

**PARAMETER OPTIMIZATION IN DESIGN OF A
MICROSTRIP PATCH ANTENNA USING ADAPTIVE
NEURO-FUZZY INFERENCE SYSTEM TECHNIQUE**

ROP, KIMUTAI VICTOR

MASTER OF SCIENCE

(Telecommunication Engineering)

**JOMO KENYATTA UNIVERSITY OF AGRICULTURE
AND TECHNOLOGY**

2013

**Parameter Optimization in Design of a Microstrip Patch Antenna
Using Adaptive Neuro-Fuzzy Inference System Technique**

Rop, Kimutai Victor

**A Thesis Submitted in Partial Fulfillment for the Degree of Master of
Science in Telecommunication Engineering in the Jomo Kenyatta
University of Science and Technology**

2013

DECLARATION

This thesis is my original work and has not been presented for award of a degree in any other University.

Signature..... Date.....

Rop, Victor Kimutai

This thesis has been submitted for examination with our approval as University supervisors

Signature..... Date.....

Prof. Dominic O. Konditi

Multimedia University College, Kenya

Signature..... Date.....

Dr. Heywood A. Ouma

University of Nairobi, Kenya

Signature..... Date.....

Dr. Stephen M. Musyoki

Jomo Kenyatta University of Science and Technology, Kenya

DEDICATION

I dedicate this work to My Loving Parents for their undying support and encouragement.

ACKNOWLEDGEMENT

I would like to express my deepest gratitude to my dedicated and untiring supervisors Prof. Konditi, Dr. Ouma, and Dr. Musyoki for their great advice, encouragement, guidance, and sharing their opinions throughout the research. They have been exemplary advisors and scholars.

My special and deepest thanks go to my parents, my brother, and my sisters for their undying support and giving me strength and courage to complete this thesis. Their support and encouragement has allowed me to reach this far in my academic career.

To all my friends, colleagues, and all those who contributed to this thesis in one way or another, I express my deepest appreciation and respect. Special thanks go to God for making it possible for me to finish this thesis.

TABLE OF CONTENTS

DECLARATION	ii
DEDICATION	iii
ACKNOWLEDGEMENT	iv
TABLE OF CONTENTS	v
LIST OF TABLES	ix
LIST OF FIGURES	x
LIST OF APPENDICES	xii
LIST OF SYMBOLS AND ABBREVIATIONS	xiii
ABSTRACT	xv
CHAPTER ONE	1
1.0. INTRODUCTION	1
1.1. Introduction	1
1.2. Problem Statement.....	2
1.3. Justification of the Study	3
1.4. Objectives	4
1.4.1. General Objective.....	4
1.4.2. Specific Objective	4
1.5. Overview of Chapters	5
CHAPTER TWO	6
2.0. LITERATURE REVIEW	6
2.1. Microstrip Patch Antennas	6
2.1.1. Background	6

2.1.2.	Physical Configuration	7
2.1.3.	Antenna Properties	10
2.1.3.1.	Gain	10
2.1.3.2.	Voltage Standing Wave Ratio (VSWR)	10
2.1.3.3.	Return Loss	11
2.1.4.	Microstrip Patch Antennas Polarization.....	11
2.1.4.1.	Linear Polarization.....	12
2.1.4.2.	Circular Polarization	12
2.1.5.	Advantages and Disadvantages of Microstrip Patch Antennas.....	13
2.1.5.1.	Advantages of Microstrip Patch Antennas	14
2.1.5.2.	Disadvantages of Microstrip Patch Antennas	14
2.1.6.	Microstrip Antennas Feed Techniques.....	15
2.1.6.1.	Coaxial Probe Feed Technique	15
2.1.6.2.	Microstrip Line Feed Technique.....	16
2.1.6.3.	Aperture-Coupled Feed Technique.....	17
2.1.6.4.	Proximity-Coupled Feed Technique	18
2.1.7.	Application of Microstrip Patch Antennas.....	20
2.1.7.1.	Mobile and Satellite Communication Application	20
2.1.7.2.	Global Positioning System Application.....	21
2.1.7.3.	Radio Frequency Identification (RFID).....	21
2.1.7.4.	Worldwide Interoperability for Microwave Access (WiMAX).....	21
2.1.7.5.	Radar Application	21
2.1.7.6.	Telemedicine Application.....	22

2.2.	Artificial Intelligence Techniques	23
2.2.1.	Fuzzy Logic.....	23
2.2.1.1.	Fuzzy sets.....	24
2.2.1.2.	Membership Functions.....	25
2.2.1.3.	Fuzzy If-Then Rules	25
2.2.1.4.	Fuzzy Inference Systems (FIS).....	26
2.2.1.4.1.	Mamdani Fuzzy Model.....	27
2.2.1.4.2.	Sugeno	27
2.2.2.	Artificial Neural Networks.....	28
2.2.2.1.	Supervised Learning	29
2.2.2.2.	Unsupervised Learning	30
2.2.3.	Neuro-Fuzzy Systems	31
2.2.3.1.	Adaptive Neuro-Fuzzy Inference System (ANFIS).....	31
2.2.3.2.	Architecture of Adaptive Neuro-Fuzzy Inference System.....	32
2.2.3.3.	ANFIS Learning Technique.....	36
CHAPTER THREE		38
3.0.	DESIGN METHODOLOGY	38
3.1.	Rectangular Microstrip Antenna Design	38
3.2.	Design Specifications	38
3.3.	Application of ANFIS in the design of a Rectangular Microstrip Patch Antenna.....	41
3.4.	ANFIS Design Procedure	43

CHAPTER FOUR	46
4.0. RESULTS AND DISCUSSIONS	46
4.1. ANFIS Simulation Results	46
4.2. Antenna Magus Software Simulation Results	55
4.3. Validation of ANFIS Model	58
4.3.1. Validation using Simulated Results	58
4.2.2. Experimental Results.....	66
5.0. CONCLUSION AND RECOMMENDATION	69
5.1. Conclusion	69
5.2. Recommendation	70
REFERENCES	71
APPENDICES	76

LIST OF TABLES

Table 2.1:	Comparison of Different Feed Techniques	19
Table 4.1:	Summary of ANFIS Model Variables	53
Table 4.2:	ANFIS Optimized Patch Antenna Design Parameters	54
Table 4.3:	Simulated Patch Antenna Design Parameters	56
Table 4.4:	Comparison of ANFIS Model, Antenna Magus Software,	59
Table 4.5:	Error Difference - Design Results	63

LIST OF FIGURES

Figure 2.1:	Cross-Sectional View of a MPA	8
Figure 2.2:	Representative Shapes of MPAs.....	9
Figure 2.3:	Structure of a Rectangular MPA	9
Figure 2.4:	Linearly Polarized Line-Fed MPA	12
Figure 2.5:	Circularly Polarized Line-Fed MPA.....	13
Figure 2.6:	Coaxial Probe Feed Technique.....	15
Figure 2.7:	Microstrip Line Feed Technique	16
Figure 2.8:	Aperture-Coupled Feed Technique	17
Figure 2.9:	Proximity-Coupled Feed Technique.....	18
Figure 2.10:	MPA in a Cellular Phone.....	20
Figure 2.11:	Architecture of an ANFIS.....	33
Figure 3.1:	MPA Electric Field Lines	38
Figure 3.2:	ANFIS Model for Design of Rectangular MPA	42
Figure 3.3:	Flowchart for Optimization of Rectangular MPA.....	44
Figure 4.1:	First Stage of ANFIS Model.....	47
Figure 4.2:	Second Stage of ANFIS Model	48
Figure 4.3:	Third Stage of ANFIS Model	49
Figure 4.4:	Fourth Stage of ANFIS Model	49
Figure 4.5:	ANFIS Optimized Patch Width vs Resonant Frequency.....	51
Figure 4.6:	ANFIS Optimized Patch Length vs Resonant Frequency	51

Figure 4.7: ANFIS Optimized Feed Point along Patch Width vs Resonant Frequency	52
.....	
Figure 4.8: ANFIS Optimized Feed Point along Patch Length vs Resonant Frequency	52
.....	
Figure 4.9: Return Loss of Rectangular MPA	54
Figure 4.10: Gain of Rectangular MPA (3D Graphical)	55
Figure 4.11: VSWR of Rectangular Microstrip Patch Antenna at 2GHz	57
Figure 4.12: Gain of Rectangular MPA at 2GHz (3D Graphical Plot)	58
Figure 4.13: Return Loss of Rectangular MPA (From ANFIS Data)	60
Figure 4.14: Rectangular MPA Gain (for ANFIS and Antenna Magus Data Respectively)	60
Figure 4.15: Patch Width Results Comparison	61
Figure 4.16: Patch Length Results Comparison	62
Figure 4.17: Feed Point along Patch Width Results Comparison	62
Figure 4.18: Feed Point along Patch Length Results Comparison	63
Figure 4.20: Patch Length Error vs. Resonance Frequency	64
Figure 4.21: Feed Point along Patch Width Error vs. Resonance Frequency	65
Figure 4.22: Feed Point along Patch Length Error vs. Resonance Frequency	65
Figure 4.23: Block Diagram of Experiment Setup	66
Figure 4.24: Fabricated Rectangular MPA	66
Figure 4.25: Experimentation Setup	67
Figure 4.26: Rectangular MPA Radiation Pattern	68

LIST OF APPENDICES

Appendix A:	MATLAB® Program Code Artificial Intelligence.....	76
Appendix B:	Training Data Sets.....	95
Appendix C:	ANFIS Parametric Design Optimized Results.....	103
Appendix D:	Computer Usage Profile Summary.....	106
Appendix E:	Publications.....	108

LIST OF SYMBOLS AND ABBREVIATIONS

AI:	Artificial Intelligence
ANFIS:	Adaptive Neuro-Fuzzy Inference System
ANN:	Artificial Neural Network
BP:	Back-propagation
BW:	Bandwidth
CP:	Circular Polarization
dB:	Decibels
FIS:	Fuzzy Inference System
HFSS:	High Frequency Structure Simulator
LHCP:	Left Hand Circularly Polarized
LSM:	Least-Squares Method
MF:	Membership Functions
MIC:	Microwave Integrated Circuits
MoM:	Method of Moments
MPA:	Microstrip Patch Antenna
P_i:	Input Power
P_r:	Radiated Power

RF:	Radio Frequency
RFID:	Radio Frequency Identification
RHCP:	Right Hand Circularly Polarized
RL:	Return Loss
RMSE:	Root Mean Square Error
SWR:	Standing Wave Ratio
VSWR:	Voltage Standing Wave Ratio
WiMAX:	Worldwide Interoperability for Microwave Access

ABSTRACT

The demand for small and reliable, high performance, diverse polarization, low-profile, and lightweight antennas has greatly increased. Its demand is in mobile communications, satellite communication, electronic warfare, biological telemetry, navigation, radar, and surveillance. Microstrip patch antennas are examples of low profile antennas. In the current highly demanding consumer world for microstrip patch antenna enabled systems, an effective and efficient higher manufacturing processing capability is required. There is thus the need for a fast, reliable, and effective microstrip patch antenna design procedure.

In this thesis, an artificial intelligence technique is used to optimize the parameters used in the design of rectangular microstrip patch antennas. This is achieved by using Adaptive Neuro-Fuzzy Inference Technique (ANFIS) implemented on the MATLAB[®] platform. This optimization method is simple, effective, and has low computer memory usage. Various data sets were used in performing the optimization for various antenna parameters and the optimized simulated results obtained were used in fabricating a set of rectangular microstrip patch antennas. Simulation results obtained from commercial Antenna Magus software were used to validate the proposed design method and to fabricate a second set of patch antennas. Fabricated antennas were then experimentally tested.

In this thesis, it is proven that optimization of rectangular microstrip patch antenna parameters using ANFIS provides good results which are in agreement with the results obtained using the commercial software. Also, on comparison of the experimental results, it is shown that the ANFIS method produces improved gain as compared with those of the Antenna Magus software. This shows that ANFIS can be used to effectively design microstrip patch antennas.

CHAPTER ONE

1.0. INTRODUCTION

1.1. Introduction

The explosion in information technology and wireless communications has created many opportunities for enhancing the performance of existing signal transmission and processing systems. This has provided a strong motivation for developing novel devices and systems. An indispensable element of any wireless communication system is the antenna. An antenna is a device used for radiating or receiving radio waves. The new generation of wireless systems demands effective and reliable antennas. These antennas include parabolic reflectors, patch antennas, slot antennas, and folded dipole antennas [1]. Each type of antenna has its own advantages and disadvantages but without a proper design, the signal generated by the radio frequency (RF) system will not be effectively transmitted and poor signal detection will be experienced at the receiver.

The sizes and weights of various wireless electronic systems (for example, mobile handsets) have rapidly reduced due to the development of modern integrated circuit technology. In many wireless communication systems, there is a requirement for low profile antennas. These antennas are less obstructive and in addition, snow, rain, or wind has less effect on their performance [1]. Microstrip patch antennas (MPAs) are examples of low profile antennas. MPAs have many attractive features such as low profile, light weight, ease of manufacture, conformability to curved surfaces, low production cost, and

compatibility with integrated circuit technology. These attractive features have recently increased MPAs popularity and applications and stimulated greater research effort to understand and improve their performance [2].

MPAs antennas are used in for example, high performance aircraft, spacecraft, space satellites, and missiles, where size, weight, cost, performance, ease of installation, and aerodynamic profile are constraints. Presently there are many other commercial applications, such as mobile radio and wireless communications that use MPAs and therefore, MPAs play a very significant role in today's world of wireless communication systems [3].

MPAs have been implemented in various configurations such as square, rectangular, circular, triangular, trapezoidal, and elliptical among others. The rectangular shaped patch antennas are very common because of the ease of analysis and fabrication and its attractive radiation characteristics especially low cross polarization radiation [3] [4]. In this thesis, the rectangular MPAs are considered as it gives an insight view of the general design of microstrip patch antennas.

1.2. Problem Statement

In the past, analytical and numerical methods have been used to design MPAs. The analytical methods, based on some fundamental simplifying physical assumptions regarding the radiation mechanism of antennas, are the most useful for practical designs

as well as for providing a good intuitive explanation of the operation of MPAs. The numerical methods are mathematically complex and cannot make a practical antenna design feasible within a reasonable period of time. They also, require strong background knowledge and have time-consuming numerical calculations which need very expensive software packages [2] [3].

Recently, many papers have reported various improved methods used in designing of MPAs including the use of artificial intelligence methods such as Genetic Algorithm, Particle Swarm Optimization, and Artificial Neural Network among others [2]. Various softwares have also been developed to ease the antenna design work. However, these softwares require large computer memory to effectively perform the design work as most of them are based on numerical method techniques and at the same time, they are expensive to acquire. This paper shows how the parameters in a design of rectangular microstrip patch can be optimized using Adaptive Neuro-Fuzzy Inference System (ANFIS) technique that takes less computer memory and is implemented in MATLAB[®].

1.3. Justification of the Study

With the ever-increasing need for microstrip patch antenna embedded systems, it is important to use a design method that is simple to use and effective. Many softwares have been developed to ease the design work for microstrip patch antenna, but still, they are not easily available locally and are very expensive. These softwares pose a challenge in their use since they are complicated and need much time for one to learn how to use them

and they also, take a lot of computer memory thus making them unpopular with many engineers. There is therefore a need to develop a better technique that performs the design work effectively with less computer memory usage.

Several design techniques have been developed using various artificial intelligence techniques [3]. Many design methodologies and various patch designs have been proved to provide better gain and radiation characteristics. This work utilizes the advantages of the ANFIS in developing an optimal parametric design procedure in modeling of a rectangular microstrip patch antenna. It demonstrates how effectively the hybrid of Fuzzy Logic and Artificial Neural Network (ANN) can be used to train and optimize the various parameters involved in the design of microstrip patch antenna.

1.4. Objectives

1.4.1. General Objective

- To develop an optimal parametric design procedure based on artificial intelligence (AI) for modeling microstrip patch antennas and practical implementation of the modeled antenna parameters.

1.4.2. Specific Objective

- To develop a rectangular microstrip patch antenna design procedure using Adaptive Neuro-Fuzzy Inference System (ANFIS) technique.

- To build a rectangular microstrip patch antenna based on optimized parameters obtained from a modeled ANFIS technique.
- To validate the ANFIS modeled experimental results with the Antenna Magus Software simulated and experimental data.

1.5. Overview of Chapters

Chapter One covers the problem background together with the objectives of the research. The literature review is elaborated in Chapter Two. This chapter presents microstrip patch antenna concept, and pertinent areas of application. It also presents the relevant artificial intelligence methods namely Fuzzy Logic, Artificial Neural Networks, and the ANFIS method. Chapter Three presents the design methodology which includes formulation and analysis of the project results describing the design procedure of the rectangular microstrip patch antenna and application of ANFIS on the same. Chapter Four analyses and discusses the simulation and experimental results. Chapter Five concludes the work performed in this thesis with suggestions for future work. And finally, the References and Appendices are included at the end of the thesis. In the Appendices, the source codes and data for various programs used in this work and execution time profile have been attached. Appendix A presents MATLAB[®] codes, Appendix B contains training data sets, Appendix C contains the ANFIS optimized results, Appendix D presents the computer usage profile summary, and finally Appendix E presents a list of publications.

CHAPTER TWO

2.0. LITERATURE REVIEW

2.1. Microstrip Patch Antennas

2.1.1. Background

An antenna is designed to transmit or receive radio waves. It is used to couple energy from a guiding structure such as transmission line or waveguide into free space and vice versa. Thus, information can be transferred between different locations without any intervening structure. Furthermore, antennas are required in situations where it is impossible, impractical or uneconomical to provide guiding structures between the transmitter and the receiver. MPA is a type of an antenna that consists of a radiating patch on one side of a dielectric substrate and a ground plane on the other side [1] [4].

The idea of microstrip radiators dates back to the year 1953 when they were proposed by Deschamps [5]. Several years later, Gutton and Baissinot [6] patented a microstrip based antenna. In spite of the publication of the concept, not much activity in microstrip antenna development occurred over the next 15 years or so except for some work by Kaloj at the U.S. Navy Missile Test Range in California. This was partly due to the lack of good microwave substrates. Also, at that time more interest was focused on stripline circuits as thinner and lower cost alternatives to waveguide components [7].

The application of microstrip radiators to design useful antennas only started in the early 1970s when the need for thin conformal antennas were required for missiles and spacecrafts and that led to the rapid development of the MPAs [8]. Since then, many papers have been written on the methods of improving and utilizing the advantages of MPAs in spite of its disadvantages [9] [10]. MPAs have been one of the most rapidly developing research fields in the last twenty years. The design of MPA elements having wider bandwidth is an area of major interest in microstrip antennas technology, particularly in the fields of electronic warfare, communication systems and wideband radar. Consequently, the bandwidth aspect of MPAs has received considerable attention [2] [9].

2.1.2. Physical Configuration

In its most basic form, a MPA consists of a radiating patch on one side of a dielectric substrate and a ground plane on the other side as shown in Figure 2.1. The bottom surface of a thin dielectric substrate is completely covered with metallization that serves as a ground plane. The metallization is usually copper or gold that has been electrodeposited or rolled on. With the former, the copper is chemically deposited on the surface, while a thin copper sheet is attached by an adhesive for the latter. The electromagnetic waves fringe off the top patch into the substrate, reflecting off the ground plane and radiates out into the air. MPAs radiate primarily because of the fringing fields between the patch edge and the ground plane [7] [8].

For a good antenna performance, a thick dielectric substrate having a low dielectric constant is desirable as it provides better efficiency, larger bandwidth and better radiation. However, such a configuration leads to a larger antenna size. To design a smaller sized MPA, higher dielectric constants must be used but it turn, it results to narrower bandwidth and less efficiency, thus a compromise must be reached between antenna dimensions and performance [2] [9] [10].

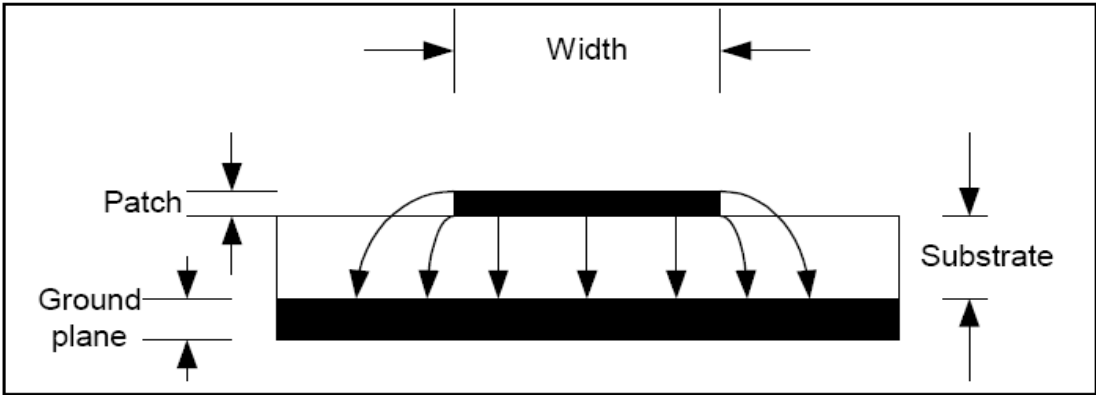


Figure 2.1: Cross-Sectional View of a MPA

The patch is normally made of conducting material and can take any possible shape as shown in Figure 2.2 [8] [9].

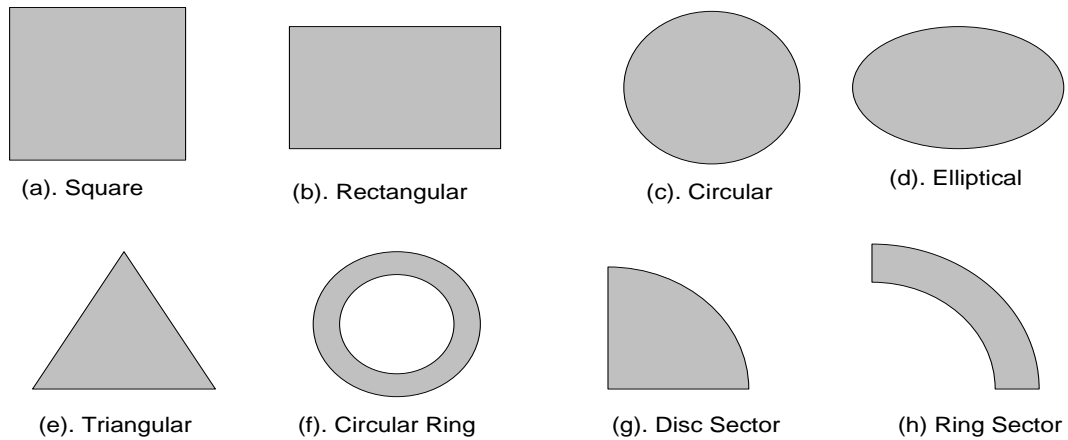


Figure 2.2: Representative Shapes of MPAs

The rectangular shaped patch antenna is the most common type of MPAs because of its ease in the analysis, fabrication, and its attractive radiation characteristics especially low cross polarization radiation. The rectangular MPA is made of a rectangular patch with dimensions width (W) and length (L) over a ground plane with a substrate thickness (h) and dielectric constants (ϵ_r) as shown in Figure 2.3 [7] [12].

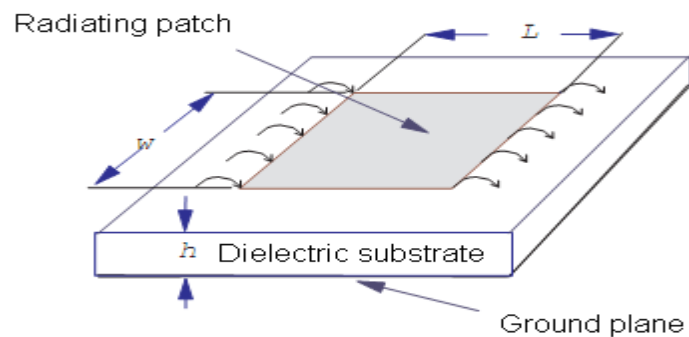


Figure 2.3: Structure of a Rectangular MPA

2.1.3. Antenna Properties

2.1.3.1. Gain

This is the quantity which describes the capability of an antenna to concentrate power in a given direction. In many instances, transmission is required between a transmitter and only one receiving station. Power is thus radiated in one direction because it is useful only in that direction. Transmitting and receiving antennas should have small power losses and should be efficient as radiators and receptors. Gain is expressed in dB and is defined as antenna directivity times a factor representing the radiation efficiency and its expression is as follows;

$$G = \eta \times D \quad (2-1)$$

where, G – Gain, η – The efficiency of the antenna, and D – Directivity

2.1.3.2. Voltage Standing Wave Ratio (VSWR)

Voltage Standing Wave Ratio is a measure of impedance mismatch between the feeding system and the antenna. Maximum power transfer can take place only when the input impedance of the antenna is matched to that of the feeding source impedance [11]. The higher the VSWR, the greater is the mismatch. The minimum possible value of VSWR is unity and this corresponds to perfect match

$$VSWR = \frac{1 + |\Gamma|}{1 - |\Gamma|} \quad (2-2)$$

$$\Gamma = \frac{V_r}{V_i} = \frac{Z_L - Z_c}{Z_L + Z_c} \quad (2-3)$$

where, Γ is the reflection coefficient, V_r is the amplitude of the reflected wave, V_i is the amplitude of the incident wave, Z_c is the characteristic impedance of the feeder cable, and Z_L is the load/antenna impedance.

2.1.3.3. Return Loss

Return loss (RL) is a ratio of power transferred to the load to power reflected back. To obtain a perfect matching between the feeding system and the antenna; $\Gamma = 0$, and RL = -infinity, thus no power is reflected back. *RL* is given as;

$$RL = -20 \log|\Gamma| \text{ (dB)} \quad (2-4)$$

2.1.4. Microstrip Patch Antennas Polarization

The polarization of an antenna refers to the polarization of the electric field vector of the radiated wave. It is the orientation of the electric fields as observed from the source versus time. A transmit antenna needs a receiving antenna with the same polarization for optimum operation [8]. Depending upon their geometry, MPAs can produce different polarization. The common and typical types of polarization are the linear (horizontal or vertical) and circular (right hand or the left hand) polarization [8] [13] [14].

2.1.4.1. Linear Polarization

Linearly polarized waves are defined with respect to a local ground plane as shown in Figure 2.4. A horizontally polarized wave has an electric field vector that oscillates in a direction parallel to the ground plane, while the electric field vector of a vertically polarized wave has a component that is orthogonal to the ground plane. When the antenna and wave polarizations are identical, the antenna extracts the maximum power from an incident wave. On the other hand, no power can be received when the polarizations are orthogonal to each other, as, for example, vertical and horizontal polarizations. Normally, conventional rectangular MPAs are linearly polarized radiating structures [8] [13] [14].

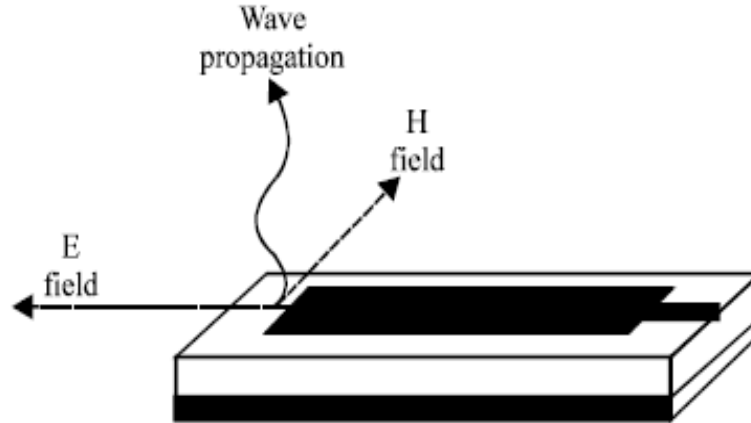


Figure 2.4: Linearly Polarized Line-Fed MPA

2.1.4.2. Circular Polarization

Circular polarization (CP) is a result of orthogonally fed signal input. When two signals of equal amplitude have 90° phases, the resulting wave is circularly polarized as show in

Figure 2.5. CP can result in left hand circularly polarized (LHCP) wave with anticlockwise, or right hand circularly polarized (RHCP) wave with clockwise rotation. The main advantage of CP is that regardless of receiver orientation, it will always be able to receive a component of the signal. This reception is due to the resulting wave having an angular variation [13] [14].

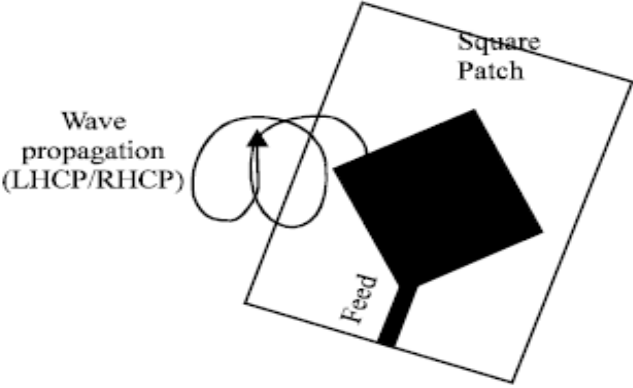


Figure 2.5: Circularly Polarized Line-Fed MPA

2.1.5. Advantages and Disadvantages of Microstrip Patch Antennas

In the recent past, the use of MPA in wireless communication has increased significantly. This is mainly due to their low-profile structure amongst other merits. However, they do possess a number of disadvantages as any other type of an antenna.

2.1.5.1. Advantages of Microstrip Patch Antennas

Some of the advantages of patch antennas as discussed in [7] [16] [14] [10] [15] are;

- Light weight and low volume.
- Low profile planar configuration easily made conformal to host surface.
- Low fabrication cost, hence mass production.
- Support of both linear and circular polarization.
- Capability of dual and triple frequency operations.
- Possibility of simultaneous fabrication of feed lines and matching network.
- Ease of integration with microwave integrated circuits (MICs).

2.1.5.2. Disadvantages of Microstrip Patch Antennas

Microstrip patch antennas suffer from a number of disadvantages as compared to conventional antennas as discussed in [7] [16] [14] [10] [15], such as;

- Narrow bandwidth and low gain with low efficiency.
- Computational (numerical) intensive design with computer memory intensive design softwares.
- Surface wave excitation and extraneous radiation from feeds and junctions
- Low power handling capacity.
- Complex feed structures requiring high performance arrays.

2.1.6. Microstrip Antennas Feed Techniques

MPAs can be fed by a variety of methods which are classified into two categories; contacting and non-contacting. Contacting feed technique is where the power is fed directly to the radiating patch through the connecting element such as microstrip line. Non-contacting technique is where an electromagnetic magnetic coupling is done to transfer the power between the microstrip line and the radiating patch. The most popular contacting feed techniques used are the microstrip line feed and coaxial probe feed, while the most popular non-contacting feed techniques are aperture coupling feed and proximity coupling feed [12] [13].

2.1.6.1. Coaxial Probe Feed Technique

This is the most common feed technique used in the design of MPAs. As seen in Figure 2.6, the external or the outer conductor is connected to the ground plane and the inner conductor of the coaxial connector extends through the dielectric and is soldered to that of the radiating patch.

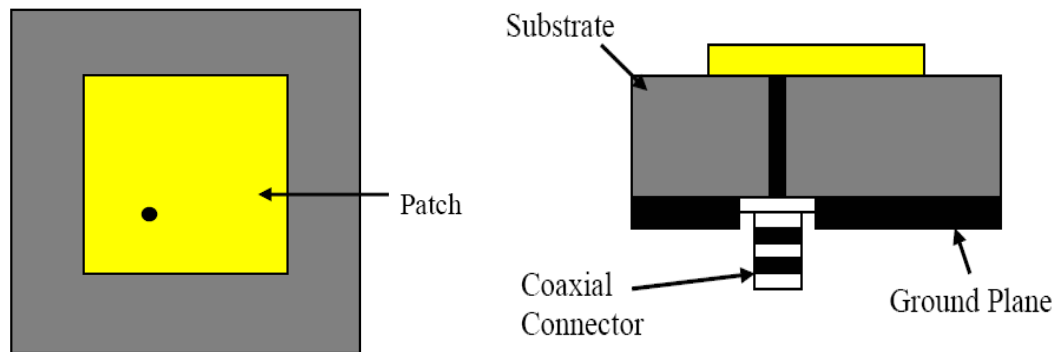


Figure 2.6: Coaxial Probe Feed Technique

Unlike the other feed techniques, coaxial probe feed has the flexibility of placing the feed anywhere in the patch in order to match the input impedance. This gives an easy way for the fabrication and it has low spurious radiation. The disadvantage of this type of feed is the narrow bandwidth. Also with the extended or the increase probe length, the input impedance becomes more inductive, which leads to the impedance matching challenges [8] [12] [13].

2.1.6.2. Microstrip Line Feed Technique

This type of feed technique uses conducting strip that is directly connected to the edge of the microstrip patch as shown in Figure 2.7. The conducting strip and the patch both can be fabricated simultaneously on the same substrate to provide a planar structure. The width of a conducting strip is smaller than that of the patch.

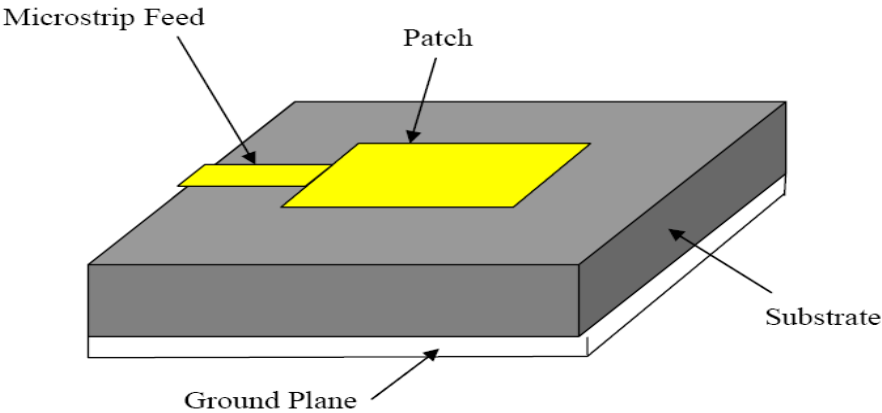


Figure 2.7: Microstrip Line Feed Technique

This method provides an easy and a simple way in the fabrication, modeling, and especially in the impedance matching. However, the surface waves and the spurious feed radiation increases as the thickness of the dielectric substrate increases which obviously hampers the bandwidth of the antenna. Also, the serious drawbacks of this feed structure are the strong parasitic radiation thus, it requires a transformer for impedance matching which restricts the broadband capability of the antenna [8] [12] [13].

2.1.6.3. Aperture-Coupled Feed Technique

This type of method falls under the non-contacting feed techniques. In this type of feed technique, the radiating patch and the microstrip feed line are divided by the ground plane as shown in Figure 2.8.

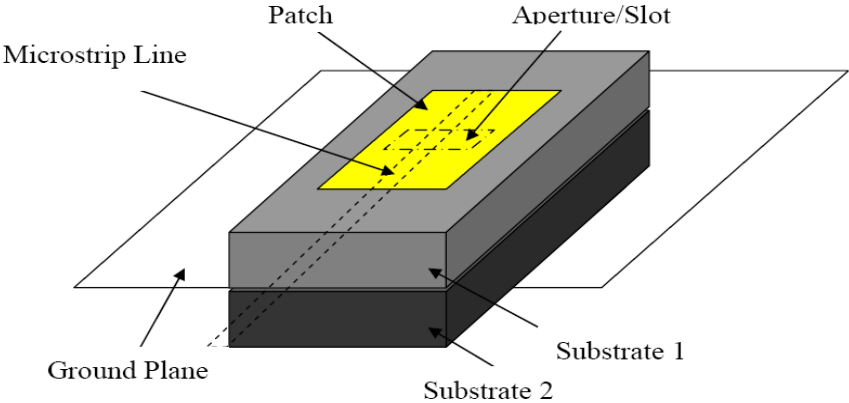


Figure 2.8: Aperture-Coupled Feed Technique

On the bottom side of lower substrate, there is a microstrip feed line whose energy is coupled to the patch through a slot on the ground plane separating two substrates. The

amount of coupling depends on the size, shape and also the location of the aperture. Since the ground plane separates the patch and the feed line, spurious radiation is minimized. Generally, a high dielectric material is used for the bottom substrate and a thick, low dielectric constant material is used for the top substrate to optimize radiation from the patch. The main outstanding feature in this particular feed technique is the wider bandwidth. It has all of the advantages of the former two structures and it also isolates the radiation from the feed network thereby leaving the main antenna radiation uncontaminated. The major disadvantage of this feed technique is that it is difficult to fabricate due to multiple layers, which also increases the antenna thickness [8] [13] [16].

2.1.6.4. Proximity-Coupled Feed Technique

This type of feed technique is also called the electromagnetic coupling scheme. As shown in Figure 2.9, two dielectric substrates are used such that the feed line is in between the two substrates and the radiating patch is on top of the upper substrate.

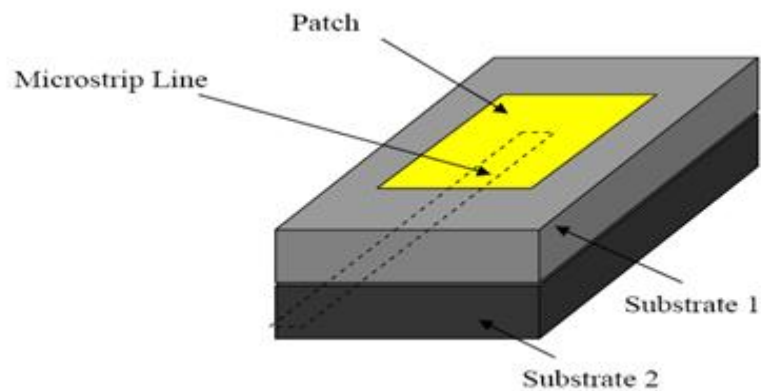


Figure 2.9: Proximity-Coupled Feed Technique

The main advantage of this feed technique is that it eliminates spurious feed radiation and provides very high bandwidth (as high as 13%) [16]. This proximity-coupled feed technique also provides choices between two different dielectric media; one for the patch and one for the feed line to optimize the individual performances. Matching can be achieved by controlling the length of the feed line and the width-to-line ratio of the patch. The major disadvantage of this feed scheme is that it is difficult to fabricate because of the two dielectric layers which need proper alignment. Also, there is an increase in the overall thickness of the antenna [16] [12] [13].

Table 2.1 summarizes the characteristics of microstrip line feed, coaxial probe feed, aperture-coupled feed, and proximity-coupled feed techniques [13] [16].

Table 2.1: Comparison of Different Feed Techniques

Characteristics	Coaxial Probe Feed	Microstrip Line Feed	Aperture-Coupled Feed	Proximity-Coupled Feed
Configuration	Non Planar	Coplanar	Planar	Planar
Ease of Fabrication	Soldering and drilling needed	Easy	Alignment required	Alignment required
Spurious Feed Radiation	More	More	Less	Minimum
Reliability	Poor due to soldering	Better	Good	Good
Impedance Matching	Easy	Easy	Easy	Easy
Polarization Purity	Poor	Poor	Excellent	Poor
Bandwidth	2-5%	2-5%	About 15%	About 13%

2.1.7. Application of Microstrip Patch Antennas

The usage of the MPAs is spreading widely in both commercial and non-commercial aspects due to the low cost of the substrate material and ease of fabrication, with the most applications being on mobile communication systems. MPAs are mostly applicable where small, lightweight, low profile, and low-cost conformal structures are required. As discussed in [8] [10] [13] [16], some of the applications include;

2.1.7.1. Mobile and Satellite Communication Application

MPAs are widely used in mobile communication systems. An example is shown in the Figure 2.10. In the case of satellite communication, circularly polarized radiation patterns are usually used and can be realized using either square or circular patch with one or two feed points.

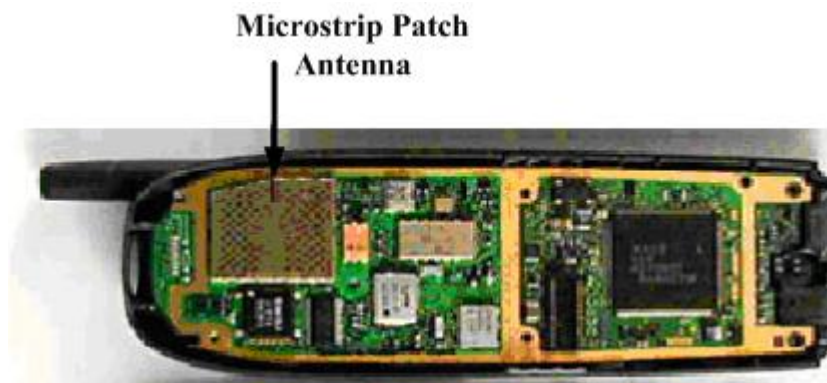


Figure 2.10: MPA in a Cellular Phone

Other applications of MPAs include the following among others;

2.1.7.2. Global Positioning System Application

MPAs are used for global positioning system due to its ease in integration of a low noise amplifier on the substrate used for the feeding circuitry. These antennas are usually circularly polarized. Most of the GPS receivers are used by the general population for land vehicles, aircraft, and maritime vessels.

2.1.7.3. Radio Frequency Identification (RFID)

RFID systems consist of a tag or transponder and a transceiver or reader RFID and are used in different areas like mobile communication, logistics, manufacturing, transportation, and health care. They generally use frequencies between 30 Hz and 5.8 GHz depending on its applications.

2.1.7.4. Worldwide Interoperability for Microwave Access (WiMAX)

Microstrip patch antennas are used for WiMAX as they meet the IEEE 802.16 standard [14].

2.1.7.5. Radar Application

Radar can be used for detecting moving targets such as people and vehicles. It demands a low profile light weight antenna subsystem making MPAs the most ideal choice.

2.1.7.6. Telemedicine Application

In telemedicine application, the antennas mostly used operate at 2.45 GHz. A semi directional radiation pattern is preferred over the omni-directional pattern to overcome unnecessary radiation to the user's body, thus MPAs are suitable for telemedicine applications. Also, it has been proved that in the treatment of malignant tumors, microwave energy is the most effective way of inducing hyperthermia [16]. The design of the particular radiator which is to be used for this purpose should possess light weight, easy in handling, and to be rugged and therefore, the patch radiator fulfills these requirements.

2.2. Artificial Intelligence Techniques

Artificial intelligence (AI) is the ability of a computer or any other machine to perform those activities that are normally thought to require intelligence by evaluating information and making decisions according to pre-established criteria. AI borrows its meaning from the word intelligence which is defined as the ability to apply past and present experience to satisfactorily solve present and future problems. In AI, the basic paradigm of intelligent action is that of searching through a space of partial solutions (called the problem space) for a goal situation. Fuzzy logic, artificial neural networks, genetic algorithms, and particle swarm optimization, among others are examples of AI techniques that are applicable in every day's life [17] [22]. Artificial intelligence techniques have gained popularity in engineering design in recent years due to their efficiency and effectiveness [22]. Various papers have been published in the recent past on the design of antennas using AI techniques as seen in [2] [15] [26] [33] [36].

2.2.1. Fuzzy Logic

Fuzzy logic is a form of multi-valued logic derived from fuzzy set theory to deal with reasoning that is approximate rather than precise. It is a problem-solving control system methodology that deals with the use of logical rules to solve nonlinear and complex problems by employing the use of linguistic terms that deal with the causal relationship between the input and output variables, thus treating the variables as continuous rather than discrete [22]. This system is implemented in MATLAB® Fuzzy Toolbox. Various

researches have shown that human thinking does not always follow crisp “yes”/“no” logic, but rather it is often vague, qualitative, uncertain, imprecise, or fuzzy in nature. Therefore, fuzzy system provides parameters of the fuzzy control paradigm which is a collection of rules and fuzzy set membership functions [18] [19]. Among the reasons for using fuzzy logic technique is that it;

- Is conceptually easy to understand.
- Is flexible.
- Is tolerant of imprecise data.
- Can be blended with conventional control techniques.
- Is based on natural language.

2.2.1.1. Fuzzy sets

Fuzzy set is classification of a set without crisp or clearly defined boundary. Fuzzy set can contain elements with only a partial degree of membership. Unlike classical set based on Boolean logic, a particular object has a degree of membership in a given set that may be anywhere in the range of 0 (completely not in the set) to 1 (completely in the set), thus, it is often defined as multi-valued logic (or 0-1) [18].

2.2.1.2. Membership Functions

A membership function (MF) is a curve that defines how each point in the input space is mapped to a membership value (or degree of membership) between 0 and 1. A fuzzy set can be defined by enumerating membership values of the elements in the set if it is discrete or by defining the membership function mathematically if it is continuous. Although there exist numerous types of membership functions, the most commonly used in practice are triangles, trapezoids, Gaussian, and bell curves [19] [20].

2.2.1.3. Fuzzy If-Then Rules

Fuzzy if-then rules are a knowledge representation scheme for capturing knowledge (typically human knowledge) that is imprecise and inexact by nature. Generally, this is achieved by using linguistic variables to describe elastic conditions (that is, conditions that can be satisfied to a degree) in the “if” part of fuzzy rules and to perform inference under partial matching. A fuzzy if-then rule takes the form:

$$\text{IF } x \text{ is } A_k \text{ THEN } y \text{ is } B_k(x) \quad (2-5)$$

where, A_k and B_k are linguistic values defined by fuzzy sets on universes x and y respectively. Often, the “if” part is called antecedent or premise, while the “then” part is called consequence or conclusion. The fuzzy sets in a rule’s antecedent define a fuzzy region of the input space covered by the rule (that is, the input situations that fit the rule’s

condition completely or partially), whereas the fuzzy sets in a rule's consequent describe the vagueness of the rule's conclusion [18] [20].

2.2.1.4. Fuzzy Inference Systems (FIS)

Fuzzy inference is the actual process of mapping from a given input to an output using fuzzy logic. A typical FIS consists of membership functions, a rule base and an inference procedure. The basic structure of a FIS consists of three conceptual components:

- i. A rule base, which contains a selection of fuzzy rules;
- ii. A database, which defines the membership functions used in the fuzzy rules;
- iii. A reasoning mechanism, which performs the inference procedure upon the rules and given facts to derive a reasonable output or conclusion.

The inputs of fuzzy inference system can either be fuzzy sets or crisp values (which are viewed as fuzzy singletons). If the system produces fuzzy sets as output while a crisp output is needed, then a method of defuzzification is required to extract a crisp value that best represents the fuzzy set [18] [20].

Depending on the types of fuzzy reasoning and fuzzy if-then rules employed, most fuzzy inference systems can be classified into two types namely Mamdani and Sugeno fuzzy models.

2.2.1.4.1. Mamdani Fuzzy Model

Mamdani fuzzy model was proposed Mamdani (1975) [19] as an attempt to control a steam engine and boiler combination by a set of linguistic control rules. A Mamdani fuzzy system uses fuzzy sets as rule consequent. The fuzzy rule in this model is in the form of:

$$\text{IF } x_1 \text{ is } A_{i1} \dots \text{and/or } x_n \text{ is } A_{in} \text{ THEN } y \text{ is } C_i \quad (2-6)$$

where, x_j ($j=1, 2, \dots, n$) are the input variables, y is the output variable, and A_{ij} and C_i are fuzzy sets for x_j and y respectively [19] [20].

2.2.1.4.2. Sugeno Fuzzy Model

Sugeno fuzzy model was proposed by Takagi, Sugeno, and Kang [19] in an effort to develop a systematic approach of generating fuzzy rules from a given input-output data set. A typical two-input fuzzy rule in this model is in the form of:

$$\text{IF } x_1 \text{ is } A \text{ and } x_2 \text{ is } B \text{ THEN } y = f(x_1, x_2). \quad (2-7)$$

where, A and B are fuzzy sets in the antecedent and $y = f(x_1, x_2)$ is a crisp function in the consequent. Usually, $f(x_1, x_2)$ is a polynomial function of the input variables x_1 and x_2 , but it can be any function as long as it can appropriately describe the output of the model within the fuzzy region specified by the antecedent of the rule. When $f(x_1, x_2)$ is a first-order polynomial function, the resulting fuzzy inference system is called a first-order Sugeno fuzzy model. When $f(x_1, x_2)$ is a constant, the system is referred as a zero-order Sugeno fuzzy model [19] [20]. Because it is a more compact and computationally efficient

representation than a Mamdani system, the Sugeno system lends itself to the use of adaptive techniques for constructing fuzzy models. These adaptive techniques can be used to customize the membership functions so that the fuzzy system best models the data.

2.2.2. Artificial Neural Networks

Artificial Neural Network (ANN) is information processing technique with the capability of performing computations similar to human brain or biological neural network. ANN is a technique that seeks to build an intelligent program to implement intelligence similar to that of a human brain processing. ANN uses models that simulate the inter-connection of neurons, such that neuron outputs are connected (through weights), to all other neurons including themselves. Just like the way human brain remembers and learns, an ANN system works in a similar manner. With the set of input data patterns, the network can be trained (not programmed) to give corresponding desired patterns at the output [21] [22]. Some of the reasons why this AI technique has gained popularity are;

- Their ability to derive meaning from complicated or imprecise data
- Adaptive learning: An ability to learn how to do tasks based on the data given for training or initial experience.
- Self-Organization: An ANN can create its own organization or representation of the information it receives during learning time.
- Real Time Operation: ANN computations may be carried out in parallel with simulations.

- **Parallel Computation:** ANN is a fast and massive parallel input parallel output multidimensional computing system.

Learning methods used for ANN can be classified into two major categories namely supervised and unsupervised learning.

2.2.2.1. Supervised Learning

The goal of supervised learning is to shape the input-output mappings of the network based on a given training data set. As the term suggests, first, the desired input-output data sets must be known; then the resulting networks need to have adjustable parameters that are updated by a supervised learning rule. The adjustable parameters are often referred to as weights. In supervised training, both the inputs and the outputs are provided. The network then processes the inputs and compares its resulting outputs against the desired outputs. Errors are then propagated back through the system, causing the system to adjust the weights which control the network. This process occurs over and over as the weights are continually tweaked [22]. The set of data which enables the training is called the ‘training set’. During the training of a network, the same set of data is processed many times as the connection weights are ever refined. An important issue concerning supervised learning is the problem of error convergence, that is, the minimization of error between the desired and computed unit values. The aim is to determine a set of weights which minimizes the error [23].

Back-propagation (BP), also known as back error propagation or the generalized delta rule is an example of supervised learning method. The training process involves two steps; a forward propagating step and a backward propagating step. In the forward pass, the training input data is presented to the input layer. The data propagates on through the hidden layers, until it reaches the output layer, where it is displayed as the output pattern. In the backward pass, the error term is calculated and propagated back to change the assigned weights of the inputs. The magnitude of the error value indicates how large an adjustment needs to be made and the sign of the error value gives the direction of the change [24].

2.2.2.2. Unsupervised Learning

In unsupervised training, the network is provided with inputs but not with desired outputs. The system itself must then decide what features it will use to group the input data. This is often referred to as self-organization or adaption. Unsupervised learning is learning with no information available regarding the desired outputs; the network updates weights only on the basis of the input patterns. Self-organizing implies the ability to acquire knowledge through a trial and error learning process involving organizing and reorganizing in response to external stimuli [22] [24]. Kohonen self-organizing maps also known as Kohonen self-organizing feature maps, are one of the common unsupervised learning paradigms [24].

2.2.3. Neuro-Fuzzy Systems

Neural networks and fuzzy logic are two complementary technologies as discussed earlier. This is because neural networks have the learning ability which can learn knowledge using training examples, while fuzzy inference systems can deduce knowledge from the given fuzzy rules. Therefore, the combination of these two outperforms either neural network or fuzzy logic method used exclusively [25]. Fast and accurate learning, excellent explanation facilities in the form of semantically meaningful fuzzy rules, the ability to accommodate both data and existing expert knowledge about the problem, and good generalization capability features have made neuro-fuzzy systems popular in the recent past [23] [24].

2.2.3.1. Adaptive Neuro-Fuzzy Inference System (ANFIS)

Fundamentally, ANFIS is about taking a FIS and tuning it with an ANN algorithm based on some collection of input-output data. Using a given input/output data set, the toolbox function ANFIS constructs a FIS whose membership function parameters are tuned (adjusted) using either a back-propagation algorithm alone or in combination with a least squares type of method. This adjustment allows the fuzzy systems to learn from the data they are modeling [24] [28]. The parameters associated with the membership functions changes through the learning process. The computation of these parameters (or their adjustment) is facilitated by a gradient vector. This gradient vector provides a measure of how well the fuzzy inference system is modeling the input/output data for a given set of

parameters. When the gradient vector is obtained, any of several optimization routines can be applied in order to adjust the parameters and to reduce some error measure. This error measure is usually defined by the sum of the squared difference between actual and desired outputs [25] [29]. This process is referred as supervised learning in neural network literature. By combining the advantages of imprecise data sampling of fuzzy logic and the intelligence of ANN, the neuro-fuzzy outsmarts the two AI and therefore, this AI method was chosen for this work so as to show that it can be used to design MPAs with the results that are in agreement with the conventional design results.

2.2.3.2. Architecture of Adaptive Neuro-Fuzzy Inference System

ANFIS network is organized into two parts like fuzzy systems. The first part is the antecedent and the second part is the conclusion, and the two are connected to each other by rules to form a network. A step in the learning process has two passes: In the first pass, training data is brought to the inputs while the premise parameters are assumed to be fixed and the optimal consequent parameters are estimated by an iterative least mean square procedure. In the second pass, the patterns are propagated again but this time the consequent parameters are assumed to be fixed and back-propagation is used to modify the premise parameters [28] [25]. The process will repeat itself depending on the number of epochs (iterations) specified.

The ANFIS architecture consists of five layers namely; fuzzy layer, product layer, normalized layer, de-fuzzy layer, and summation (total output) layer as shown in Figure 2.11. In the figure, a circle indicates a fixed node, whereas a square indicates an adaptive node [8].

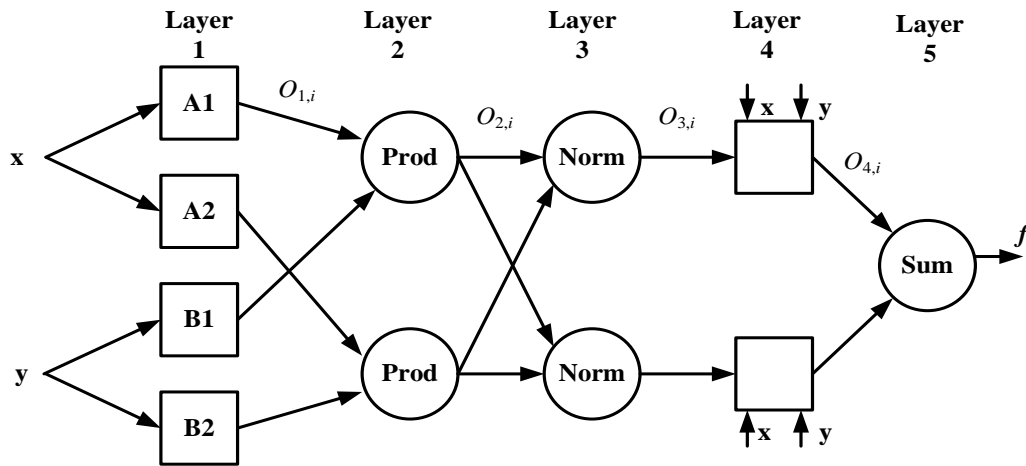


Figure 2.111: Architecture of an ANFIS

Assume that the fuzzy inference system under consideration has two inputs x and y and one output f . Based on a first-order Sugeno model, a typical rule set with two fuzzy if-then rules can be expressed as;

$$\text{Rule1: If } x \text{ is } A_1 \text{ and } y \text{ is } B_1, \text{ then } f_1 = p_1x + q_1y + r_1 \quad (2-8)$$

$$\text{Rule2: If } x \text{ is } A_2 \text{ and } y \text{ is } B_2, \text{ then } f_2 = p_2x + q_2y + r_2 \quad (2-9)$$

where, A_1, B_1, A_2, B_2 are fuzzy sets, p_i, q_i and r_i ($i = 1, 2$) are the coefficients of the first-order polynomial linear functions.

The following section discusses in depth the relationship between the input and output of the five layers in ANFIS architecture as outlined in [20] [26] [27] [28].

Layer 1 is *the Fuzzy Layer*, in which x and y are the input of nodes A_1 , B_1 , and A_2 , B_2 respectively. A_1 , B_1 , A_2 , and B_2 are the linguistic labels used in the fuzzy theory for dividing the membership functions. The membership relationship between the output and input functions of this layer can be expressed as;

$$O_{1,i} = \mu_{A_i}(x), \quad i = 1, 2 \quad (2-10)$$

$$O_{1,j} = \mu_{B_j}(y), \quad j = 1, 2 \quad (2-11)$$

where $O_{1,i}$ and $O_{1,j}$ denote the output functions, whereas μ_{A_i} and μ_{B_j} denote the membership functions respectively.

Layer 2 is *the Product Layer* that consists of two nodes labeled Prod. The output w_1 and w_2 are the weight functions of the next layer. Each node calculates the firing strength of a rule via multiplication. The output of this layer ($O_{2,i}$) is the product of the input signal, and is defined as;

$$O_{2,i} = w_i = \mu_{A_i}(x)\mu_{B_j}(y), \quad i, j = 1, 2 \quad (2-12)$$

Layer 3 is *the Normalized Layer* whose nodes are labeled Norm. Its function is to normalize the weight function, that is, the firing strength from previous layer. It calculates the ratio of the i^{th} rule's firing strength to the sum of the entire rule's firing strengths. The output is denoted as $O_{3,i}$ and is defined in Eq. 2-13.

$$O_{3,i} = \bar{w}_i = \frac{w_i}{w_1 + w_2}, i = 1,2 \quad (2-13)$$

Layer 4 is the *De-fuzzy Layer* whose nodes are adaptive. p_i , q_i and r_i denote the linear parameters which are also called consequent parameters of the node. The de-fuzzy relationship between the input and output of this layer can be defined as Eq. 2-14, where $O_{4,i}$ denotes the Layer 4 output. The output of each node is simply the product of the normalized firing strength and a first order polynomial.

$$O_{4,i} = \bar{w}_i f_i = \bar{w}_i (p_i x + q_i y + r_i) \quad (2-14)$$

Layer 5 is the *Total Output Layer* whose single node is labeled as Sum. The output of this layer denoted as $O_{5,1}$ is the total of input signals. The results can be expressed as;

$$O_{5,1} = \sum_i \bar{w}_i f_i = \frac{\sum_i w_i f_i}{\sum_i w_i} \quad (2-15)$$

The output of ANFIS can be therefore, be written as;

$$f = \frac{w_1}{w_1 + w_2} f_1 + \frac{w_2}{w_1 + w_2} f_2 \quad (2-16)$$

Substituting Eq. 2-13 into Eq. 2-16 yields

$$f = \bar{w}_1 f_1 + \bar{w}_2 f_2 \quad (2-17)$$

Substituting the fuzzy if-then rules in Eq. 2-8 and 2-9 into Eq. 2-17, then yields

$$f = \bar{w}_1 (p_1 x + q_1 y + r_1) + \bar{w}_2 (p_2 x + q_2 y + r_2) \quad (2-18)$$

The output can therefore, be expressed as a linear combination of the consequent parameters:

$$f = (\bar{w}_1 x) p_1 + (\bar{w}_1 y) q_1 + \bar{w}_1 r_1 + (\bar{w}_2 x) p_2 + (\bar{w}_2 y) q_2 + \bar{w}_2 r_2 \quad (2-19)$$

In this ANFIS architecture, there are two adaptive layers (layer 1 and 4). Layer 1 has modifiable parameters pertaining to the input MFs. These parameters are called premise parameters. Layer 4 has three modifiable parameters (p_i , q_i and r_i) pertaining to the first order polynomial. These parameters are called consequent parameters [28].

2.2.3.3. ANFIS Learning Technique

To identify the parameters in the nonlinear neuro-fuzzy model, the gradient descent method [25] in conjunction with error BP process [25] [26] could be used for neural network learning. However, this optimization method usually takes a long time to converge. An alternative is the Least-Squares Method (LSM) which is a powerful and well developed tool that is widely employed in areas such as adaptive control, signal processing and statistics. The hybrid learning algorithm combining the LSM and the BP algorithm can be used to solve the problem of convergence. This algorithm converges much faster, since it reduces the dimension of the search space of the BP algorithm [25] [18]. During the learning process, the premise parameters in the layer 1 and the consequent parameters in the layer 4 are tuned until the desired response of the FIS is achieved. The

hybrid learning algorithm is a two-step process. First, while holding the premise parameters fixed, the functional signals are propagated forward to layer 4, where the consequent parameters are identified by the LSM. Then, the consequent parameters are held fixed while the error signals, the derivative of the error measure with respect to each node output, are propagated from the output end to the input end, and the premise parameters are updated by the standard BP algorithm. This process is repeated until the results are deemed satisfactory (when the error becomes zero) or once the process reaches a specified epoch number [10] [26].

CHAPTER THREE

3.0. DESIGN METHODOLOGY

3.1. Rectangular Microstrip Antenna Design

The rectangular MPA is made of a rectangular patch with dimensions width (W) and length (L) over a ground plane with a substrate thickness (h) and dielectric constant (ϵ_r).

This work concentrates only on the basic geometry of the MPAs ignoring the various complex structures adopted for the enhancement of bandwidth, directivity, and gain.

3.2. Design Specifications

There are various methods of analysis for MPAs namely; transmission-line, cavity, and full-wave (methods of moments). In this thesis, the transmission-line method is used as it gives good physical insight and is easy to model. Figure 3.1 shows the electric fields of a basic rectangular MPA.

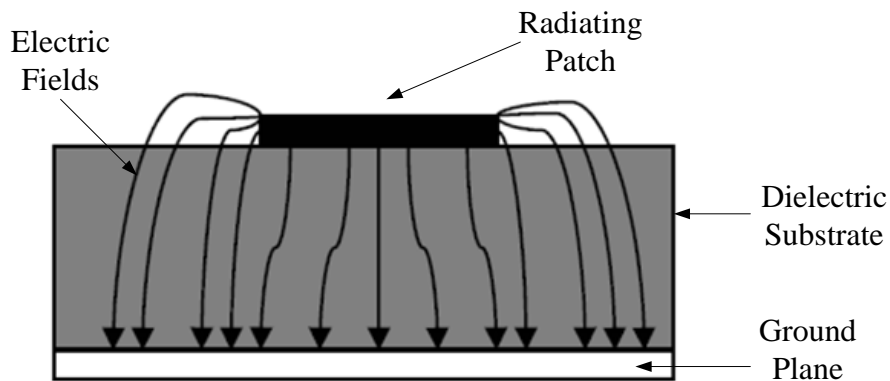


Figure 3.1: MPA Electric Field Lines

The transmission-line method is the most commonly used method in the design of rectangular MPAs. The steps followed in the design of rectangular MPAs as discussed in [7] [8] [12] [35] are as follows;

Step 1: Calculating the Patch Width (W) – For efficient radiation, the patch width W is given as;

$$W = \frac{c}{2f_r} \sqrt{\frac{2}{\epsilon_r + 1}} \quad (3-1)$$

where, W is the Patch width, c is the speed of light, f_r is the resonant frequency, and ϵ_r is the dielectric constant of the substrate.

Step 2: Calculating the Effective Dielectric Constant (ϵ_{reff}) – As seen in Figure 3.1, most of the electric field lines reside in the substrate and parts of some lines in air. An effective dielectric constant (ϵ_{reff}) must be obtained in order to account for the fringing effect and the wave propagation in the line.

$$\epsilon_{reff} = \frac{\epsilon_r + 1}{2} + \frac{\epsilon_r - 1}{2} \left[1 + 12 \frac{h}{W} \right]^{-\frac{1}{2}} \quad (3-2)$$

where, ϵ_{reff} is the effective dielectric constant and h is the height of the dielectric substrate.

Step 3: Calculating the Effective Length (L_{eff}) – For a given resonance frequency f_r , the effective patch length is given as;

$$L_{eff} = \frac{c}{2f_r \sqrt{\epsilon_{reff}}} \quad (3-3)$$

where, L_{eff} is the effective length.

Step 4: Determining the Length Extension (ΔL) – The fringing fields along the width can be modeled as radiating slots and electrically, the patch of the MPA looks greater than its physical dimensions. The dimensions of the patch along its length have now been extended on each end by a distance ΔL , which is given as;

$$\Delta L = 0.412h \frac{\left(\epsilon_{reff} + 0.3 \right) \left(\frac{W}{h} + 0.264 \right)}{\left(\epsilon_{reff} - 0.258 \right) \left(\frac{W}{h} + 0.8 \right)} \quad (3-4)$$

where, ΔL is the patch length extension.

Step 5: Determining the Patch Length (L) – The actual patch length now becomes;

$$L = L_{eff} - 2 \Delta L \quad (3-5)$$

where, L is the actual patch length.

Step 6: Calculating the Bandwidth (BW)

$$BW \% = 3.77 \left(\frac{\epsilon_r - 1}{\epsilon_r^2} \right) \left(\frac{W}{L} \right) \left(\frac{h}{\lambda_o} \right) * 100\% \quad (3-6)$$

where, λ_o is the wavelength in free space.

Step 7: Determining the Feed Co-ordinates – Using coaxial probe-fed technique, the feed points are calculated as;

$$Y_f = W/2 \quad (3-7)$$

$$x_f = \frac{L}{2\sqrt{\epsilon_{reff}}} \quad (3-8)$$

where, Y_f and X_f are the feed co-ordinates along the patch width and length respectively

Step 8: Determining the Plane Ground Dimensions – It has been shown that MPAs produces good results if the size of the ground plane is greater than the patch dimensions by approximately six times the substrate thickness all around the periphery [35] [37].

$$L_g = 6h + L \quad (3-9)$$

$$W_g = 6h + W \quad (3-10)$$

where, L_g and W_g are the plane ground dimensions along the patch length and width respectively

3.3. Application of ANFIS in the design of a Rectangular Microstrip Patch Antenna

As discussed in Chapter 2, ANFIS uses a set of data for training of its network. There are two types of data generators (measurements and simulations) for antenna applications. The selection of a data generator depends on the application and the availability of the data generator. In this work, the ANFIS model shown in Figure 3.2 with the inputs

substrate height (h), resonant frequency (f_r), and dielectric constant (ϵ_r) and the outputs patch width (W_t), patch length (L_t), and the feed point along the width and length (Y_f, X_f) respectively, illustrates how parameters used in the design of rectangular MPA are optimized to achieve a goal of improved antenna gain.

The ANFIS can simulate and analyze the mapping relation between the input and output data through a learning algorithm so as to optimize the parameters used in design of MPAs.

The data presented to ANFIS for training (estimating) membership function parameters should be fully representative of the features of the data that the trained FIS is intended to model. To ensure that the data sets are representative, the testing data sets are also included in the system. The training and testing data sets used in this work have been obtained from both simulations and previous experimental works which are documented in various refereed journals [2] [9] [13] [31] [33] [35].

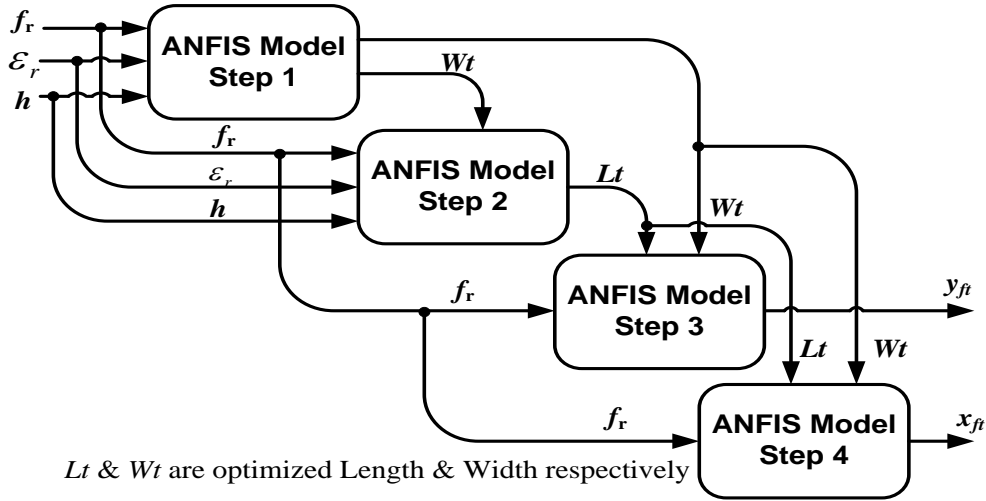


Figure 3.2: ANFIS Model for Design of Rectangular MPA

3.4. ANFIS Design Procedure

Figure 3.3 is an optimization design procedure followed in this work. Using MATLAB®, a program was developed comprising of the design formulas illustrated in Eq. 3-1 to Eq. 3-10. This program (Appendix A-1) was then used to generate the data sets for training of ANFIS. Here, all the formulas used in designing of basic rectangular MPA were put into consideration. The program allows for computer human interaction as it allows the user to input specific resonant frequency, substrate height, and dielectric constant of a specific material under consideration. The generated data comprising of design parameters were saved to be used in optimizing the patch dimensions data at a later stage. In the second step, a program containing test data sets available in literature from the previous experimental works published in several sources ([2] [9] [10] [13] [26] [31] [33] [35] [36]) was developed as shown in Appendix A-2. These test data sets are arranged in a matrix format depending on the number of parameters to be used in the optimization procedure. Another MATLAB® program with the ANFIS model for optimizing parameters was developed as shown in Appendix A-3. In this program, the membership function type and number is specified beforehand together with the number of epochs for training. The optimization using ANFIS can be illustrated in a flowchart in Figure 3.3 where the output can be achieved once the specified number of epochs is achieved or the error becomes zero.

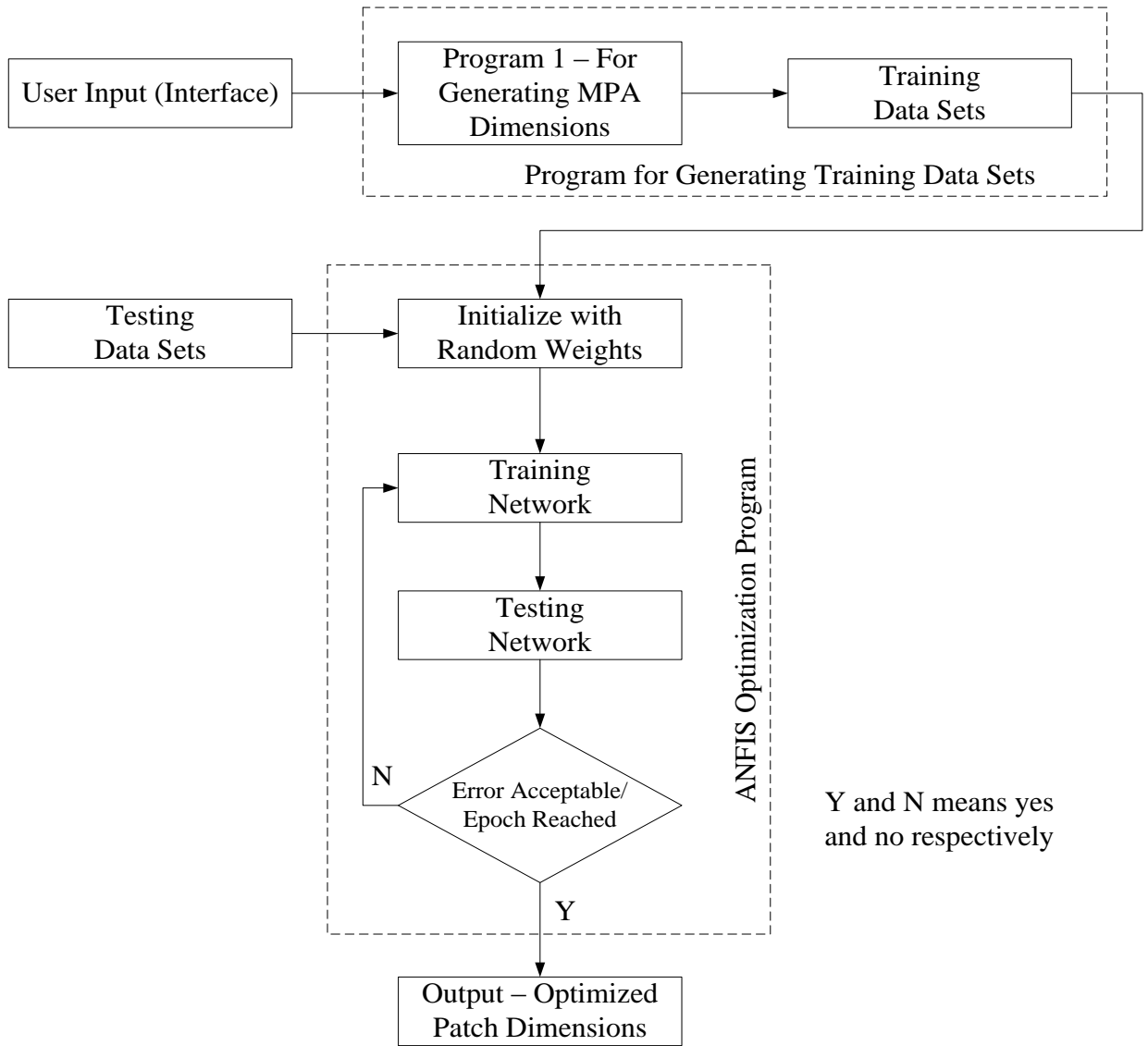


Figure 3.3: Flowchart for Optimization of Rectangular MPA

As illustrated in Figure 3.2, the ANFIS model contains four stages. In the first stage, resonant frequency, dielectric constant, and substrate height are used in optimizing the patch width (W) of the antenna. 90 data sets were used for training while 18 data sets were used as test data sets as shown in Appendix B-1. The MFs for the input variables f_r , ϵ_r , and h , are 4, 3, and 3 respectively. The number of rules is then 36 ($4 \times 3 \times 3$) and the number

of epochs specified as 700. In the second stage, the antenna patch length (L) is optimized. The three input variables used in first stage are maintained with the addition of the optimized patch width (W_t) as an input variable, therefore, variables f_r , ϵ_r , h , and W_t are used as inputs with L as the output variable to be optimized. 90 training and 16 testing data sets shown in Appendix B-2 were used in this stage. The MFs for the input variables f_r , ϵ_r , h , and W_t are 4, 2, 2, and 4 respectively thus, the number of rules is 64 ($4 \times 2 \times 2 \times 4$) with the number of epochs specified as 700. The third stage in the ANFIS model is used for optimizing the feed point (Y_f) along the patch width. In this stage, the number of epochs is specified as 600 with 90 training data sets and 15 testing data sets (Appendix B-3) used. The variables f_r , W_t , and L_t are used as inputs with the MFs as 3, 4, and 4 respectively. This gives the number of rules as 48 ($3 \times 4 \times 4$). Finally, the input variables f_r , W_t , and L_t are used in optimizing the feed point X_f along the path length of the antenna. With 90 training data sets and 15 testing data (Appendix B-3) used, the number of iterations was specified as 600. The input variables f_r , W_t , and L_t were each allocate the MFs values as 3, 4, and 4 respectively, making the number of rules as 48 ($3 \times 4 \times 4$).

Figure 3.3 shows the procedure of generating the optimized parametric data. These data are based on optimizing the antenna gain which is explained in the next chapter.

After running the above mentioned MATLAB[®] program and the optimized parameter values noted down (see Appendix C), commercial antenna design software was then used to design an antenna and the parameter values noted down. Finally, the two pairs of rectangular microstrip patch antennas were fabricated based on the results.

CHAPTER FOUR

4.0. RESULTS AND DISCUSSIONS

The simulation results that were obtained by using Antenna Magus software (a product of Magus (Pty) Ltd) to validate the performance of the proposed ANFIS model for design of rectangular microstrip patch antennas is presented. Two sets of antennas (one set based on ANFIS model and the other Antenna Magus software results respectively) were fabricated in the lab and their performance characteristics experimentally measured and analyzed. Two sets of rectangular MPAs were fabricate so as to compare the results based on the design method (ANFIS and Antenna Magus Simulations).

4.1. ANFIS Simulation Results

As illustrated in Figure 3.2, ANFIS model used in this work has four stages. In each stage, optimization is carried out as per the specified number of epochs. Using the Eq. 3-1 to 3-10, training data sets were generated. Testing data sets were also collected (from refereed journals and simulations as indicated in Chapter 3) and the overall ANFIS design model formulated. Since ANFIS model is singleton (has one output), four similar design stages were formulated. Finally, in order to view the rectangular MPA characteristic based on the optimized parameters, Ansoft HFSS (High Frequency Structure Simulator) software was fed with the optimized results.

In every microstrip patch antenna design, the resonant frequency and substrate material type used are crucial in determining other physical parameters. Figure 4.1 illustrates the first stage indicating the number of variables used.

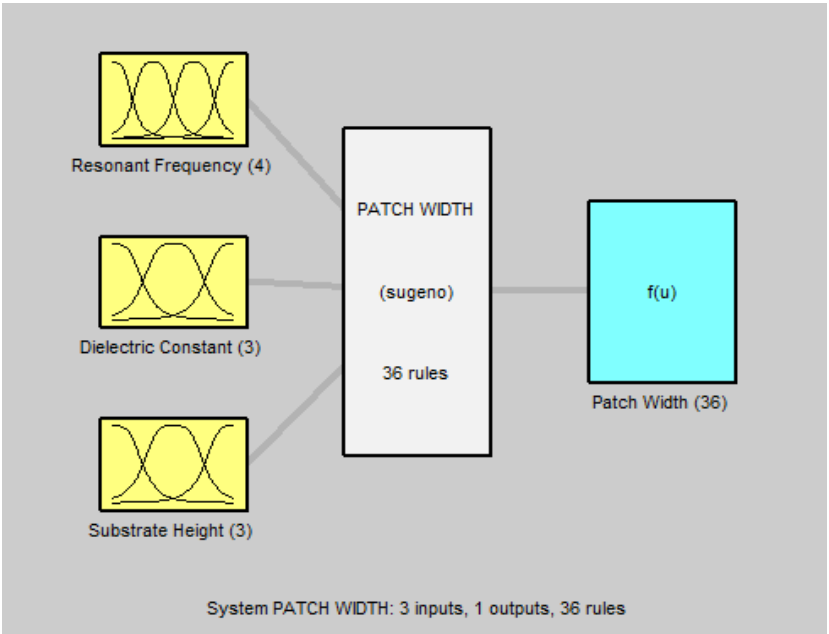


Figure 4.1: First Stage of ANFIS Model

As illustrated earlier, the membership values were specified such that the total number of rules was 36. At the end of the training, the root mean square error (RMSE) was 0.5180 at epoch number 700. The optimized patch width was then used in optimization in the next stage.

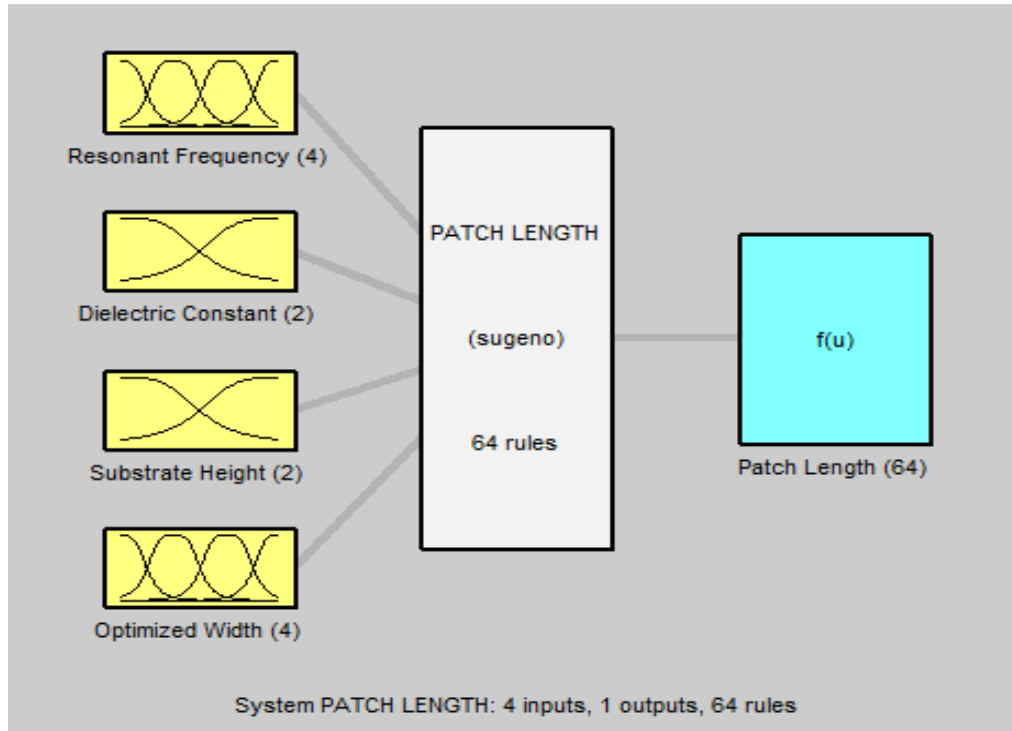


Figure 4.2: Second Stage of ANFIS Model

The second stage of ANFIS model produced an optimized patch length. With four variable (shown in Figure 4.2) specified as inputs, optimization was carried out resulting in an RMSE error of 0.0052. Figure 4.3 shows how the input and output variables were arranged in the third stage.

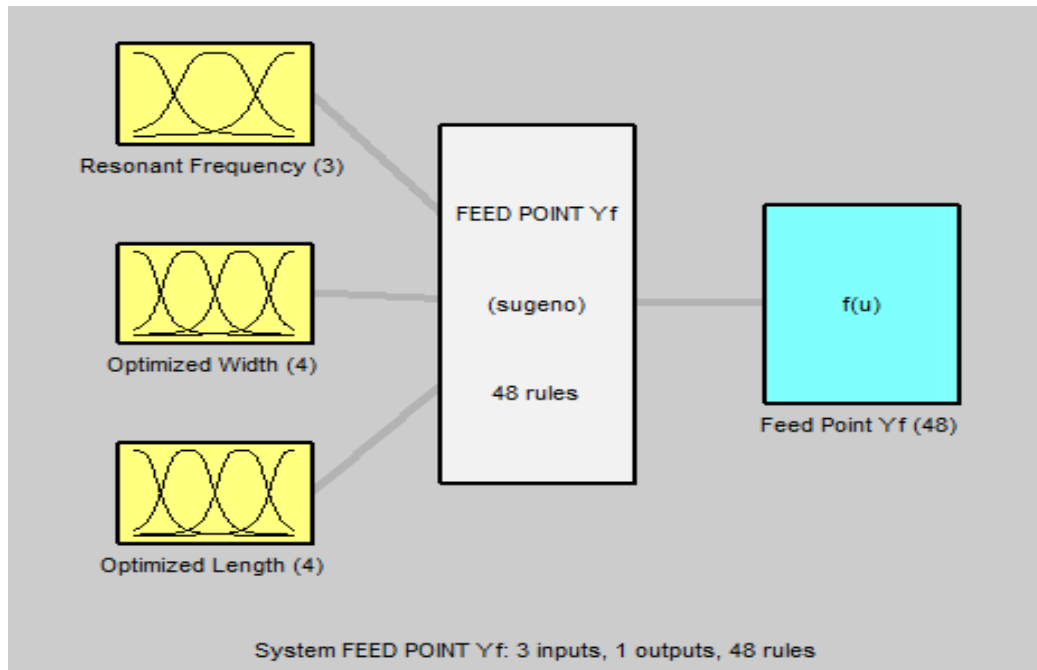


Figure 4.3: Third Stage of ANFIS Model

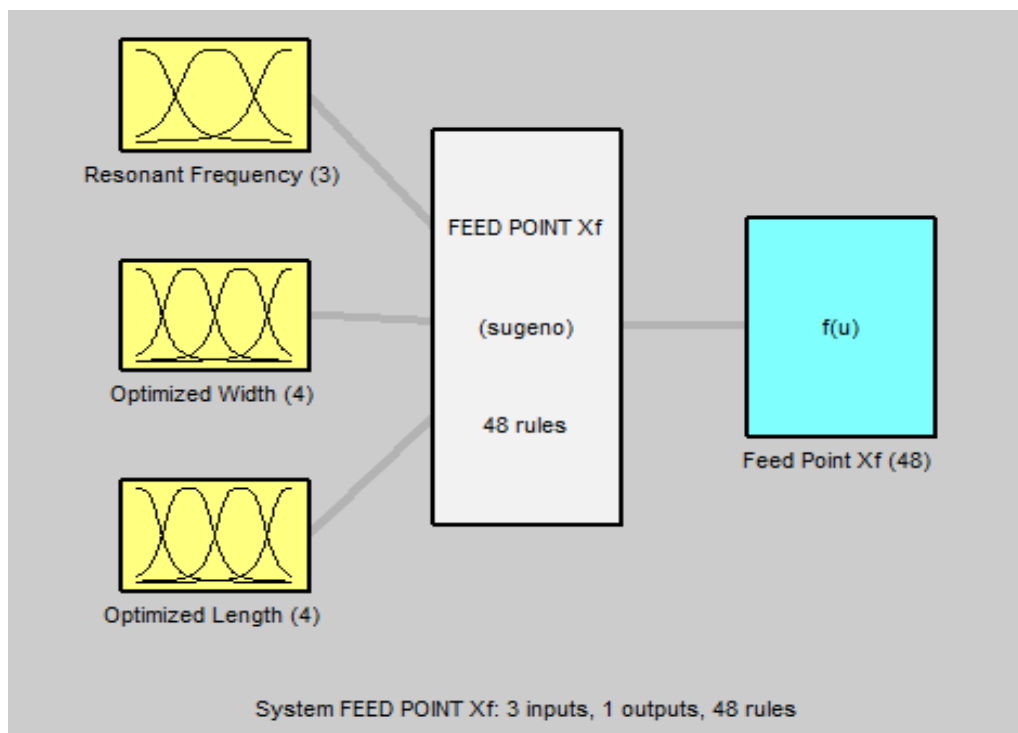


Figure 4.4: Fourth Stage of ANFIS Model

Figure 4.3 and Figure 4.4 shows how the variables used in optimization of feed point along the patch width and length were carried out respectively.

With the emphasis on FR4 Glass-Epoxy substrate (with dielectric constant of 4.35 and substrate height of 1.6mm) operating at 2GHz, various substrates (FR4 Glass-Epoxy, Duroid 5880, DiClad880, Silicon, and Alumina substrates) were used in determining the best possible parametric values for rectangular microstrip patch antenna. Figure 4.5 to 4.8 plots various optimized parameters with relation to resonant frequency. As mentioned earlier, the program allows for human interaction therefore, in this work, quartz substrate material with dielectric constant of 3.8 and substrate thickness of 1.5mm was used for testing purposes and labeled as input in subsequent figures. Quartz substrate was chosen as its dielectric constant value falls on the lower side of the dielectric constant value range of 2.2 to 12, and also the lower the dielectric constant the higher the antenna gain and bandwidth. [37].

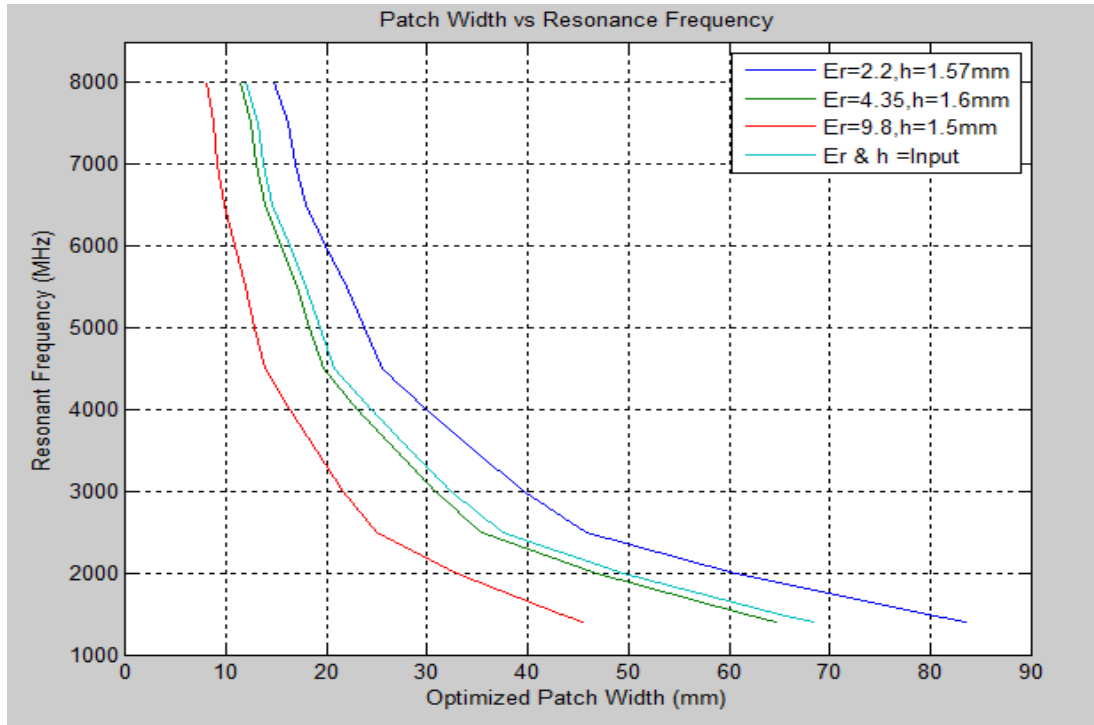


Figure 4.5: ANFIS Optimized Patch Width vs Resonant Frequency

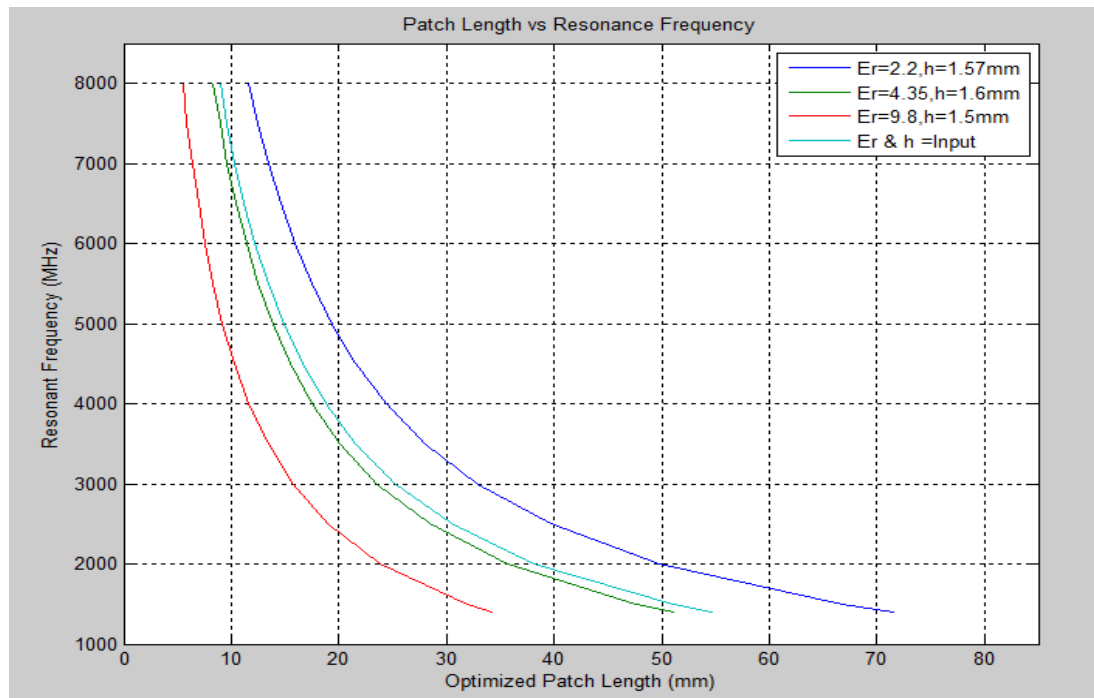


Figure 4.6: ANFIS Optimized Patch Length vs Resonant Frequency

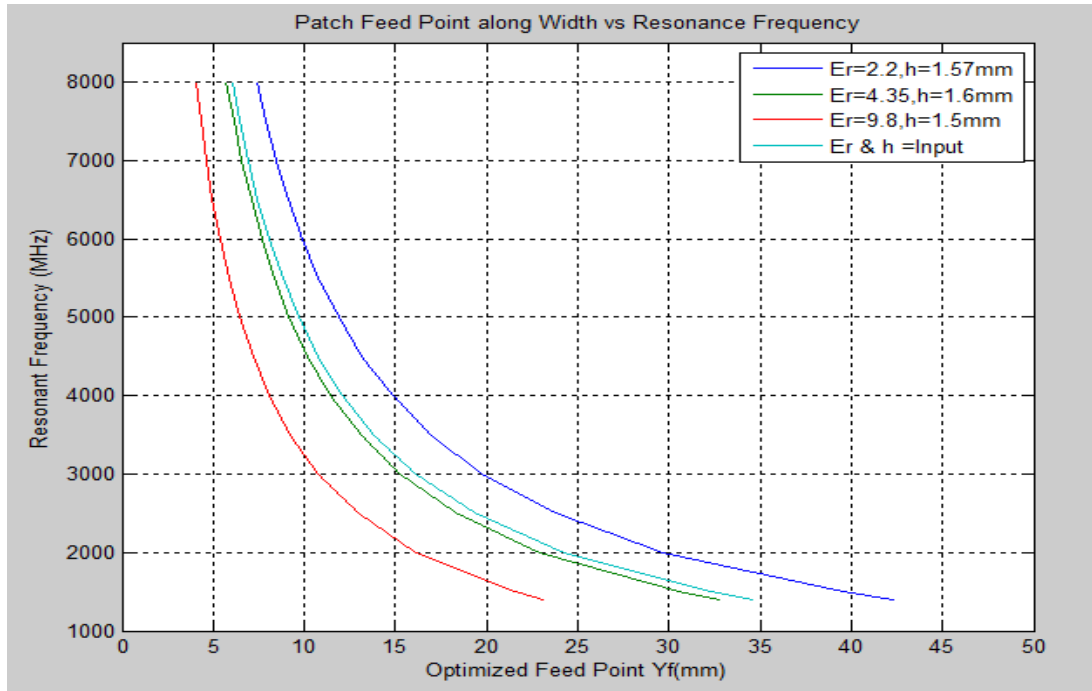


Figure 4.7: ANFIS Optimized Feed Point along Patch Width vs Resonant Frequency

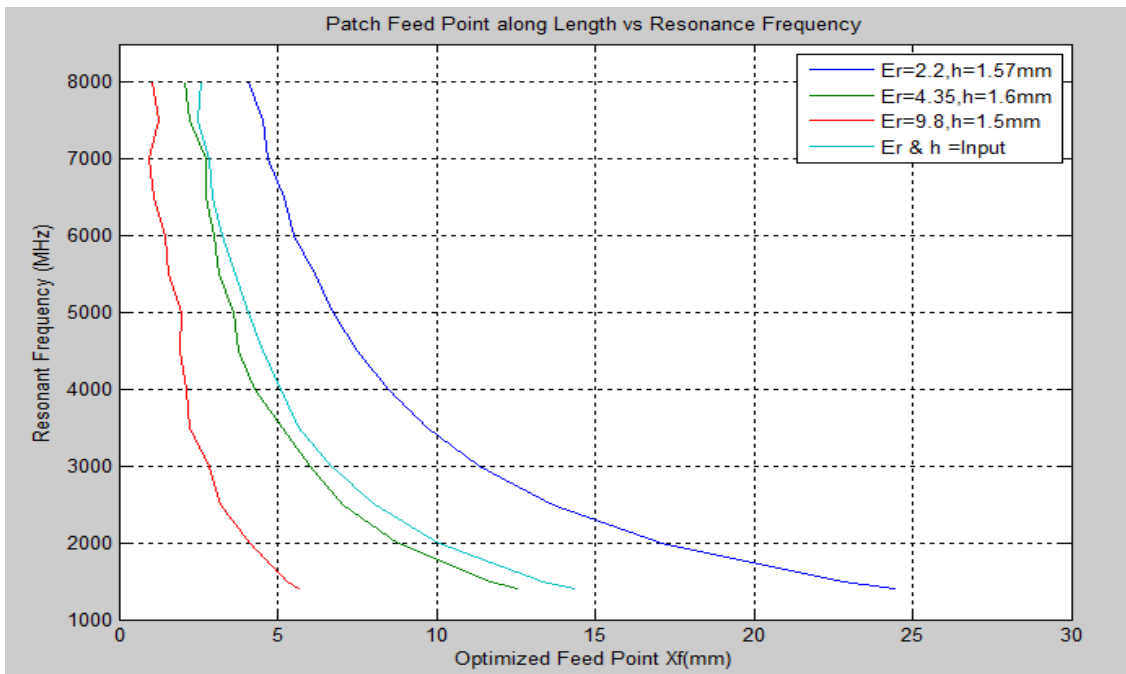


Figure 4.8: ANFIS Optimized Feed Point along Patch Length vs Resonant Frequency

As depicted in Figure 4.5 to Figure 4.8, the patch dimensions vary as per the type of substrate material used in relation to resonant frequency. To plot the above rectangular MPA optimized parameters, the substrates Duroid 5880 with dielectric constant of 2.2 and substrate thickness of 1.57mm, FR4 Glass-Epoxy with substrate thickness of 1.6mm and dielectric constant of 4.35, aluminum with dielectric constant of 9.8 and substrate thickness of 1.5mm, and quartz with dielectric constant of 3.8 and substrate thickness of 1.5mm were used. Also, it can be seen that the higher the resonant frequency the smaller the patch antenna therefore, it is not practical to use this type of an antenna for operational frequencies above 6GHz because the fabrication process for relatively small sized antennas is quite difficult and its power handling capability is greatly reduced.

Table 4.1: Summary of ANFIS Model Variables

ANFIS Stage	Output Variable	Input Variables	RMSE Prediction
1	W_t	f_r, ϵ_r, h	0.5180
2	L_t	f_r, ϵ_r, h, W_t	0.0052
3	Y_{ft}	f_r, W_t, L_t	0.0194
4	X_{ft}	f_r, W_t, L_t	0.1770

Table 4.1 shows a summary of some of the specified design parameters and the output RMSE. The error goal was set at default 0 with the initial step size set at 0.04 and the decrease and increase step size learning rate set at 0.9 and 1.1 respectively. Due to the specification of the Antenna Trainer Kit used for testing the MPA, the rectangular MPA was designed with the operating frequency of 2GHz. Table 4.2 shows the ANFIS

optimized MPA design parameters which were used in fabricating the antenna. This data is extracted from the results table on Appendix C, row 18. As indicated earlier, FR4 Glass-Epoxy substrate material was used due to its availability.

Table 4.2: ANFIS Optimized Patch Antenna Design Parameters

f_r	2 GHz	W_t	46.818mm	X_{ft}	8.819mm
ϵ_r	4.35	L_t	35.631mm	W_g	55.456mm
h	1.6mm	Y_{ft}	22.927mm	L_g	45.241mm

To check the ANFIS designed patch antenna characteristics, the optimized parameters namely; patch width, patch length, and feed point were fed onto HFSS simulation tool. The resonant frequency was specified as 2GHz.

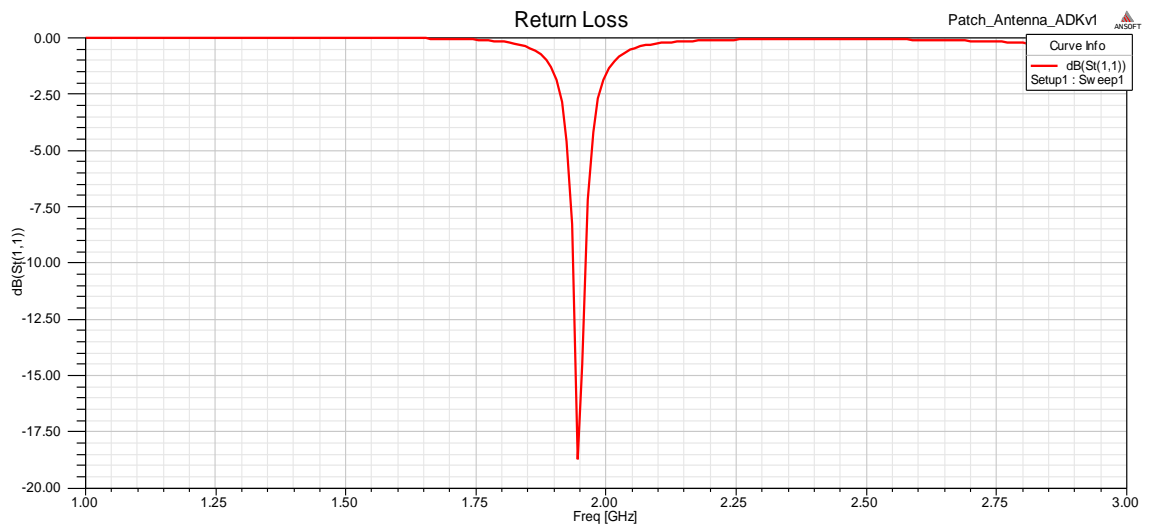


Figure 4.9: Return Loss of Rectangular MPA

As illustrated in Chapter 2, a return loss of 0dB is unwanted as it signifies a reflection of all incident power. From Figure 4.9, it can be seen that the return loss is lowest at about 1.96GHz. An antenna resonating at a frequency of 2.0GHz returned losses of about -2.25dB. A slight impedance mismatch in the MPA produced the lowest return loss at 1.96GHz as compared to the designed resonating frequency of 2GHz, but still lie on the safe antenna resonating frequency of $\pm 5\%$. Figure 4.10 shows the gain of the designed antenna as generated by Ansoft HFSS. The highest gain point is in the z-direction with the gain of about 6.5dB operating at 2GHz.

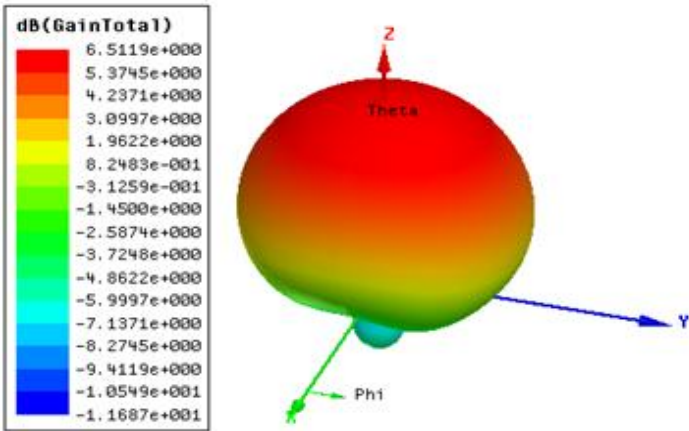


Figure 4.10: Gain of Rectangular MPA (3D Graphical)

4.2. Antenna Magus Software Simulation Results

The software used to simulate the rectangular MPA and validate the ANFIS model is Antenna Magus software. Antenna Magus is a full-wave electromagnetic simulator that

is widely used in conjunction with FEKO software and used in the design of patch antennas, wire antennas, and other RF/wireless antennas.

On specifying the frequency of 2GHz, substrate height of 1.6mm, and dielectric constant of 4.35, simulation was carried out to establish the antenna parameters and characteristics for a FR4 substrate. Table 4.3 shows the antenna parameters values as simulated on Antenna Magus.

Table 4.3: Simulated Patch Antenna Design Parameters

f_r	2 GHz	W	45.825mm	X_f	12.749mm
ϵ_r	4.35	L	35.243mm	W_g	91.649mm
h	1.6mm	Y_f	22.913mm	L_g	70.486mm

On comparison between Table 4.2 and 4.3, a significant difference was noted on the values of X_f , W_g , and L_g . This can be attributed to the type of formulas Antenna Magus software is based on and the ANFIS model design procedure followed. A significant difference in patch width, length, and feed point will affect the antenna performance, but a variation in ground plane (W_g and L_g) should not affect the antenna performance so long as the minimum ground plane is larger than six times the substrate height plus the corresponding patch dimension as shown in Eq. 3-9 and 3-10. In Table 4.2, the transmission-line method was used in the design procedure, while a full-wave electromagnetic simulator Antenna Magus software was used to simulate the results in Table 4.3.

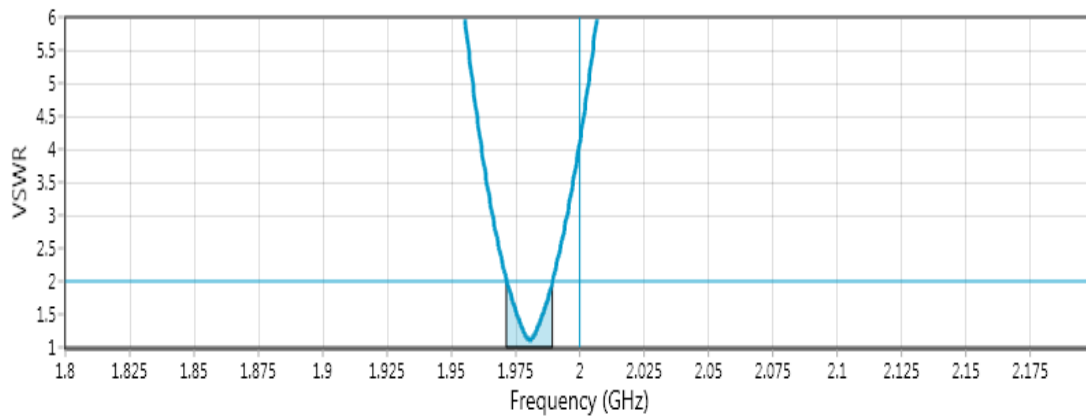


Figure 4.11: VSWR of Rectangular Microstrip Patch Antenna at 2GHz

As discussed in the literature review, the value of VSWR should always be less than 2 for proper operation of MPA. As shown in Figure 4.11 from Antenna Magus software simulation, this MPA functions well within the frequency range of approximately 1.971GHz and 1.989GHz where the VSWR is less than 2. VSWR is minimum (1.107) at a frequency of 1.98GHz. From Figure 4.11, VSWR at exactly 2GHz is about 4, and therefore, a significant transmitted power loss. This loss can be greatly attributed to the impedance mismatch. Applying Eq. 2.2 and a VSWR of 4, yields a return loss of 4.44dB. On comparison between -2.5dB return loss from Figure 4.9 and 4.44dB from Figure 4.11, it can be seen that the later has higher return losses that the former.

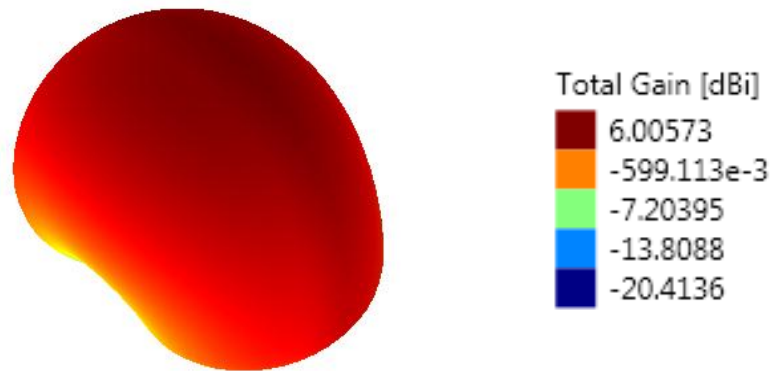


Figure 4.12: Gain of Rectangular MPA at 2GHz (3D Graphical Plot)

Figure 4.12 show the gain of a rectangular MPA as simulate on Antenna Magus software. The gain is maximum (about 6dB) at a frequency of about 2.04GHz. From Figure 4.10, the gain was found to be around 6.5dB on simulating the ANFIS parametric values on Ansoft HFSS software. Similarly, Antenna Magus simulated software was used to validate the ANFIS results and the results (antenna gain) shown in Figure 4.12.

4.3. Validation of ANFIS Model

4.3.1. Validation using Simulated Results

ANFIS, implemented in MATLAB[®] is a powerful design tool that can be customized to solve various problems. In this thesis, ANFIS model results were validated with both the theoretical results and simulation results using Antenna Magus software. With the emphasis on the FR4 Glass-Epoxy substrate, the theoretical values were determined using Eq. 3.1 to Eq. 3.10. Also, simulation was carried out for a frequency range of 1.4GHz to

6GHz. The theoretical (labelled as training data sets in Appendix B) and simulated results were used for validation since a significant difference in the position of feed point was noted.

Table 4.4 shows the comparison between theoretical, Antenna Magus simulated data, and ANFIS model simulated data operating at 2GHz.

Table 4.4: Comparison of ANFIS Model, Antenna Magus Software, and Theoretical Results

Antenna Parameters	ANFIS Model	Antenna Magus	Theoretical (From Equations)
W (mm)	46.818	45.825	45.856
L (mm)	35.631	35.243	35.641
Y_f (mm)	22.927	22.913	22.928
X_f (mm)	8.819	12.749	8.821

To compare the antenna characteristics for both the ANFIS model and Antenna Magus simulated data, their respective simulated data were fed onto the same platform Ansoft HFSS Software and their return loss and gain graphs plotted as in Figure 4.13 and 4.14 respectively. On Figure 4.13, the red line represents the return loss from Antenna Magus Data while the blue line represents the return loss from ANFIS model data.

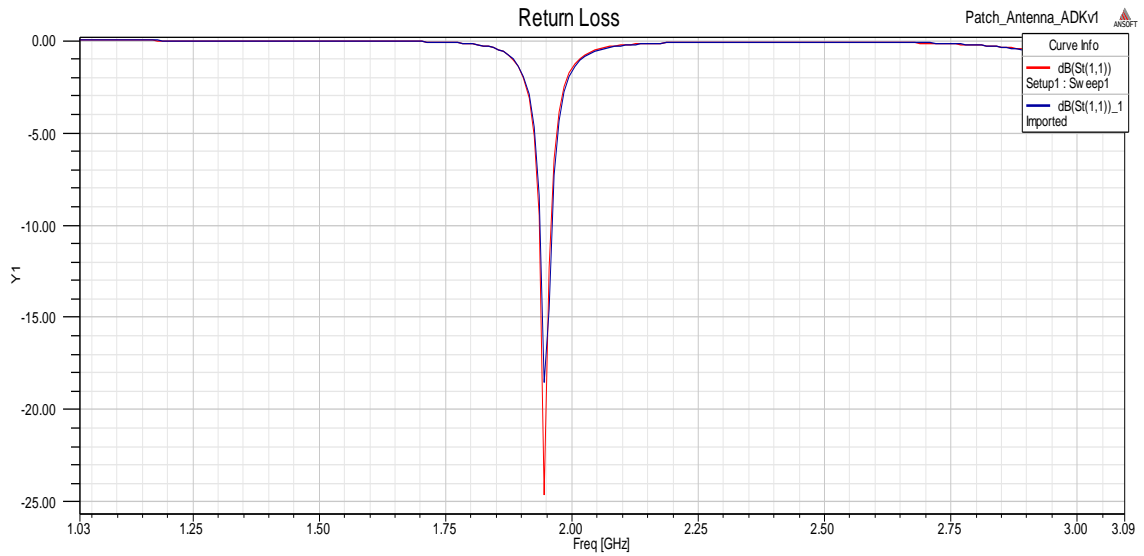


Figure 4.13: Return Loss of Rectangular MPA (From ANFIS Data)

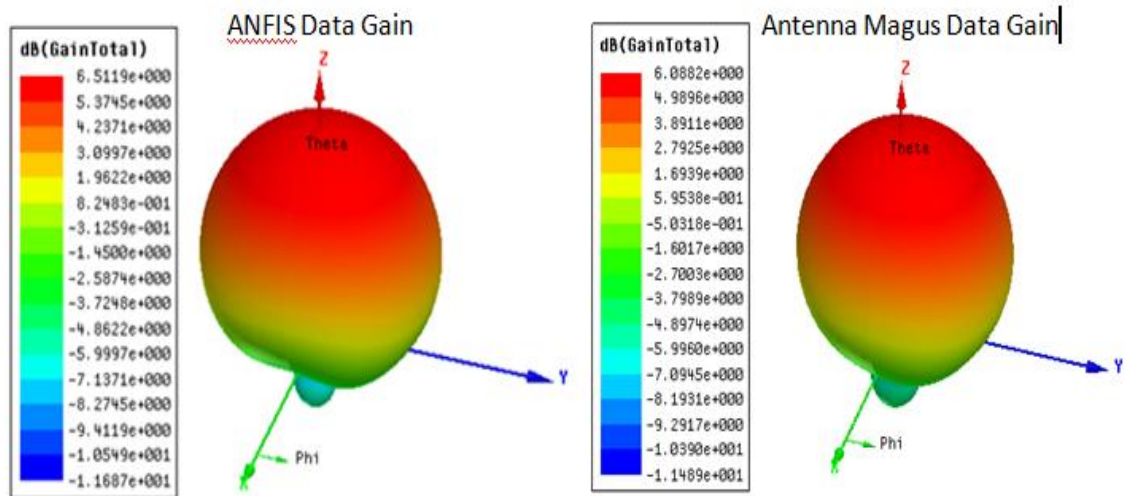


Figure 4.14: Rectangular MPA Gain (for ANFIS and Antenna Magus Data Respectively)

From Figure 4.13, and 4.14, a comparison can be made of data results from both the ANFIS and Antenna Magus simulations as plotted on the Ansoft HFSS software. The ANFIS simulated data produced an improved gain as compared to the Antenna Magus

simulated data. This improvement can be attributed to the optimized antenna parameters especially the feed point along the patch length.

Table 4.4 can be presented in form of figures as shown in Figure 4.15 to 4.18 with antenna parameters plotted against resonance frequency.

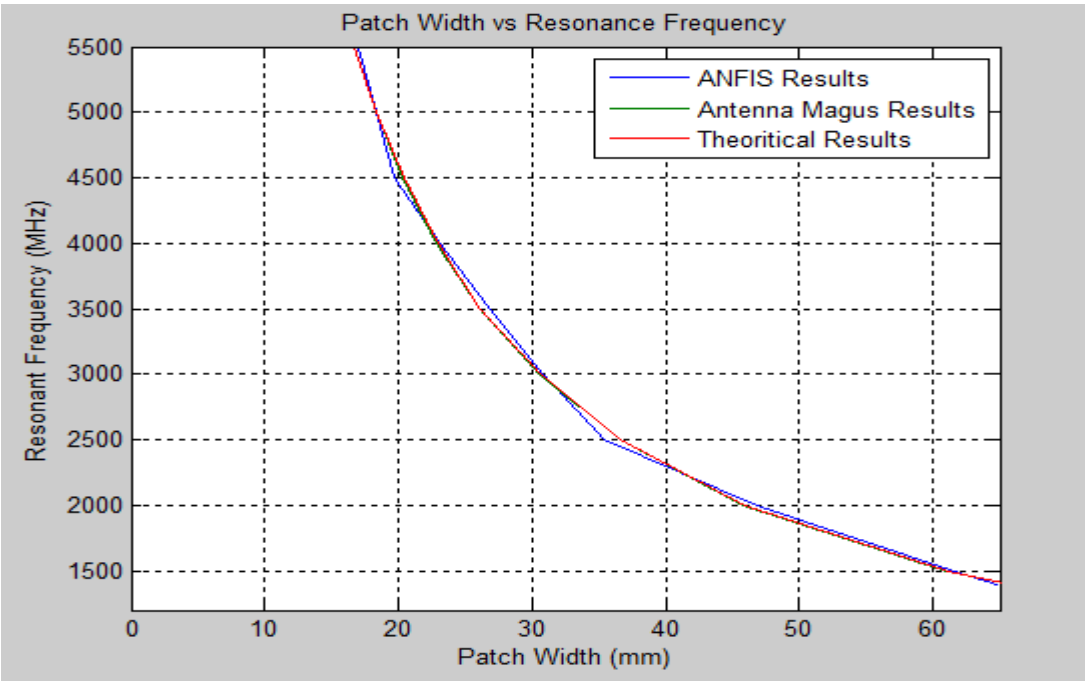


Figure 4.15: Patch Width Results Comparison

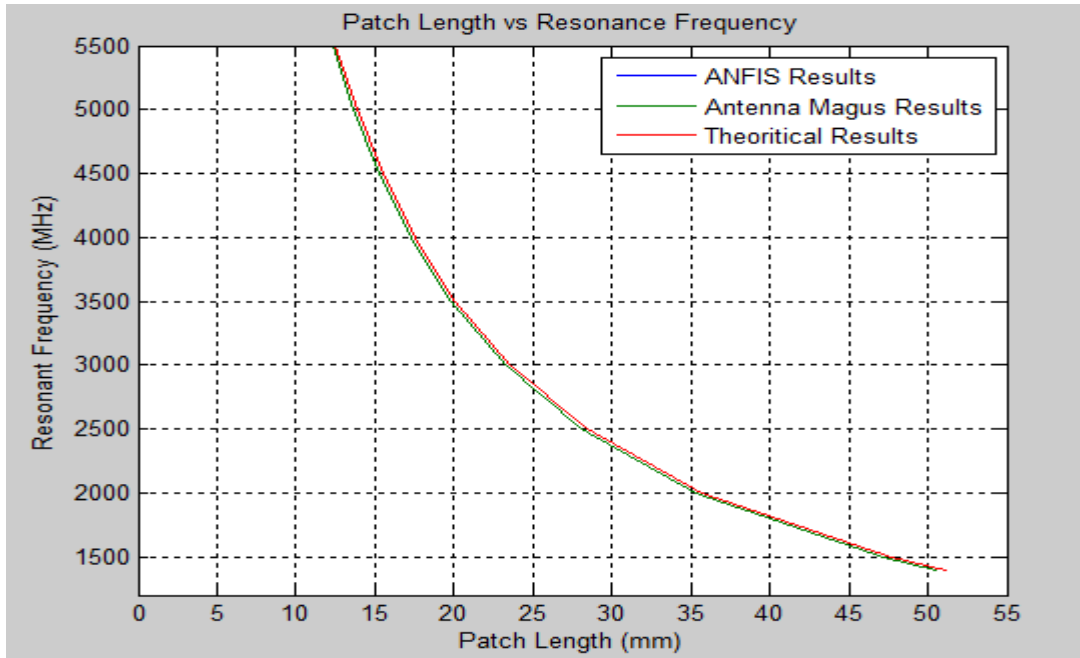


Figure 4.16: Patch Length Results Comparison

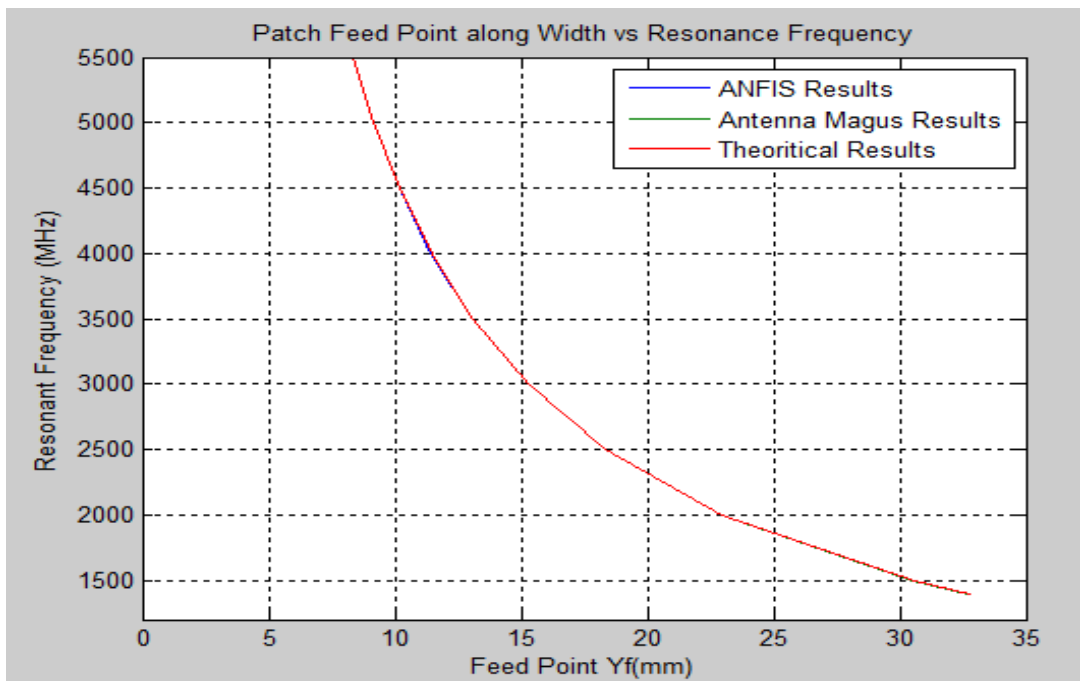


Figure 4.17: Feed Point along Patch Width Results Comparison

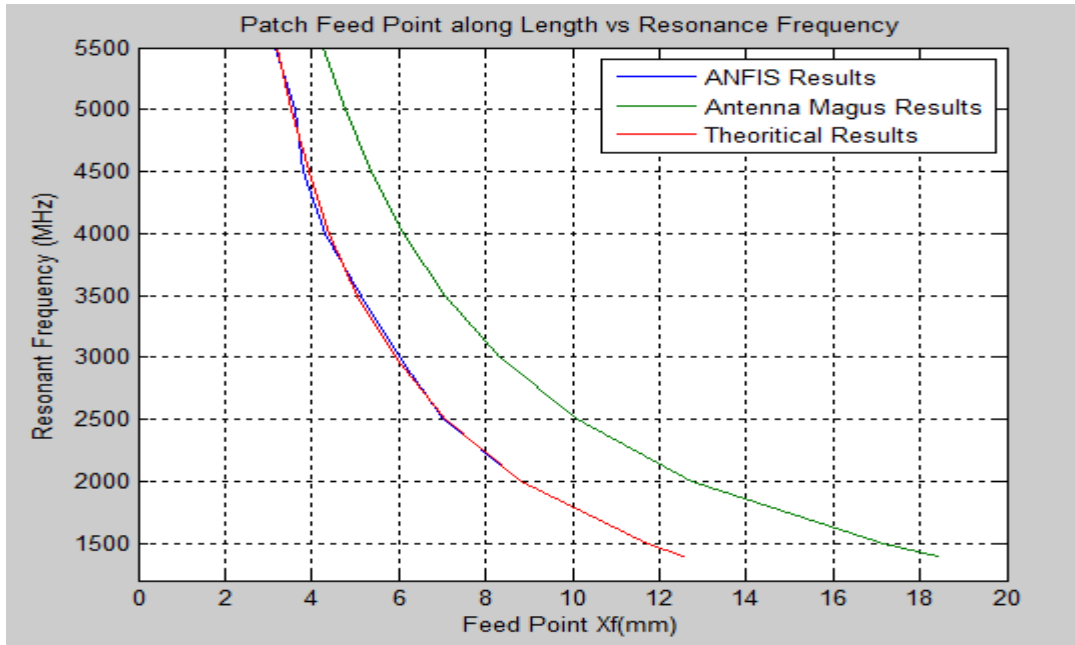


Figure 4.18: Feed Point along Patch Length Results Comparison

From Figure 4.15 to 4.18, it can be seen that the error difference between the results produced by the proposed ANFIS model, Antenna Magus software, and theoretical is minimal. Table 4.5 show the error difference at 2GHz

Table 4.5: Error Difference - Design Results

Antenna Parameters	ANFIS Model	Antenna Magus	Theoretical (From Equations)	Error Difference	
				Antenna Magus (%)	Theoretical (%)
W (mm)	46.818	45.825	45.856	2.121	2.06
L (mm)	35.631	35.243	35.641	1.089	-0.03
Y _f (mm)	22.927	22.913	22.928	0.061	0
X _f (mm)	8.819	12.749	8.821	-44.56	0.02

Figure 4.19 to 4.22 shows the error results plotted against a range of operational frequencies. The ANFIS results are taken as reference point.

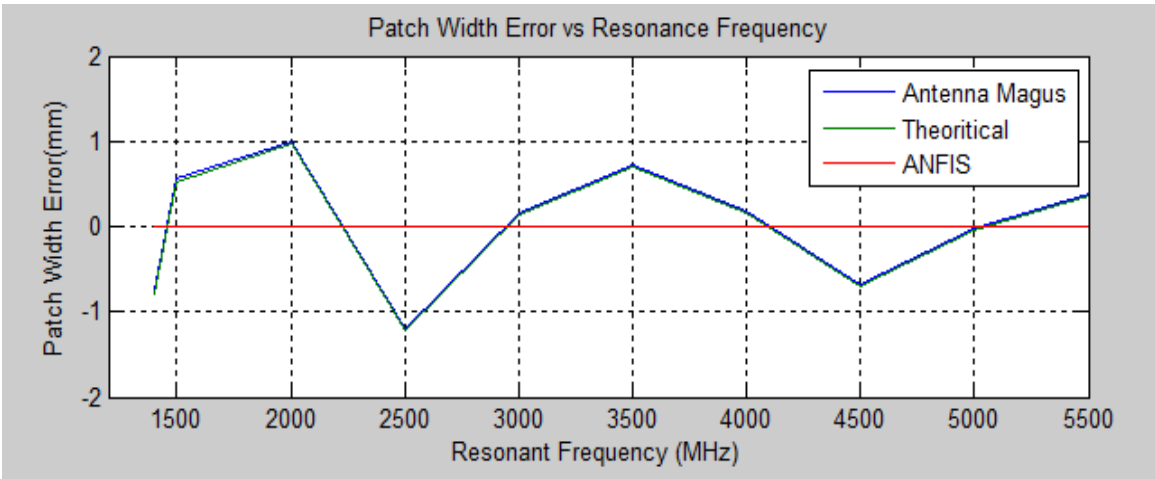


Figure 4.19: Patch Width Error vs. Resonance Frequency

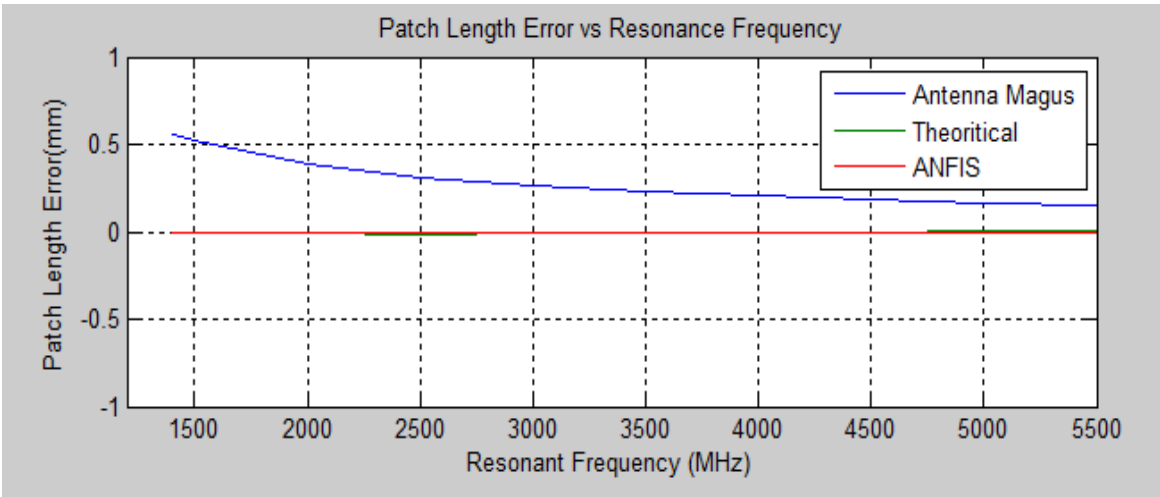


Figure 4.20: Patch Length Error vs. Resonance Frequency

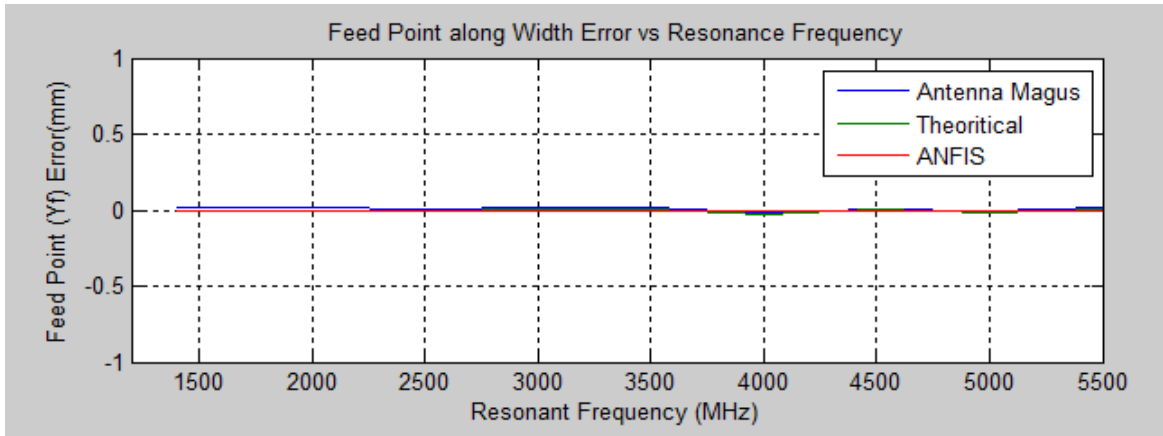


Figure 4.21: Feed Point along Patch Width Error vs. Resonance Frequency

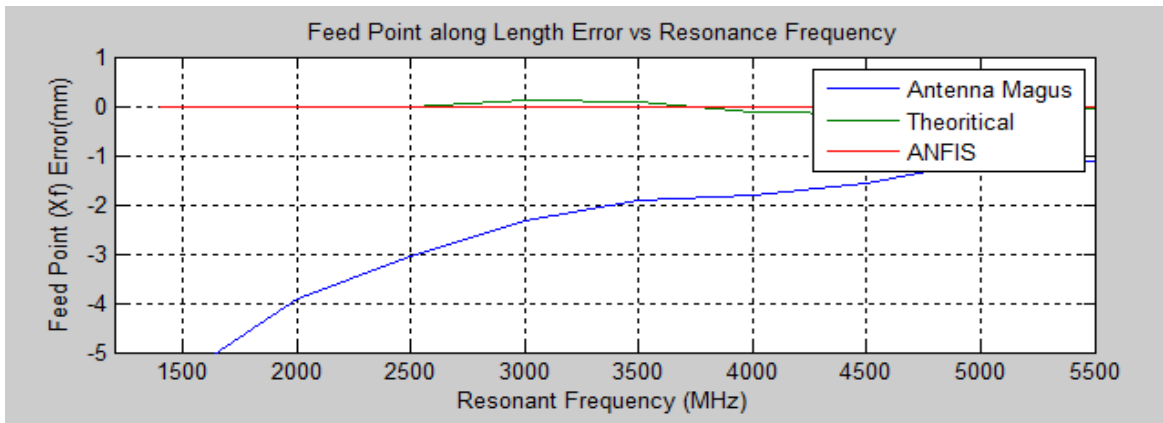


Figure 4.22: Feed Point along Patch Length Error vs. Resonance Frequency

The simulations were carried out on the same computer so as to be able to monitor the time taken by each software to complete the respective simulations. Running an ANFIS simulation on MAL^TAB[®] took approximately 6 minutes. On the other hand, simulation using Ansoft HFSS software took approximately 28 minutes to complete the modeling. It can therefore, be seen that simulating antenna using Ansoft HFSS takes a longer time as compared to ANFIS simulation. A complete computer usage time profile summary is shown in Appendix D.

4.2.2. Experimental Results

Practical implementation of the simulated data was carried out so as to validate the ANFIS model. Figure 4.23 shows a block diagram of the experimental setup used in testing the patch antenna. Figure 4.24 and 4.25 shows fabricated antenna and practical setup of patch antennas in the laboratory respectively.

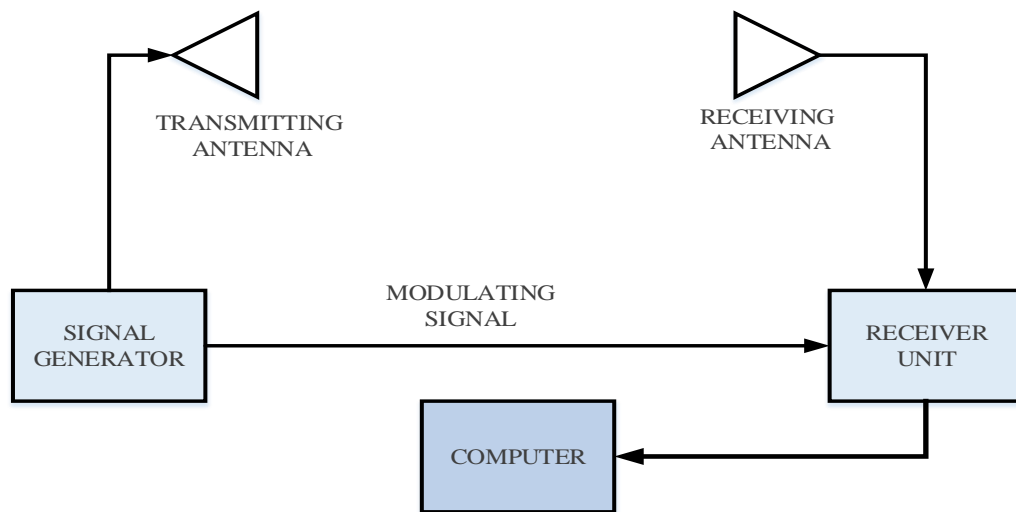


Figure 4.23: Block Diagram of Experiment Setup

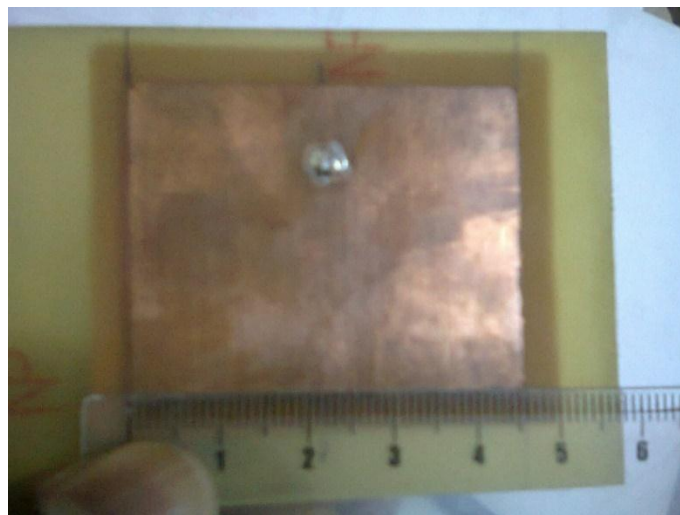


Figure 4.24: Fabricated Rectangular MPA

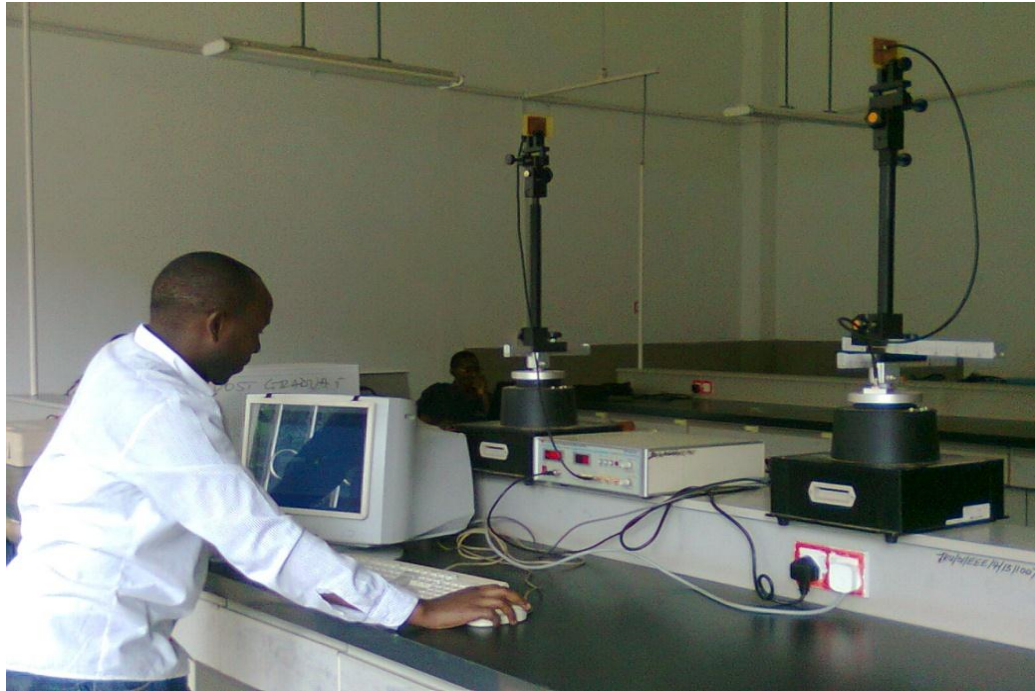


Figure 4.25: Experimentation Setup

ED-3200 Antenna Trainer Kit was used in practically testing the performance of microstrip patch antenna in their far field. Antenna kit enables tests at frequencies of 500MHz, 2GHz, and 10GHz. As shown in Figure 4.25, two sets of patch antennas were tested and mapped together. The first patch (patch1) was fabricated based on Antenna Magus simulated data while the second patch (patch 2) was fabricated based on ANFIS simulated data as seen in Figure 4.26. The antenna trainer kit signal generator connects both the transmitter and receiver units as seen in Figure 4.23. It provides transmission signal to the transmitter and a modulating signal to the receiver. The receiver unit then rotates in a clockwise direction through a 360° angle. This rotation allows plotting of a radiation pattern as seen in Figure 4.26.

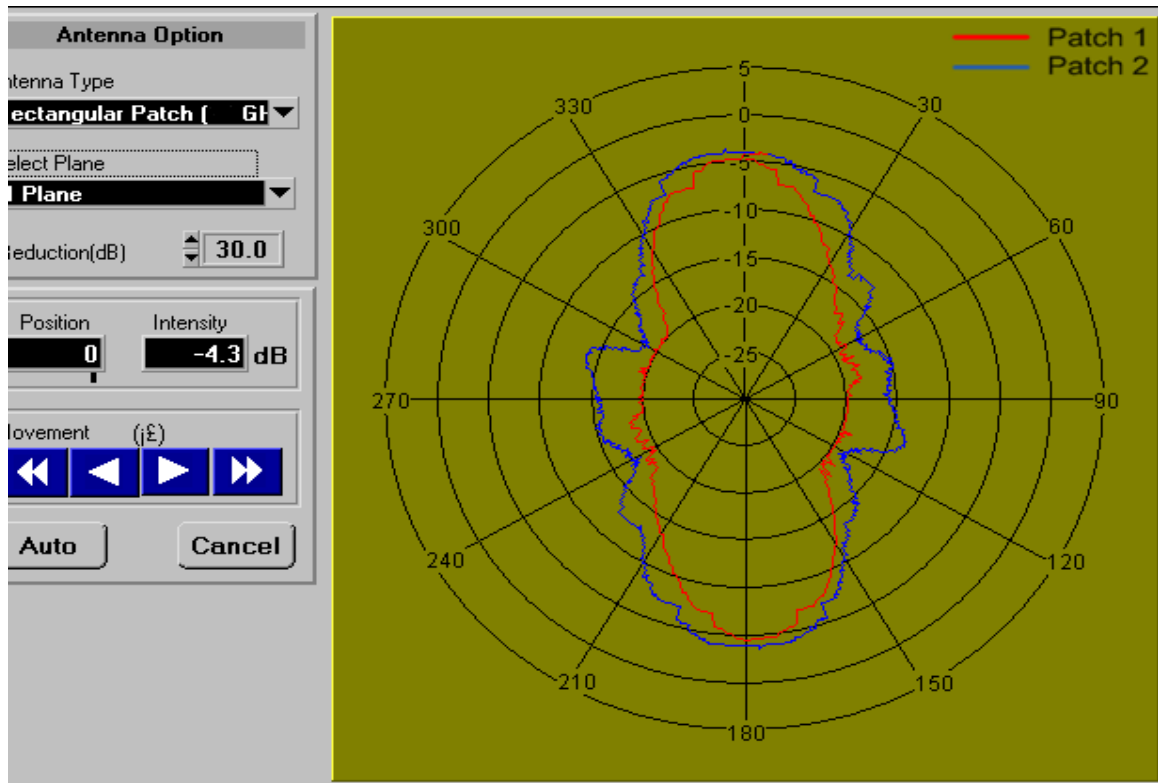


Figure 4.26: Rectangular MPA Radiation Pattern

Figure 4.26 shows the E-Plane electric field radiation pattern indicating the radiation intensity in dB. It was observed that ANFIS model produced slightly improved radiation intensity of -0.2dB with the radiation intensity of -4.1dB as compared to results from Antenna Magus simulated practical data which had a radiation intensity of -4.3dB. This shows that based on validation with Antenna Magus software, ANFIS can be effectively used to design MPAs. From the experimental set up, it was noted that the gain was lower than the expected. This is because the set up was carried out in an open area (laboratory), thus, other external factors (including reflections) affected the strength of signal. Also, soldering the coaxial cable onto the antenna might have led to emission of spurious radiation by the antenna.

CHAPTER FIVE

5.0. CONCLUSION AND RECOMMENDATION

5.1. Conclusion

In this thesis, a rectangular microstrip patch antenna has been successfully designed using adaptive neuro-fuzzy inference optimization technique. The microstrip antenna designed is completely planar in nature and does not have any cross-layered structures as have been proposed elsewhere for bandwidth, gain, and radiation efficiency enhancement. The proposed antenna was designed to operate at $2.0 \pm 5\%$ GHz.

From the simulation results, it was observed that the formulated ANFIS model produces results which are in agreement with simulated data from Antenna Magus software. The main parameters that influence the antenna design are the dielectric constant of the dielectric substrate, the feed location, patch length, and patch width.

A comparison of the ANFIS model simulation with the Antenna Magus simulation and the theoretical results shows that there is a minimal difference of about 3% in the patch dimensions with ANFIS model producing an improved simulated gain. Simulating an antenna using HFSS took a significant time (about twenty eight minutes) with incidences of memory overload. These simulations were carried out on a computer with a processor of 2.2GHz core2duo and RAM of 2GB. Simulation using ANFIS took a significantly less time (6 minutes) as compared to HFSS (28 minutes) thus has the advantage of less computer time and memory usage. This demonstrates that ANFIS being fast and accurate

design methodology can be used to effectively design MPAs with complex structures and other related work.

The overall performance of the prototype and the design goals were achieved. It was also, observed that ANFIS can work hand in hand with another antenna design software so as to plot various antenna characteristics.

5.2. Recommendation

The optimization routine of an antenna by ANFIS has a primary goal of minimizing the design error as well as maximizing the antenna gain. Future work could focus on further improving the ANFIS design methodology by formulating it to display various antenna radiation characteristics.

When using commercial antenna design softwares to design antennas, convergence may prove to be a challenge in the absence of a powerful central processing unit when simulating structures with multiple layers. ANFIS can be used to aid in this design by formulating a model that incorporates various types of multilayered antennas since ANFIS model implemented in MATLAB[®] platform takes less computer memory and time to optimize antenna parameters.

In this thesis, the rectangular patch antenna with only one specific band of frequencies was considered. Patch antennas with multiband Frequencies can be designed using ANFIS simulations.

REFERENCES

- [1]. W. Stuart, "Fundamentals of Electromagnetics with Engineering Applications", John Wiley & Sons, NJ, USA, pp. 442-445, 2005
- [2]. K. Guney and N. Sarikaya, "Adaptive neuro-fuzzy inference system for computing the resonant frequency of circular microstrip antennas", *Aces Journal*, Vol. 19, No. 3, pp. 188-197, November 2004
- [3]. Chang Kai, "RF and Microwave Wireless Systems", John Wiley & Sons, Inc., New York, pp. 90-98, 2000
- [4]. Er Nitin Agarwal, Dr. D.C.Dhubkarya, Er Rinkesh Mittal, "Designing & Testing of Rectangular Micro strip antenna operating at 2.0 GHz using IE3D", *Global Journal of Researches in Engineering*, Vol. 11, No. 1, pp. 44-48, February 2011
- [5]. Deschamps, G.A., "Microstrip Microwave Antennas", 3rd USAF Sysmp. Antennas, University of Illinois, Urbana, 1953.
- [6]. Gutton, H., and G. Baussinot, "Flat Aerial for Ultra High Frequencies," French Patent No. 703113, 1955.
- [7]. Sainati, Robert A., "CAD of Microstrip Antennas for Wireless Applications", The Artec House Antenna Library, pp 1-18, January 1996
- [8]. Balanis, Contantine A., "Antenna Theory – Analysis and Design", 2nd Edition, John Wiley & Sons Inc., pp. 722-751, 1997
- [9]. K. Guney, and N. Sarikaya, "Comparison of adaptive-network-based fuzzy inference systems for bandwidth calculation of rectangular microstrip antennas", *Expert Systems with Applications* 36, Elsevier Ltd., pp. 3522–3535, 2009.

- [10]. K. Guney, and N. Sarikaya, "Adaptive Neuro-Fuzzy Inference Systems for Computation of the Bandwidth of Electrically Thin and Thick Rectangular Microstrip Antennas", *Electrical Engineering Journal* 88, ©Springler-Verlag, pp. 201–210, 2006
- [11]. Marine Corps, "Field Antenna Handbook", Navy Department, Headquarters United States Marine Corps Washington, D.C., pp. 48-51, 1999.
- [12]. Dafalla, Z. I., Kuan, W. T. Y., Abdel Rahman, A. M., and Shudakar, S. C.: "Design of a Rectangular Microstrip Patch Antenna at 1 GHz." RF and Microwave Conference, Subang, Selangor, Malaysia, October 2004
- [13]. Mehmet Kara, "Design Considerations for Rectangular Microstrip Antenna Elements with Various Substrate Thicknesses", *Microwave and Optical Technology Letters / Vol. 19, No. 2*, pp. 111-121, October 1998.
- [14]. Saeed, A. Rashid and Khatum, Sabira, "Design of Microstrip Antenna for WLAN", *Journal of Applied Sciences* 5 (1), ©Asian Network for Scientific Information, pp. 47-51, 2005
- [15]. Bratislav Milovanovic, Marija Milijic, Aleksandar Atanaskovic, and Zoran Stankovic, "Modeling of Patch Antennas using Neural Networks", *Telskiks, Serbia and Montenegro*, ©IEEE, 2005
- [16]. Indrasen Singh et al, "Microstrip Patch Antenna and its Applications: a Survey", *Int. J. Comp. Tech. Appl.*, Vol. 2, pp. 1595-1599, 2011

- [17]. Papi, D. G., “An Artificial Intelligence Applications for Architectural Textures Analysis”, The International Archives of the Photogrammetry, Remote Sensing and Spatial Information Sciences, Vol. XXXIV, Part 5/W12, 2003
- [18]. Jang and Gulley, ‘MATLAB Fuzzy Logic Toolbox’, The MathWorks, Inc., pp. 16-41, 84-93, 1997
- [19]. Lofti A. Zadeh, ‘Fuzzy Logic – Computing with Words’, IEEE Transactions on Fuzzy Systems, Vol. 4, No. 2, pp. 103-111, May 1996
- [20]. S. N. Sivanandam, S. Sumathi and S. N. Deepa, “Introduction to Fuzzy Logic using MATLAB”, Springer-Verlag Berlin Heidelberg, pp. 10-127, 2007
- [21]. Ben Krose and Patric Van Der Smagt, “An Introduction to Neural Networks”, 8th Edition, University of Amsterdam, pp. 1-45, 1996.
- [22]. Kasabov, K. Nikola, “Foundations of Neural Networks, Fuzzy Systems, and Knowledge Engineering”, The MIT Press Cambridge, Massachusetts London, England, pp. 1-19, 167-329, 1998
- [23]. Robert Fuller, “Neural Fuzzy Systems”, Abo Akademi University, ISBN 951-650-624-0, 1995
- [24]. Jang et.al, “Neuro-Fuzzy and Soft Computing”, Prentice Hall Upper Saddle River, pp. 1-42, 197-223, 333-360, 1997
- [25]. Ariffin, Kasuma Bin, “On Neuro-Fuzzy Applications for Automatic Control, Supervision, and Fault Diagnosis for Water Treatment Plant”, A Thesis submitted to the Faculty of Electrical Engineering, Universiti Teknologi, Malaysia, 2007.

- [26]. K. Guney, and N. Sarikaya, "Adaptive Neuro-Fuzzy Inference System for Computing Patch Radius of Circular Microstrip Antennas", *Microwave and Optical Technology Letters*, Vol. 48, No. 8, pp. 1606–1610, Feb. 2007
- [27]. N. Sarikaya, K. Guney, and C. Yildiz, "Adaptive Neuro-Fuzzy Inference System for the Computational of the Characteristic Impedance and the Effective Permittivity of the Micro-Planar Strip Line", Faculty of Engineering, Erciyes University, Kayseri, ©IEEE, 2005
- [28]. Zoltan Himer, et.al, "Control of Combustion Base on Neuro-Fuzzy Model", Systems Engineering Laboratory, University of Oulu, Finland, 2006
- [29]. Jang, Roger, "ANFIS: Adaptive-Network-Based Fuzzy Inference System", *IEEE Transactions on Systems, MAN, and Cybernetics*, Vol. 23, No. 3, pp. 665-685, 1993
- [30]. Kapil Goswami *et.al*, "Design and Analysis of Rectangular Microstrip Antenna with PBG Structure for Enhancement of Bandwidth", *Global Journal of Research Engineering*, Vol. 11, Issue 2, Version 1.0, pp. 22-28, March 2011
- [31]. A. Hameed and B. Khalaf, "Design and Simulation of Broadband Rectangular Microstrip Antenna", *Eng. Tech.*, Vol. 26, No. 1, pp. 93-121, 2008
- [32]. Vivekananda L. Subrahmanya, "Pattern Analysis of Rectangular Microstrip Patch Antenna", A Thesis submitted to the School of Engineering, University College of Boras, Boras, 2009.
- [33]. N. Turker, *et.al*, "Artificial Neural Design of Microstrip Antennas", *Turk J Elec. Engin.*, Vol. 14, No. 3, pp. 445-453, 2006

- [34]. K. Guney, "Simple and Accurate Formulas for the Physical Dimensions of Rectangular Microstrip Antennas with Thin and Thick Substrates", *Microwave and Optical Technology Letters*, Vol. 44, No. 3, pp. 257-259, February 2005
- [35]. A.B. Mutiara, R. Refianti, and Rachmansyah, "Design of Microstrip Antenna for Wireless Communication at 2.4GHz", *Journal of Theoretical and Applied Information Technology*, Vol. 33, No. 2, pp. 184-192, November 2011
- [36]. V.V. Thakare and Singhal, "Analysis of Feed Point Coordinates of a Coaxial Feed Rectangular Microstrip Antenna using Mlpffbp Artificial Neural Network", *ICIT 5th International Conference on Information Technology*, pp. 1-6, 2011
- [37]. Ali Dheyab and Karim Hamad, "Improving Bandwidth of Rectangular Patch Antenna using Different Thickness of Dielectric Substrate", *ARNP Journal of Engineering and Applied Sciences*, Vol. 6, No. 4, pp. 16-21, April 2011
- [38]. John Ojha and Marc Peters, "Microwave and Millimeter Wave Technologies – Modern UWB Antennas and Equipment", In Tech Publishers, Europe, ISBN 978-953-7619-67-1, March 2010.

APPENDICES

APPENDIX A: MATLAB® PROGRAM CODE

APPENDIX A-1: Training Data Sets Generation MATLAB® Program Code

```
function final = antennaparameters

v = 3e8; %Speed of Light (m/s)
c = v; %Speed of Light (m/s)
fo_in = input(' Please enter the Resonant Frequency = ' )
fo = [fo_in (1.5e9:500e6:8e9)]; %Resonant Frequency
Erin = input(' Please enter the Dielectric constant = ' )
hin = input(' Please enter the substrate thickness in Metres = ' )
wavelength = c./fo; %Calculates the Wavelength.
Erd = 2.2; %Dielectric Constant of the Duroid 5880 Substrate
hd = 0.00157; %Height of the Duroid 5880 Substrate in Metres
Erg = 4.35; %Dielectric Constant of the FR4 Glass Epoxy Substrate
hg = 0.0016; %Height of the FR4 Glass Epoxy Substrate in Metres
Eru = 10; %Dielectric Constant of DiClad880 Substrate
hu = 0.0022;%Height of DiClad880 Substrate in Metres
Ers = 11.9; %Dielectric Constant of a Silicon Substrate
hs = 0.0015; %Height of Silicon Substrate in Metres
Era = 9.8; %Dielectric Constant of Alumina Substrate
ha = 0.0015; %Height of Alumina Substrate in Metres

%-----
----

%The Patch Width (W)

    Wd = v./(2.*fo)*sqrt(2/(Erd+1)); %Width of Duroid 5880 Substrate in
(M)
    Wdmm = 1000.*Wd; %Patch Width of Duroid 5880 Substrate in mm

    Wg = v./(2.*fo)*sqrt(2/(Erg+1)); %Width of FR4 Glass Epoxy
Substrate (M)
    Wgmm = 1000.*Wg; %Patch Width of FR4 Glass Epoxy Substrate in
mm

    Wu = v./(2.*fo)*sqrt(2/(Eru+1)); %Patch Width of DiClad880
Substrate (M)
    Wumm = 1000.*Wu; %Patch Width of DiClad880 Substrate in mm
```

```
Ws = v./(2.*fo)*sqrt(2/(Ers+1)); %Patch Width of Silicon Substrate
(M)
```

```
Wsmm = 1000.*Ws; %Patch Width of Silicon Substrate in mm
```

```
Wa = v./(2.*fo)*sqrt(2/(Era+1)); %Patch Width of Alumina Substrate
(M)
```

```
Wamm = 1000.*Wa; %Patch Width of Alumina Substrate in mm
```

```
%-----
----
```

```
%Effective Dielectric Constant (Ereff)
```

```
Ereffd = ((Erd+1)/2)+((Erd-1)/2)*(1./sqrt(1+(hd.*12./Wd)));
%Effective Dielectric Constant (Ereff) of Duroid 5880 Substrate
```

```
Ereffg = ((Erg+1)/2)+((Erg-1)/2)*(1./sqrt(1+(hg.*12./Wg)));
%Effective Dielectric Constant (Ereff) of FR4 Glass Epoxy Substrate
```

```
Ereffu = ((Eru+1)/2)+((Eru-1)/2)*(1./sqrt(1+(hu.*12./Wu)));
%Effective Dielectric Constant (Ereff) of DiClad880 Substrate
```

```
Ereffs = ((Ers+1)/2)+((Ers-1)/2)*(1./sqrt(1+(hs.*12./Ws)));
%Effective Dielectric Constant (Ereff) of Silicon Substrate
```

```
Ereffa = ((Era+1)/2)+((Era-1)/2)*(1./sqrt(1+(ha.*12./Wa)));
%Effective Dielectric Constant (Ereff) of Alumina Substrate
```

```
%-----
----
```

```
%Effective Length (Leff)
```

```
%Calculates the Effective Length for the corresponding Effective
%Dielectric constant in metres respectively.
```

```
Leffd = c./(2.*fo.*sqrt(Ereffd));
```

```
Leffg = c./(2.*fo.*sqrt(Ereffg));
```

```
Leffu = c./(2.*fo.*sqrt(Ereffu));
```

```
Leffs = c./(2.*fo.*sqrt(Ereffs));
```

```
Leffa = c./(2.*fo.*sqrt(Ereffa));
```

```
%-----
----
```

```

%Length Extension (Lextn)

%Calculates the Length Extension in metres respectively

Lextnd = (0.412*hd).*((Ereffd+0.3).*(Wd./hd+0.264))./((Ereffd-...
0.258).*(Wd./hd+0.8));

Lextng = (0.412*hg).*((Ereffg+0.3).*(Wg./hg+0.264))./((Ereffg-...
0.258).*(Wg./hg+0.8));

Lextnu = (0.412*hu).*((Ereffu+0.3).*(Wu./hu+0.264))./((Ereffu-...
0.258).*(Wu./hu+0.8));

Lextns = (0.412*hs).*((Ereffs+0.3).*(Ws./hs+0.264))./((Ereffs-...
0.258).*(Ws./hs+0.8));

Lextna = (0.412*ha).*((Ereffa+0.3).*(Wa./ha+0.264))./((Ereffa-...
0.258).*(Wa./ha+0.8));

```

```

%-----
----

```

```

%Patch Length (L (mm))

Ld = Leffd - 2.*Lextnd;
Ldmm = 1000*Ld; %Patch Length of Duroid 5880 Substrate in mm

Lg = Leffg - 2.*Lextng;
Lgmm = 1000*Lg; %Patch Length in of FR4 Glass Epoxy Substrate
mm

Lu = Leffu - 2.*Lextnu;
Lumm = 1000*Lu; %Patch Length of DiClad880 Substrate in mm

Ls = Leffs - 2.*Lextns;
Lsmm = 1000*Ls; %Patch Length of Silicon Substrate in mm

La = Leffa - 2.*Lextna;
Lamm = 1000*La; %Patch Length of Alumina Substrate in mm

```

```

%-----
----

```

```

%Bandwidth (BW)

BWd = 3.77*((Erd-1)./Erd^2).*(Wd./Ld).*(hd./wavelength);
BWdp = 100.*BWd; %BW of Duroid 5880 Substrate in percentage

```

```

    BWg = 3.77*((Erg-1)./Erg^2).*(Wg./Lg).*(hg./wavelength);
    BWgp = 100.*BWg; %BW of FR4 Glass Epoxy Substrate in
percentage

    BWu = 3.77*((Eru-1)./Eru^2).*(Wu./Lu).*(hu./wavelength);
    BWup = 100.*BWu; %BW of Didad880 Substrate in percentage

    BWs = 3.77*((Ers-1)./Ers^2).*(Ws./Ls).*(hs./wavelength);
    BWsp = 100.*BWs; %BW of Silicon Substrate in percentage

    BWa = 3.77*((Era-1)./Era^2).*(Wa./La).*(ha./wavelength);
    BWap = 100.*BWA; %BW of Alumina Substrate in percentage

```

```

%-----
----

```

```

%Feed Co-ordinates

```

```

%Feed Co-ordinates of Duroid 5880 Substrate

```

```

    Yfd = Wd./2; %Feed point along the Patch Width.
    Yfdmm = 1000.*Yfd; %Feed point along the Patch Width in mm.
    Xfd = Ld./(2.*sqrt(Ereffd)); %Feed Point along the Patch Legth.
    Xfdmm = 1000.*Xfd; %Feed Point along the Patch Legthin mm.

```

```

%Feed Co-ordinates of FR4 Glass Epoxy Substrate

```

```

    Yfg = Wg./2; %Feed point along the Patch Width.
    Yfgmm = 1000.*Yfg; %Feed point along the Patch Width in mm.
    Xfg = Lg./(2.*sqrt(Ereffg)); %Feed Point along the Patch Legth.
    Xfgmm = 1000.*Xfg; %Feed Point along the Patch Legthin mm.

```

```

%Feed Co-ordinates of Didad880 Substrate

```

```

    Yfu = Wu./2; %Feed point along the Patch Width.
    Yfummm = 1000.*Yfu; %Feed point along the Patch Width in mm.
    Xfu = Ld./(2.*sqrt(Ereffu)); %Feed Point along the Patch Legth.
    Xfummm = 1000.*Xfu; %Feed Point along the Patch Legthin mm.

```

```

%Feed Co-ordinates of Silicon Substrate

```

```

    Yfs = Ws./2; %Feed point along the Patch Width.
    Yfsmm = 1000.*Yfs; %Feed point along the Patch Width in mm.
    Xfs = Ls./(2.*sqrt(Ereffs)); %Feed Point along the Patch Legth.
    Xfsmm = 1000.*Xfs; %Feed Point along the Patch Legthin mm.

```

```

%Feed Co-ordinates of Alumina Substrate

```

```

    Yfa = Wa./2; %Feed point along the Patch Width.
    Yfammm = 1000.*Yfa; %Feed point along the Patch Width in mm.
    Xfa = La./(2.*sqrt(Ereffa)); %Feed Point along the Patch Legth.
    Xfammm = 1000.*Xfa; %Feed Point along the Patch Legthin mm.

```

```

%-----
----

```



```

%Plane Ground Dimensions

%Plane Ground Dimensions of Duroid 5880 Substrate
Lgd = 1000*((6*hd)+Ld); %Plane Ground Dimension along the Lenght.
Wgd = 1000*((6*hd)+Wd); %Plane Ground Dimension along the Width.

%Plane Ground Dimensions of FR4 Glass Epoxy Substrate
Lgg = 1000*((6*hg)+Lg); %Plane Ground Dimension along the Lenght.
Wgg = 1000*((6*hg)+Wg); %Plane Ground Dimension along the Width.

%Plane Ground Dimensions of Didad880 Substrate
Lgu = 1000*((6*hu)+Lu); %Plane Ground Dimension along the Lenght.
Wgu = 1000*((6*hu)+Wu); %Plane Ground Dimension along the Width.

%Plane Ground Dimensions of Silicon Substrate
Lgs = 1000*((6*hs)+Ls); %Plane Ground Dimension along the Lenght.
Wgs = 1000*((6*hs)+Ws); %Plane Ground Dimension along the Width.

%Plane Ground Dimensions of Alumina Substrate
Lga = 1000*((6*ha)+La); %Plane Ground Dimension along the Lenght.
Wga = 1000*((6*ha)+Wa); %Plane Ground Dimension along the Width.

%-----
----

%Calculations for the patch material being experimented.
%Specific input figures are got from an interactive Matlab
workspace.

Win = v./(2*fo).*sqrt(2/(Erin+1)); %Patch Width in Metres
Winmm = 1000*Win; %Patch Width of Substrate material (mm)

Ereffin = ((Erin+1)/2)+((Erin-
1)/2)*(1./sqrt(1+(hin.*12./Win)));
%Effective Dielectric Constant (Ereff)

Leffin = c./(2.*fo.*sqrt(Ereffin)); %Effective Length
Lextnin = (0.412*hin).*((Ereffin+0.3).*(Win./hin+...
0.264))./(Ereffin-0.258).*(Win./hin+0.8));
%Calculates the Length Extension in metres respectively

Lin = Leffin - 2.*Lextnin;
Linmm = 1000*Lin; %Patch Length in mm

BWin = 3.77*((Erin-
1)./Erin^2).*(Win./Lin).*(hin./wavelenght));
BWinp = 100.*BWin; %BW of in percentage

WLdin = c./(fo.*sqrt(Erin));%Wavelength of Dielectric Substrate

```

```

    haWLdin = (hin./WLdin).*1000;

    %Feed Co-ordinates of a Substrate
    Yfin = Win./2; %Feed point along the Patch Width.
    Yfinmm = 1000.*Yfin; %Feed point along the Patch Width in mm.
    Xfin = Lin./(2.*sqrt(Ereffin)); %Feed Point along the Patch
Legth.
    Xfinmm = 1000.*Xfin; %Feed Point along the Patch Legthin mm.

    %Plane Ground Dimensions of a Substrate
    Lgin = 1000*((6*hin)+Lin); %Plane Ground Dimension along the
Lenght
    Wgin = 1000*((6*hin)+Win); %Plane Ground Dimension along the
Width.

%-----
----

%Arranging the Dielectric Constants of various materials and their
%respective Substrate Dielectric Heights into columns.
    n = ones(1,15);
    z1 = Erd*n;
    z2 = Erg*n;
    z3 = Eru*n;
    z4 = Ers*n;
    z5 = Era*n;
    zin = Erin*n;

    y1 = hd*n*1000;
    y2 = hg*n*1000;
    y3 = hu*n*1000;
    y4 = hs*n*1000;
    y5 = ha*n*1000;
    yin = hin*n*1000;

%-----
----

%Converting the Resonant Frequency to MHz

    fo2 = fo./1e6;

%-----
----

%The simulation results are then re-arranged to be used as data set in
%ANFIS training as follows;

%First, the columns to be used for optimization are arranged as per the
%columns as follows where,
%Column 1 - Resonant Frequency, Column 2 - Dielectric Constants, Column
3 -

```

%Dielectric Substrate Heights, Column 4 - Patch Width, Column 5 - Patch
 %Length, Column 6a - Feed Point along the Patch Width, Column 6b - Feed
 %Point along the Patch Length.

```

trncolumn1 = [fo2';fo2';fo2';fo2';fo2';fo2'];
trncolumn2 = [z1';z2';z3';z4';z5';zin'];
trncolumn3 = [y1';y2';y3';y4';y5';yin'];
    trnset1 = [trncolumn1 trncolumn2 trncolumn3];
        save trnset1

trncolumn4 = [Wdmm';Wgmm';Wumm';Wsmm';Wamm';Winmm'];
        save trncolumn4

trncolumn5 = [Ldmm';Lgmm';Lumm';Lsmm';Lamm';Linmm'];
        save trncolumn5

trncolumn6a = [Yfdmm';Yfgmm';Yfummm';Yfsmm';Yfamm';Yfinmm'];
        save trncolumn6a

trncolumn6b = [Xfdmm';Xfgmm';Xfummm';Xfsmm';Xfamm';Xfinmm'];
        save trncolumn6b

Lgall = [Lgd';Lgg';Lgu';Lgs';Lga';Lgin'];
Wgall = [Wgd';Wgg';Wgu';Wgs';Wga';Wgin'];
BWall = [BWdp';BWgp';BWup';BWsp';BWap';BWinp'];

final = [trnset1 trncolumn4 trncolumn5 trncolumn6a trncolumn6b...
        Lgall Wgall BWall];
        save final
end

```

APPENDIX A-2: Testing Data Sets MATLAB® Program Code

%In this page, the testing/checking data used in ANFIS optimization is
%listed below;

```
%-----
----
%First, the data used in the first phase comprising of Frequency,
%Dielectric Constant, Height of Substrate and Patch Width are listed as
%shown below
%-----
----
```

%	Frequency	Er	Height	Width
%	GHz		(mm)	(mm)
chkcolumn1 =	[2310	2.33	3.175	57;...
	4805	2.33	1.57	18.1;...
	8000	3.78	1.7	12.13;...
	2000	4.3	1.6	46.07;...
	3000	10	2.2	21.32;...
	5600	2.33	0.254	20.76;...
	5820	2.55	4.76	10.00;...
	3200	2.55	12.81	10.30;...
	3580	2.55	9.52	12.56;...
	2200	2.5	1.524	68.58;...
	5100	2.55	4.76	13.75;...
	1500	11.9	1.5	39.375;...
	2000	4.3	1.6	46.072;...
	3500	2.45	0.483	32.631;...
	3500	9.8	1.5	18.443;...
	5000	11.9	1.5	11.813;...
	7500	4.3	1.5	12.286;...
	5060	2.33	1.57	17.2];

save chkcolumn1

```
%-----
----
%Secondly, the data used in the second phase comprising of Frequency,
%Dielectric Constant, Height of Substrate and Patch Width, and Patch
%Length are listed as shown below
%-----
----
```

%	Frequency	Er	Height	Width	Length
%	GHz		(mm)	(mm)	(mm)
chkcolumn2 =	[2310	2.33	3.175	57	38.00;...
	4805	2.33	1.57	18.1	19.60;...
	8000	3.78	1.7	12.13	6.885;...
	5600	10.20	1.27	10.00	9.10;...

```

5820      2.55      4.76      10.00      15.20;...
3200      2.55      12.81     10.30      33.80;...
3580      2.55      9.52      12.56      27.56;...
2200      2.5      1.524     68.58      41.40;...
5100      2.55      4.76      13.75      15.80;...
1500      11.9     1.5       39.375     28.925;...
2000      4.3       1.6       46.072     35.846;...
3500      2.45     0.483     32.631     27.206;...
3500      9.8      1.5       18.443     13.409;...
5000      11.9     1.5       11.813     8.317;...
7500      4.3      1.5       12.286     9.046;...
5060      2.33     1.57      17.2       18.60];

```

```
save chkcolumn2
```

```

%-----
----
%Also, the data used in the third phase comprising of Frequency,
%Dielectric Constant, Height of Substrate and Patch Width, Patch
Length,
%and Feed Point (Yf) along the Patch Width are listed as shown below
%-----
----

```

```

%      Frequency      Width      Length      Feed Point
%      GHz            (mm)      (mm)      Yf (mm)
chkcolumn3 = [2440    29.22    24.33    16.56;...
              1700    34.12    23.66    22.71;...
              8000    12.13    6.885    2.40;...
              2000    30.22    23.60    17.36;...
              1910    30.45    24.11    18.575;...
              2400    62.04    46.23    20.0;...
              2450    37.86    29.66    7.52;...
              1912    31.1     22.80    0.0;...
              2290    29.77    22.10    22.635;...
              1500    11.9     1.5     19.688;...
              2000    4.3      1.6     23.036;...
              3500    2.45     0.483   16.315;...
              3500    9.8      1.5     9.221;...
              5000    11.9     1.5     5.906;...
              7500    4.3      1.5     6.143];

```

```
save chkcolumn3
```

```

%-----
----
%Finally, the data used in the fourth phase comprising of Frequency,
%Dielectric Constant, Height of Substrate and Patch Width, Patch
Length,
%and Feed Point (Xf) along the Patch Length are listed as shown below
%-----
----

```

```

%           Frequency      Width      Length      Feed Point
%           GHz           (mm)      (mm)        Xf (mm)
chkcolumn4 = [2440      29.22     24.33      17.115;...
              1700      34.12     23.66      15.38;...
              8000      12.13     6.885      6.065;...
              2000      30.22     23.60      14.05;...
              1910      30.45     24.11      21.305;...
              2400      62.04     46.23      11.0 ;...
              2450      37.86     29.66      18.78;...
              1912      31.1      22.80      4.0;...
              2290      29.77     22.10      17.5;...
              1500      11.9      1.5        4.368;...
              2000      4.3       1.6        8.921;...
              3500      2.45     0.483      9.069;...
              3500      9.8       1.5        2.296;...
              5000      11.9     1.5        1.323;...
              7500      4.3       1.5        2.351];
save chkcolumn4

```

APPENDIX A-3: ANFIS MATLAB® Program Code

This program aims at optimizing the parameters used in the design of a rectangular microstrip patch antenna by using adaptive neuro-fuzzy inference system technique.

```
clear all
run antennaparameters
run antennachkdata

%-----
----
%On the First Phase, the Patch Width is optimized based on three
parameters
%(Resonant Frequency, Dielectric Constant, & Substrate Height) as
follows;

                'OPTIMIZATION OF ANTENNA PATCH WIDTH USING ANFIS'
%-----
----
%This loads both the training and checking data used by ANFIS.

load trnset1.mat
load trncolumn4.mat
load chkcolumn1.mat
load final.mat

%-----
----

trnData1 = [trnset1 trncolumn4];
chkData1 = chkcolumn1;

numMFs = [4 3 3];
mfType = 'gbellmf';
fismat = genfis1(trnData1,numMFs,mfType);

        showfis(fismat)
        showrule(fismat)
        ruleview(fismat)
        ruleedit(fismat)

fismat = setfis(fismat, 'name','PATCH WIDTH');
fismat = setfis(fismat, 'input',1,'name','Resonant Frequency');
fismat = setfis(fismat, 'input',2,'name','Dielectric
Constant');
fismat = setfis(fismat, 'input',3,'name','Substrate Height');
fismat = setfis(fismat, 'output',1,'name','Patch Width');
```

```

        figure (1);
        plotfis(fismat);

        figure (2);
    for input_index=1:3,
        subplot(2,2,input_index)
        [x,y]=plotmf(fismat,'input',input_index)
        ;
        plot(x,y)
        axis([-inf inf 0 1.2]);
        xlabel(['Input ' int2str(input_index)]);
        title('Initial Membership Values')
    end

        numEpochs = 700;

        [fismat1,trnErr,ssl,fismat2,chkErr] = anfis(trnData1,fismat,...
            [numEpochs 0 0.04 0.9 1.1],NaN,chkData1,1);

        trnOut = evalfis([trnData1(:,1) trnData1(:,2)
            trnData1(:,3)],fismat1);
        trnRMSE1 = norm(trnOut - trnData1(:,4))/sqrt(length(trnOut));

        epoch = 1:numEpochs;

        figure (3);
        plot(epoch,trnErr,'o',epoch,chkErr,'x')
        hold on;
        plot(epoch,[trnErr chkErr]);
        hold off

        trndW = evalfis([trnData1(:,1) trnData1(:,2)
            trnData1(:,3)],fismat1);

        ' Please Press ENTER Key to Continue'
        pause

        %-----
        ----
        %On Second Phase, the Patch Length is optimized based on four
        parameters
        %(Resonant Frequency, Dielectric Constant, Optimized Width, & Substrate
        %Height) as follows;

        'OPTIMIZATION OF ANTENNA PATCH LENGTH USING ANFIS'
        %-----
        ----

        load trncolumn5.mat
        load chkcolumn2.mat

```



```

%-----
-----

trnData2 = [trnset1 trndW trncolumn5];
chkData2 = chkcolumn2;

numMFs = [4 2 2 4];
mfType = 'gbellmf';
fismat_2 = genfis1(trnData2,numMFs,mfType);

    showfis(fismat_2)
    showrule(fismat_2)
    ruleview(fismat_2)
    ruleedit(fismat_2)
fismat_2 = setfis(fismat_2,'name','PATCH LENGTH');
fismat_2 = setfis(fismat_2,'input',1,'name','Resonant
Frequency');
fismat_2 = setfis(fismat_2,'input',2,'name','Dielectric
Constant');
fismat_2 = setfis(fismat_2,'input',3,'name','Substrate
Height');
fismat_2 = setfis(fismat_2,'input',4,'name','Optimized Width');
fismat_2 = setfis(fismat_2,'output',1,'name','Patch Length');

    figure (4);
    plotfis(fismat_2)

    figure (5);
for input_index=1:4,
    subplot(2,2,input_index)
    [x,y]=plotmf(fismat_2,'input',input_index);
    plot(x,y)
    axis([-inf inf 0 1.2]);
    xlabel(['Input ' int2str(input_index)]);
    title('Initial Membership Values')
end

    numEpochs = 600;

[fismat3,trnErr2,ss2,fismat4,chkErr2] = anfis(trnData2,fismat_2,...
[numEpochs 0 0.04 0.9 1.1],NaN,chkData2,1);

trnOut2 = evalfis([trnData2(:,1) trnData2(:,2) trnData2(:,3)...
trnData2(:,4)],fismat3);
trnRMSE2 = norm(trnOut2 - trnData2(:,5))/sqrt(length(trnOut2));

    epoch = 1:numEpochs;

    figure (6);

```

```

        plot(epoch, trnErr2, 'o', epoch, chkErr2, 'x')
        hold on;
        plot(epoch, [trnErr2 chkErr2]);
        hold off

    trndL = evalfis([trnData2(:,1) trnData2(:,2) trnData2(:,3)...
        trnData2(:,4)], fismat3);

    ' Please Press ENTER Key to Continue'
    pause

    %-----
    ----
    %On the Third Phase, the Antenna Feed Point (Yf) is optimized based on
    %Five parameters (Resonant Frequency, Dielectric Constant, Substrate
    %Height, Optimized Width, & Optimized Length) as follows;

        'OPTIMIZATION OF ANTENNA FEED POINT (Yf) USING ANFIS'
    %-----
    ----

    load trncolumn6a.mat
    load chkcolumn3.mat
    %-----
    ----

    trnData3 = [trncolumn1 trndW trndL trncolumn6a];
    chkData3 = chkcolumn3;
    numMFs = [3 4 4];
    mfType = 'gbellmf';
    fismat_3 = genfis1(trnData3, numMFs, mfType);

        showfis(fismat_3)
        showrule(fismat_3)
        ruleview(fismat_3)
        ruleedit(fismat_3)

        fismat_3 = setfis(fismat_3, 'name', 'FEED POINT Yf');
        fismat_3 = setfis(fismat_3, 'input', 1, 'name', 'Resonant
Frequency');
        fismat_3 = setfis(fismat_3, 'input', 2, 'name', 'Optimized Width');
        fismat_3 = setfis(fismat_3, 'input', 3, 'name', 'Optimized
Length');
        fismat_3 = setfis(fismat_3, 'output', 1, 'name', 'Feed Point Yf');

        figure (7);
        plotfis(fismat_3)

        figure (8);
    for input_index=1:3,
        subplot(2,2,input_index)
        [x,y]=plotmf(fismat_3, 'input', input_index);

```

```

    plot(x,y)
    axis([-inf inf 0 1.2]);
    xlabel(['Input ' int2str(input_index)]);
    title('Initial Membership Values')
end

    numEpochs = 600;

    [fismat5,trnErr3,ss3,fismat6,chkErr3] = anfis(trnData3,fismat_3,...
    [numEpochs 0 0.04 0.9 1.1],NaN,chkData3,1);

    trnOut3 = evalfis([trnData3(:,1) trnData3(:,2)
trnData3(:,3)],fismat5);
    trnRMSE3 = norm(trnOut3 - trnData3(:,4))/sqrt(length(trnOut3));

    epoch3 = 1:numEpochs;

    figure (9);
    plot(epoch3,trnErr3,'o',epoch3,chkErr3,'x')
    hold on;
    plot(epoch3,[trnErr3 chkErr3]);
    hold off

    trndYf = evalfis([trnData3(:,1) trnData3(:,2)
trnData3(:,3)],fismat5);

' Please Press ENTER Key to Continue'
pause

%-----
----
%On the Third Phase, the Antenna Feed Point (Xf) is optimized based on
%Five parameters(Resonant Frequency, Dielectric Constant, Substrate
%Height, Optimized Width, & Optimized Length) as follows;

'OPTIMIZATION OF ANTENNA FEED POINT (Xf) USING ANFIS'
%-----
----

load trncolumn6b.mat
load chkcolumn4.mat

%-----
----

trnData4 = [trncolumn1 trndW trndL trncolumn6b];
chkData4 = chkcolumn4;

numMFs = [3 4 4];
mfType = 'gbellmf';

```

```

fismat_4 = genfis1(trnData4,numMFs,mfType);

    showfis(fismat_4)
    showrule(fismat_4)
    ruleview(fismat_4)
    ruleedit(fismat_4)

fismat_4 = setfis(fismat_4,'name','FEED POINT Xf');
fismat_4 = setfis(fismat_4,'input',1,'name','Resonant
Frequency');
fismat_4 = setfis(fismat_4,'input',2,'name','Optimized Width');
fismat_4 = setfis(fismat_4,'input',3,'name','Optimized
Length');
fismat_4 = setfis(fismat_4,'output',1,'name','Feed Point Xf');

figure (10);
plotfis(fismat_4)

figure (11);
for input_index=1:3,
    subplot(2,2,input_index)
    [x,y]=plotmf(fismat_4,'input',input_index);
    plot(x,y)
    axis([-inf inf 0 1.2]);
    xlabel(['Input ' int2str(input_index)]);
    title('Initial Membership Values')
end

numEpochs = 600;

[fismat7,trnErr4,ss4,fismat8,chkErr4] = anfis(trnData4,fismat_4,...
[numEpochs 0 0.04 0.9 1.1],NaN,chkData4,1);

trnOut4 = evalfis([trnData4(:,1) trnData4(:,2)
trnData4(:,3)],fismat7);
trnRMSE4 = norm(trnOut4 - trnData4(:,4))/sqrt(length(trnOut4));

epoch4 = 1:numEpochs;

figure (12);
plot(epoch4,trnErr4,'o',epoch4,chkErr4,'x')
hold on;
plot(epoch4,[trnErr4 chkErr4]);
hold off

trndXf = evalfis([trnData4(:,1) trnData4(:,2)
trnData4(:,3)],fismat7);

' Please Press ENTER Key to Continue'
pause

```

```

%-----
----
%The final optimized Antenna Design Parameters are listed in this
section
%Also, in the same section, the final design parameter values are saved
as
%an excel document under the Matlab Folder. Anytime the simulation is
%carried out, the final values are then appended in the same file named
%PATCHANTENNA.

```

'OVERALL OPTIMIZATION RESULTS'

```

%-----
----

```

```

optmzdpparameters = [trndW trndL trndYf trndXf]
    save optmzdpparameters

allparameters = {'Fr' 'Er' 'h' 'optW' 'OptL' 'OptYf' 'OptXf' 'Lg'
'Wg';...
    trncolumn1 trncolumn2 trncolumn3 trndW trndL trndYf trndXf Lgall
Wgall};

allt = [trncolumn1 trncolumn2 trncolumn3 trndW trndL trndYf trndXf
Lgall...
    Wgall];

    save allparameters

    s = xlswrite('patchantenna.xls', allparameters, 'simulation',
'B1');
    s2 = xlswrite('patchantenna.xls', allt, 'simulation', 'B3');

```

```

%-----
----

```

```

%Here, the graphs of relationship between frequency and Optimized Patch
%Width, Patch Length, Feed Point along the Width Yf, and Feed Point
along
%the Length Xf are plotted as shown below in figure 13 to 16.

```

```

fd = xlsread('patchantenna.xls', 'simulation', 'B3:B17');
fg = xlsread('patchantenna.xls', 'simulation', 'B18:B32');
fa = xlsread('patchantenna.xls', 'simulation', 'B63:B77');
fin = xlsread('patchantenna.xls', 'simulation', 'B78:B92');

Wd = xlsread('patchantenna.xls', 'simulation', 'E3:E17');
Wg = xlsread('patchantenna.xls', 'simulation', 'E18:E32');
Wa = xlsread('patchantenna.xls', 'simulation', 'E63:E77');
Win = xlsread('patchantenna.xls', 'simulation', 'E78:E92');

Ld = xlsread('patchantenna.xls', 'simulation', 'F3:F17');
Lg = xlsread('patchantenna.xls', 'simulation', 'F18:F32');

```

```

La = xlsread('patchantenna.xls', 'simulation', 'F63:F77');
Lin = xlsread('patchantenna.xls', 'simulation', 'F78:F92');

Yfd = xlsread('patchantenna.xls', 'simulation', 'G3:G17');
Yfg = xlsread('patchantenna.xls', 'simulation', 'G18:G32');
Yfa = xlsread('patchantenna.xls', 'simulation', 'G63:G77');
Yfin = xlsread('patchantenna.xls', 'simulation', 'G78:G92');
Xfd = xlsread('patchantenna.xls', 'simulation', 'H3:H17');
Xfg = xlsread('patchantenna.xls', 'simulation', 'H18:H32');
Xfa = xlsread('patchantenna.xls', 'simulation', 'H63:H77');
Xfin = xlsread('patchantenna.xls', 'simulation', 'H78:H92');

%Figure 13 plots Resonance Frequency vs Optimized Patch Width
figure (13);
plot (Wd,fd,Wg,fg,Wa,fa,Win,fin);
axis([0 90 1000 8500]);
legend('Er=2.2,h=1.57mm','Er=4.35,h=1.6mm','Er=9.8,h=1.5mm',...
'Er & h =Input')

grid
xlabel('Optimized Patch Width (mm)')
ylabel('Resonant Frequency (MHz)')
title('Patch Width vs Resonance Frequency')

%Figure 14 plots Resonance Frequency vs Optimized Patch Length
figure (14);
plot (Ld,fd,Lg,fg,La,fa,Lin,fin);
axis([0 85 1000 8500]);
legend('Er=2.2,h=1.57mm','Er=4.35,h=1.6mm','Er=9.8,h=1.5mm',...
'Er & h =Input')

grid
xlabel('Optimized Patch Length (mm)')
ylabel('Resonant Frequency (MHz)')
title('Patch Length vs Resonance Frequency')

%Figure 15 plots Resonance Frequency vs Optimized Feed Pont along the
Width
figure (15);
plot (Yfd,fd,Yfg,fg,Yfa,fa,Yfin,fin);
axis([0 50 1000 8500]);
legend('Er=2.2,h=1.57mm','Er=4.35,h=1.6mm','Er=9.8,h=1.5mm',...
'Er & h =Input')

grid
xlabel('Optimized Feed Point Yf(mm)')
ylabel('Resonant Frequency (MHz)')
title('Patch Feed Point along Width vs Resonance Frequency')

%Figure 16 plots Resonance Frequency vs Optimized Feed Pont along the
%patch Length
figure (16);
plot (Xfd,fd,Xfg,fg,Xfa,fa,Xfin,fin);
axis([0 30 1000 8500]);
legend('Er=2.2,h=1.57mm','Er=4.35,h=1.6mm','Er=9.8,h=1.5mm',...

```

```

        'Er & h =Input')
    grid
    xlabel('Optimized Feed Point Xf(mm)')
    ylabel('Resonant Frequency (MHz)')
    title('Patch Feed Point along Length vs Resonance Frequency')

%Figure 17 plots Resonance Frequency vs all the Optimized parameters.
figure (17);

subplot(2,2,1)
    plot (Wd,fd,Wg,fg,Wa,fa,Win,fin);
        axis([0 90 1000 8500]);
        legend('Er=2.2,h=1.57mm','Er=4.35,h=1.6mm','Er=9.8,h=1.5mm',...
            'Er & h =Input')
    grid
    xlabel('Patch Width (mm)')
    ylabel('Resonant Frequency (MHz)')
    title('1st Model - W vs fr')

subplot(2,2,2)
    plot (Ld,fd,Lg,fg,La,fa,Lin,fin);
        axis([0 85 1000 8500]);
        legend('Er=2.2,h=1.57mm','Er=4.35,h=1.6mm','Er=9.8,h=1.5mm',...
            'Er & h =Input')
    grid
    xlabel('Patch Length (mm)')
    ylabel('Resonant Frequency (MHz)')
    title('2nd Model - L vs fr')

subplot(2,2,3)
    plot (Yfd,fd,Yfg,fg,Yfa,fa,Yfin,fin);
        axis([0 50 1000 8500]);
        legend('Er=2.2,h=1.57mm','Er=4.35,h=1.6mm','Er=9.8,h=1.5mm',...
            'Er & h =Input')
    grid
    xlabel('Feed-Point along the Width Yf(mm)')
    ylabel('Resonant Frequency (MHz)')
    title('3rd Model - Yf vs fr')

subplot(2,2,4)
    plot (Xfd,fd,Xfg,fg,Xfa,fa,Xfin,fin);
        axis([0 30 1000 8500]);
        legend('Er=2.2,h=1.57mm','Er=4.35,h=1.6mm','Er=9.8,h=1.5mm',...
            'Er & h =Input')
    grid
    xlabel('Feed-Point along the Length Xf(mm)')
    ylabel('Resonant Frequency (MHz)')
    title('4th Model - Xf vs fr')

```

APPENDIX B: TRAINING DATA SETS

APPENDIX B-1: Training Data for Patch Width Optimization

Frequency (MHz)	Dielectric Constant (ϵ_r)	Substrate Height (mm)	Patch Width (W) (mm)
1400	2.2	1.57	84.704
1500	2.2	1.57	79.057
2000	2.2	1.57	59.293
2500	2.2	1.57	47.434
3000	2.2	1.57	39.528
3500	2.2	1.57	33.882
4000	2.2	1.57	29.646
4500	2.2	1.57	26.352
5000	2.2	1.57	23.717
5500	2.2	1.57	21.561
6000	2.2	1.57	19.764
6500	2.2	1.57	18.244
7000	2.2	1.57	16.941
7500	2.2	1.57	15.811
8000	2.2	1.57	14.823
1400	4.35	1.6	65.509
1500	4.35	1.6	61.142
2000	4.35	1.6	45.856
2500	4.35	1.6	36.685
3000	4.35	1.6	30.571
3500	4.35	1.6	26.204
4000	4.35	1.6	22.928
4500	4.35	1.6	20.381
5000	4.35	1.6	18.343
5500	4.35	1.6	16.675
6000	4.35	1.6	15.285
6500	4.35	1.6	14.110
7000	4.35	1.6	13.102
7500	4.35	1.6	12.228
8000	4.35	1.6	11.464

1400	10	2.2	45.686
1500	10	2.2	42.640
2000	10	2.2	31.980
2500	10	2.2	25.584
3000	10	2.2	21.320
3500	10	2.2	18.274
4000	10	2.2	15.990
4500	10	2.2	14.213
5000	10	2.2	12.792
5500	10	2.2	11.629
6000	10	2.2	10.660
6500	10	2.2	9.840
7000	10	2.2	9.137
7500	10	2.2	8.528
8000	10	2.2	7.995
1400	11.9	1.5	42.187
1500	11.9	1.5	39.375
2000	11.9	1.5	29.531
2500	11.9	1.5	23.625
3000	11.9	1.5	19.687
3500	11.9	1.5	16.875
4000	11.9	1.5	14.766
4500	11.9	1.5	13.125
5000	11.9	1.5	11.812
5500	11.9	1.5	10.739
6000	11.9	1.5	9.844
6500	11.9	1.5	9.087
7000	11.9	1.5	8.437
7500	11.9	1.5	7.875
8000	11.9	1.5	7.383
1400	9.8	1.5	46.107
1500	9.8	1.5	43.033
2000	9.8	1.5	32.275
2500	9.8	1.5	25.820
3000	9.8	1.5	21.517
3500	9.8	1.5	18.443
4000	9.8	1.5	16.137
4500	9.8	1.5	14.344
5000	9.8	1.5	12.910

5500	9.8	1.5	11.736
6000	9.8	1.5	10.758
6500	9.8	1.5	9.931
7000	9.8	1.5	9.221
7500	9.8	1.5	8.607
8000	9.8	1.5	8.069
1400	3.8	1.5	69.160
1500	3.8	1.5	64.550
2000	3.8	1.5	48.412
2500	3.8	1.5	38.730
3000	3.8	1.5	32.275
3500	3.8	1.5	27.664
4000	3.8	1.5	24.206
4500	3.8	1.5	21.517
5000	3.8	1.5	19.365
5500	3.8	1.5	17.604
6000	3.8	1.5	16.137
6500	3.8	1.5	14.896
7000	3.8	1.5	13.832
7500	3.8	1.5	12.910
8000	3.8	1.5	12.103

APPENDIX B-2: Training Data for Patch Length Optimization

Frequency (MHz)	Dielectric Constant (ϵ_r)	Substrate Height (mm)	Patch Width (W) (mm)	Patch Length (L) (mm)
1400	2.2	1.57	83.641	71.535
1500	2.2	1.57	79.714	66.712
2000	2.2	1.57	60.572	49.820
2500	2.2	1.57	45.860	39.674
3000	2.2	1.57	39.677	32.903
3500	2.2	1.57	34.763	28.060
4000	2.2	1.57	29.859	24.423
4500	2.2	1.57	25.466	21.592
5000	2.2	1.57	23.659	19.324
5500	2.2	1.57	22.025	17.466
6000	2.2	1.57	19.922	15.916
6500	2.2	1.57	17.886	14.604

7000	2.2	1.57	16.844	13.478
7500	2.2	1.57	16.095	12.501
8000	2.2	1.57	14.678	11.645
1400	4.35	1.6	64.713	51.119
1500	4.35	1.6	61.665	47.682
2000	4.35	1.6	46.818	35.641
2500	4.35	1.6	35.461	28.401
3000	4.35	1.6	30.716	23.564
3500	4.35	1.6	26.908	20.100
4000	4.35	1.6	23.096	17.497
4500	4.35	1.6	19.689	15.468
5000	4.35	1.6	18.307	13.841
5500	4.35	1.6	17.044	12.507
6000	4.35	1.6	15.409	11.394
6500	4.35	1.6	13.826	10.450
7000	4.35	1.6	13.029	9.639
7500	4.35	1.6	12.453	8.936
8000	4.35	1.6	11.347	8.320
1400	10	2.2	45.139	33.672
1500	10	2.2	43.015	31.389
2000	10	2.2	32.661	23.375
2500	10	2.2	24.726	18.543
3000	10	2.2	21.404	15.305
3500	10	2.2	18.752	12.983
4000	10	2.2	16.103	11.235
4500	10	2.2	13.736	9.870
5000	10	2.2	12.775	8.775
5500	10	2.2	11.889	7.877
6000	10	2.2	10.743	7.127
6500	10	2.2	9.636	6.491
7000	10	2.2	9.084	5.945
7500	10	2.2	8.686	5.472
8000	10	2.2	7.913	5.057
1400	11.9	1.5	41.728	31.010
1500	11.9	1.5	39.752	28.925
2000	11.9	1.5	30.136	21.612
2500	11.9	1.5	22.821	17.207
3000	11.9	1.5	19.793	14.259
3500	11.9	1.5	17.336	12.145

4000	11.9	1.5	14.870	10.554
4500	11.9	1.5	12.670	9.313
5000	11.9	1.5	11.793	8.317
5500	11.9	1.5	10.981	7.500
6000	11.9	1.5	9.923	6.817
6500	11.9	1.5	8.899	6.238
7000	11.9	1.5	8.391	5.741
7500	11.9	1.5	8.024	5.309
8000	11.9	1.5	7.305	4.930
1400	9.8	1.5	45.522	34.165
1500	9.8	1.5	43.389	31.869
2000	9.8	1.5	32.989	23.820
2500	9.8	1.5	24.976	18.974
3000	9.8	1.5	21.597	15.732
3500	9.8	1.5	18.926	13.409
4000	9.8	1.5	16.264	11.660
4500	9.8	1.5	13.874	10.296
5000	9.8	1.5	12.879	9.202
5500	9.8	1.5	11.987	8.304
6000	9.8	1.5	10.846	7.554
6500	9.8	1.5	9.740	6.918
7000	9.8	1.5	9.168	6.371
7500	9.8	1.5	8.759	5.897
8000	9.8	1.5	7.992	5.481
1400	3.8	1.5	68.323	54.680
1500	3.8	1.5	65.104	51.006
2000	3.8	1.5	49.424	38.135
2500	3.8	1.5	37.436	30.398
3000	3.8	1.5	32.431	25.231
3500	3.8	1.5	28.408	21.533
4000	3.8	1.5	24.382	18.754
4500	3.8	1.5	20.785	16.589
5000	3.8	1.5	19.330	14.853
5500	3.8	1.5	17.995	13.430
6000	3.8	1.5	16.267	12.243
6500	3.8	1.5	14.595	11.236
7000	3.8	1.5	13.756	10.372
7500	3.8	1.5	13.150	9.623
8000	3.8	1.5	11.978	8.966

**APPENDIX B-3: Training Data for Feed Point along Patch Width & Length
Optimization**

Frequency (MHz)	Patch Width (W) (mm)	Patch Length (L) (mm)
1400	83.641	71.507
1500	79.714	66.705
2000	60.572	49.810
2500	45.860	39.663
3000	39.677	32.884
3500	34.763	28.065
4000	29.859	24.433
4500	25.466	21.594
5000	23.659	19.310
5500	22.025	17.458
6000	19.922	15.914
6500	17.886	14.603
7000	16.844	13.480
7500	16.095	12.500
8000	14.678	11.644
1400	64.713	51.115
1500	61.665	47.678
2000	46.818	35.631
2500	35.461	28.389
3000	30.716	23.559
3500	26.908	20.099
4000	23.096	17.496
4500	19.689	15.468
5000	18.307	13.843
5500	17.044	12.511
6000	15.409	11.398
6500	13.826	10.454
7000	13.029	9.641
7500	12.453	8.936
8000	11.347	8.318
1400	45.139	33.680
1500	43.015	31.384

2000	32.661	23.369
2500	24.726	18.539
3000	21.404	15.303
3500	18.752	12.980
4000	16.103	11.234
4500	13.736	9.870
5000	12.775	8.777
5500	11.889	7.879
6000	10.743	7.128
6500	9.636	6.491
7000	9.084	5.945
7500	8.686	5.471
8000	7.913	5.057
1400	41.728	31.000
1500	39.752	28.925
2000	30.136	21.612
2500	22.821	17.207
3000	19.793	14.258
3500	17.336	12.145
4000	14.870	10.554
4500	12.670	9.313
5000	11.793	8.317
5500	10.981	7.500
6000	9.923	6.817
6500	8.899	6.238
7000	8.391	5.741
7500	8.024	5.309
8000	7.305	4.930
1400	45.522	34.165
1500	43.389	31.869
2000	32.989	23.820
2500	24.976	18.974
3000	21.597	15.732
3500	18.926	13.409
4000	16.264	11.660
4500	13.874	10.296
5000	12.879	9.202
5500	11.987	8.304
6000	10.846	7.554

6500	9.740	6.918
7000	9.168	6.371
7500	8.759	5.897
8000	7.992	5.481
1400	68.323	54.680
1500	65.104	51.006
2000	49.424	38.135
2500	37.436	30.398
3000	32.431	25.231
3500	28.408	21.533
4000	24.382	18.754
4500	20.785	16.588
5000	19.330	14.853
5500	17.995	13.430
6000	16.267	12.243
6500	14.595	11.236
7000	13.756	10.373
7500	13.150	9.623
8000	11.978	8.966

APPENDIX C: ANFIS PARAMETRIC DESIGN OPTIMIZED RESULTS

Frequency (MHz)	Dielectric Constant (ϵ_r)	Substrate Height (mm)	Optimized Patch Width (W_t)(mm)	Optimized Patch Length (L_t)(mm)	Optimized Patch Width (Y_{ft})(mm)	Optimized Patch Width (X_{ft})(mm)	Plane Ground Dimension along Width (W_g)(mm)	Plane Ground Dimension along Length (L_g)(mm)
1400	2.2	1.57	83.576	71.444	42.413	24.427	94.124	80.955
1500	2.2	1.57	79.688	66.705	39.529	22.809	88.477	76.132
2000	2.2	1.57	60.679	49.807	29.673	17.102	68.713	59.240
2500	2.2	1.57	45.767	39.652	23.719	13.669	56.854	49.094
3000	2.2	1.57	39.669	33.081	19.758	11.362	48.948	42.323
3500	2.2	1.57	34.821	28.060	16.941	9.739	43.302	37.480
4000	2.2	1.57	29.835	24.425	14.822	8.475	39.066	33.843
4500	2.2	1.57	25.424	21.594	13.176	7.526	35.772	31.012
5000	2.2	1.57	23.662	19.325	11.860	6.762	33.137	28.744
5500	2.2	1.57	22.022	17.467	10.782	6.125	30.981	26.886
6000	2.2	1.57	19.909	15.916	9.881	5.550	29.184	25.336
6500	2.2	1.57	17.868	14.605	9.122	5.110	27.664	24.024
7000	2.2	1.57	16.852	13.477	8.479	4.854	26.361	22.898
7500	2.2	1.57	16.089	12.501	7.905	4.407	25.231	21.921
8000	2.2	1.57	14.678	11.645	7.408	4.055	24.243	21.065
1400	4.35	1.6	64.662	51.119	32.756	12.550	75.109	60.719
1500	4.35	1.6	61.649	47.682	30.572	11.722	70.742	57.282
2000	4.35	1.6	46.818	35.631	22.927	8.819	55.456	45.241
2500	4.35	1.6	35.400	28.401	18.339	7.016	46.285	38.001
3000	4.35	1.6	30.702	23.563	15.293	5.968	40.171	33.164
3500	4.35	1.6	26.950	20.101	13.111	5.211	35.804	29.700
4000	4.35	1.6	23.087	17.496	11.440	4.142	32.528	27.097
4500	4.35	1.6	19.672	15.468	10.190	3.785	29.981	25.068
5000	4.35	1.6	18.316	13.841	9.162	3.606	27.943	23.441
5500	4.35	1.6	17.048	12.507	8.334	3.174	26.275	22.107
6000	4.35	1.6	15.411	11.394	7.663	3.184	24.885	20.994
6500	4.35	1.6	13.828	10.450	7.070	2.637	23.710	20.050
7000	4.35	1.6	13.038	9.640	6.567	2.855	22.702	19.239
7500	4.35	1.6	12.446	8.935	6.120	2.299	21.828	18.536
8000	4.35	1.6	11.352	8.321	5.712	2.053	21.064	17.920
1400	10	2.2	45.109	33.672	22.837	11.751	58.886	46.872
1500	10	2.2	43.008	31.389	21.323	11.125	55.840	44.589
2000	10	2.2	32.738	23.375	15.961	7.881	45.180	36.575
2500	10	2.2	24.697	18.543	12.769	6.464	38.784	31.743
3000	10	2.2	21.414	15.305	10.654	5.448	34.520	28.505
3500	10	2.2	18.790	12.983	9.154	5.162	31.474	26.183

4000	10	2.2	16.094	11.235	7.947	3.420	29.190	24.435
4500	10	2.2	13.728	9.870	7.017	2.757	27.413	23.070
5000	10	2.2	12.808	8.775	6.383	3.226	25.992	21.975
5500	10	2.2	11.911	7.876	5.818	3.173	24.829	21.077
6000	10	2.2	10.744	7.127	5.311	2.562	23.860	20.327
6500	10	2.2	9.622	6.491	4.876	2.164	23.040	19.691
7000	10	2.2	9.089	5.945	4.548	2.385	22.337	19.145
7500	10	2.2	8.688	5.472	4.291	2.491	21.728	18.672
8000	10	2.2	7.912	5.057	3.945	1.696	21.195	18.257
1400	11.9	1.5	41.656	31.010	21.093	4.651	51.187	40.010
1500	11.9	1.5	39.714	28.925	19.687	4.362	48.375	37.925
2000	11.9	1.5	30.222	21.612	14.777	3.485	38.531	30.612
2500	11.9	1.5	22.797	17.207	11.823	2.785	32.625	26.207
3000	11.9	1.5	19.776	14.259	9.823	1.944	28.687	23.259
3500	11.9	1.5	17.359	12.145	8.439	2.031	25.875	21.145
4000	11.9	1.5	14.869	10.554	7.466	2.511	23.766	19.554
4500	11.9	1.5	12.668	9.313	6.539	1.128	22.125	18.313
5000	11.9	1.5	11.795	8.317	5.915	1.343	20.812	17.317
5500	11.9	1.5	10.978	7.500	5.374	1.307	19.739	16.500
6000	11.9	1.5	9.923	6.818	4.950	1.401	18.844	15.817
6500	11.9	1.5	8.903	6.238	4.545	1.178	18.087	15.238
7000	11.9	1.5	8.396	5.741	4.202	0.916	17.437	14.741
7500	11.9	1.5	8.015	5.309	3.989	1.157	16.875	14.309
8000	11.9	1.5	7.310	4.931	3.692	0.731	16.383	13.930
1400	9.8	1.5	45.513	34.165	23.058	5.745	55.107	43.165
1500	9.8	1.5	43.392	31.869	21.516	5.309	52.033	40.869
2000	9.8	1.5	33.030	23.820	16.160	4.369	41.275	32.820
2500	9.8	1.5	24.917	18.974	12.914	3.218	34.820	27.974
3000	9.8	1.5	21.611	15.732	10.783	3.104	30.517	24.732
3500	9.8	1.5	18.969	13.408	9.213	2.085	27.443	22.409
4000	9.8	1.5	16.249	11.661	8.079	2.249	25.137	20.660
4500	9.8	1.5	13.845	10.295	7.194	2.131	23.344	19.296
5000	9.8	1.5	12.892	9.202	6.481	2.123	21.910	18.202
5500	9.8	1.5	11.998	8.304	5.892	1.865	20.736	17.304
6000	9.8	1.5	10.844	7.554	5.393	1.208	19.758	16.554
6500	9.8	1.5	9.729	6.918	4.947	0.838	18.931	15.918
7000	9.8	1.5	9.175	6.372	4.602	1.074	18.221	15.371
7500	9.8	1.5	8.760	5.897	4.353	1.334	17.607	14.897
8000	9.8	1.5	7.989	5.481	4.027	1.058	17.069	14.481
1400	3.8	1.5	68.270	54.680	34.580	14.314	78.160	63.680
1500	3.8	1.5	65.089	51.006	32.275	13.372	73.550	60.006
2000	3.8	1.5	49.544	38.135	24.206	10.056	57.412	47.135
2500	3.8	1.5	37.375	30.398	19.367	8.084	47.730	39.398
3000	3.8	1.5	32.416	25.231	16.135	6.737	41.275	34.231
3500	3.8	1.5	28.453	21.532	13.821	5.592	36.664	30.533

4000	3.8	1.5	24.372	18.755	12.118	5.201	33.206	27.754
4500	3.8	1.5	20.767	16.588	10.755	4.501	30.517	25.589
5000	3.8	1.5	19.336	14.853	9.705	4.298	28.365	23.853
5500	3.8	1.5	17.996	13.431	8.810	3.578	26.604	22.430
6000	3.8	1.5	16.265	12.243	8.039	3.071	25.137	21.243
6500	3.8	1.5	14.593	11.235	7.440	2.872	23.896	20.236
7000	3.8	1.5	13.763	10.373	6.906	3.003	22.832	19.372
7500	3.8	1.5	13.140	9.624	6.447	2.449	21.910	18.623
8000	3.8	1.5	11.983	8.965	6.066	2.563	21.103	17.966

APPENDIX D: COMPUTER USAGE PROFILE SUMMARY

APPENDIX D-1: ANFIS MATLAB Time Usage Profile

Profile Summary

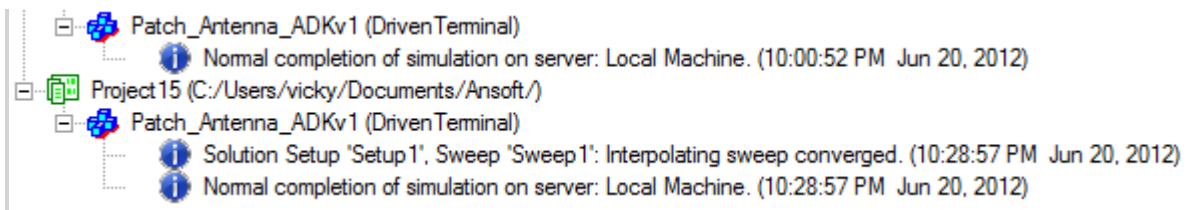
Generated 18-Jun-2012 10:49:10 using cpu time.

<u>Function Name</u>	<u>Calls</u>	<u>Total Time</u>	<u>Self Time*</u>	Total Time Plot (dark band = self time)
antennaanfis	1	383.642 s	108.902 s	
anfis	4	229.481 s	0.015 s	
anfismex (MEX-function)	4	229.434 s	229.434 s	
run	2	19.329 s	0.015 s	
antennaparameters	1	19.282 s	19.282 s	
xlsread	20	14.133 s	5.083 s	
actxserver	22	9.892 s	9.892 s	
xlswrite	2	2.433 s	0.031 s	
legendcolorbarlayout>doLayout	240	2.263 s	0.174 s	
legendcolorbarlayout>doLayoutCB	216	2.072 s	0.063 s	
ruleedit	8	1.776 s	1.495 s	
ruleview	8	1.481 s	1.122 s	
xlswrite>ExecuteWrite	2	1.357 s	1.248 s	
legend	8	1.031 s	0.016 s	
legendcolorbarlayout>doinOutLayout	240	1.025 s	0.174 s	
legend>make_legend	8	1.015 s	0.031 s	
scribe.legend.methods	336	1.007 s	0.000 s	
scribe.legend.legend	8	0.904 s	0.109 s	
scribe.legend.methods>getsize	248	0.712 s	0.031 s	
showfis	4	0.702 s	0.218 s	
scribe.legend.methods>getsizeinfo	248	0.696 s	0.093 s	
legendcolorbarlayout>getPixelBounds	240	0.692 s	0.174 s	
title	76	0.639 s	0.093 s	
legendcolorbarlayout>doParentResize	8	0.624 s	0.016 s	
scribe.legend.methods>strsize	992	0.587 s	0.556 s	
scribe.legend.init	8	0.577 s	0.063 s	
plotfis	4	0.562 s	0.500 s	
xlabel	42	0.545 s	0.032 s	
closereq	16	0.518 s	0.518 s	
ylabel	16	0.498 s	0.000 s	

gcbf	48	0 s	0.000 s	
gcbo	48	0 s	0.000 s	
filesep	24	0 s	0.000 s	
strmatch	2	0 s	0.000 s	
pwd	2	0 s	0.000 s	
winfun\private\newprogid	22	0 s	0.000 s	
xlswrite>base27dec	2	0 s	0.000 s	
xlswrite>calculate_range	2	0 s	0.000 s	
repmat	2	0 s	0.000 s	
ind2sub	2	0 s	0.000 s	
xlswrite>create@()\cleaner(Excel,file)	2	0 s	0.000 s	
onCleanup>onCleanup.onCleanup	2	0 s	0.000 s	
xlswrite>activate_sheet	2	0 s	0.000 s	
xlsread>trim_arrays	20	0 s	0.000 s	
legend>find_legend	8	0 s	0.000 s	
legend>process_inputs	8	0 s	0.000 s	
scribe.legend.schema>edgeColorSetter	8	0 s	0.000 s	
hggetbehavior>localPeek	40	0 s	0.000 s	
hgbehaviorfactory>localGetBehaviorInfo	40	0 s	0.000 s	
...loteditbehavior.schema>doEnableAction	8	0 s	0.000 s	
graphics.panbehavior.dosupport	8	0 s	0.000 s	
graphics.zoombehavior.dosupport	8	0 s	0.000 s	
graphics.rotate3dbehavior.dosupport	8	0 s	0.000 s	
graphics.datacursorbehavior.dosupport	8	0 s	0.000 s	
graphics.ploteditbehavior.dosupport	8	0 s	0.000 s	
legend.colorbarlayout>initProperties	8	0 s	0.000 s	
...layout>create@(obj,evd)(doLayout(ax))	8	0 s	0.000 s	
scribe.legend.init>setWidthHeight	16	0 s	0.000 s	

Self time is the time spent in a function excluding the time spent in its child functions. Self time also includes overhead resulting from the process of profiling.

APPENDIX D-2: ANSOFT HFSS Time Usage Profile



APPENDIX E: PUBLICATIONS

APPENDIX E-1: Journal Papers

1. K.V. Rop, D.B.O. Konditi, H.A. Ouma, S. Musyoki “Parameter Optimization in Design of a Rectangular Microstrip Patch Antenna using Adaptive Neuro-Fuzzy Inference System Technique”, International Journal on Technical and Physical Problems of Engineering (IJTPE), Issue 12, Vol. 4, No. 3, pp16-23, September 2012
2. K.V. Rop, D.B.O. Konditi. “Performance Analysis of a Rectangular Microstrip Patch Antenna on Different Dielectric Substrates”, International Institute for Science Technology and Education (IISTE) - Innovative Systems Design and Engineering, Vol. 3, No. 8, pp. 7-14, August 2012

APPENDIX E-2: Conference Papers

1. K.V. Rop, D.B.O. Konditi, H.A. Ouma, S. Musyoki “Parameter Optimization in Design of a Rectangular Microstrip Patch Antenna using Adaptive Neuro-Fuzzy Inference System Technique”, Annual Interdisciplinary Conference, The Catholic University of Eastern Africa, Nairobi Kenya, June 2012
2. K.V. Rop, D.B.O. Konditi. “Analysis of a Rectangular Microstrip Patch Antenna on Different Dielectric Substrates”, KSEEE-JSAEM 2012 International Engineering Conference, African Institute for Capacity Development (AICAD), Juja Kenya, pp. 11-16, August, 2012